SPATIOTEMPORAL REGULATION OF CAMP/PKA SIGNALING IN CELLULAR PROCESSES

by
Jessica R. Yang

A dissertation submitted to Johns Hopkins University in conformity with the requirements for the degree of Doctor of Philosophy

Baltimore, Maryland
August 2015

Abstract

Cells respond to extracellular stimuli by modulating intricately intertwined signaling pathways. To achieve specific responses, these pathways are tightly controlled in space and time by regulating second messenger concentrations and kinase activity dynamics. The 3'-5'-cyclic adenosine monophosphate (cAMP)/cAMP-dependent protein kinase (PKA) pathway is spatiotemporally compartmentalized at various levels in order to elicit specific cellular activities. At the second messenger level, cAMP concentration gradients are maintained by actively controlling its accumulation and degradation. PKA activity is also modulated in space and time by the spatiotemporal compartmentalization of upstream components, including cAMP gradients, and is itself spatially localized to specific subcellular compartments, contributing to highly specific substrate recognition. Moreover, interactions with signaling molecules from other signaling pathways serve as another source of regulation of the cAMP/PKA pathway. To study cAMP and PKA in their native environment, wherein the entire signaling network remains intact, we used fluorescence resonance energy transfer (FRET)-based biosensors to capture their endogenous signaling dynamics.

This dissertation is composed of two parts. The first part consists of two studies, which investigate the role of spatiotemporally compartmentalized PKA signaling in two separately important biological processes. In the first study, we used FRET-based PKA reporter (AKAR4-Kras) to study how cells tune PKA activity to transition between different modes of migration in response to different degree of physical confinement. We demonstrate the importance of crosstalk between different signaling pathways in regulating PKA activity to enable cells to adapt to their microenvironment and migrate

efficiently. In the second study we also employed FRET-based reporters to profile compartment-specific Akt activity dynamics in PC12 cells. We observed spatial differences of Akt as well as interesting temporal dynamics in response to EGF and NGF. While dissecting the molecular mechanisms governing compartment-specific Akt activity, we demonstrated a complex interaction between PKA and Akt that could regulate the differentiation of PC12 cells.

The second portion of the dissertation involves developing enhanced BRET- and FRET-based reporters to sensitively monitor kinase activity (Bim-BRET-KARs) and cAMP levels (ICUE4), respectively. We demonstrated the ability of Bim-BRET-KARs in detecting various kinase activities with high spatial resolution, and the applicability of these reporters to be used in combination with fluorescent molecules and optogenetic tools. We also generated a cAMP reporter that can detect low cAMP levels that were previously undetectable by current FRET-based cAMP reporters.

Taken together, the studies presented herein highlight various modes and roles of spatiotemporally compartmentalized cAMP/PKA signaling in modulating specific cellular processes. Moreover, utilizing the newly developed tools, we have elucidated dynamics of the cAMP/PKA signaling that we previously could not visualize. These studies enhance our understanding of the cAMP/PKA pathway and unveil unknown roles it plays in biological processes.

Thesis Advisor: Dr. Jin Zhang

Second Thesis Reader: Joy Yang

Acknowledgements

For the past five years, I have been extremely fortunate to be surrounded by supportive and selfless group of colleagues, friends and family members.

First, I would like to express my appreciation for being able to work with and learn from Dr. Jin Zhang. I could have not asked for a more understanding and encouraging advisor to work with. Thank-you for sticking by me and believing in me at times when I almost want to give up. Thank-you for being there and making me a better scientist by encouraging me to be more diligent and teaching me about how to formulate questions and convey succinct scientific ideas to others.

I also want to thank each member of the Zhang lab, past and present, for also guiding me through the most difficult times of my graduate career and always making time to help me with a task. Mostly I want to thank everyone for making the lab a fun and enjoyable environment. I want to especially thank Sohum Mehta, Xin Zhou, Ambhi Ganesan, and Nwe-Nwe for always willing to drop whatever they are doing and listen to my complaints about life and struggles with my projects. I feel like I cannot repay you all enough for the amount of time you all spend helping me. I want to give Sohum a big thank-you for spending time working with me on my thesis. Thank-you Xin and Nwe-Nwe for sharing your tips and insights on how to improve my experimental techniques. Also thank-you Ambhi for sharing in the struggle with working on the PC12 project.

I also want to thank Terri for being so helpful when I have a lot on my plate. I am so thankful you joined the lab so that I can have another person to talk to and hang out with other than the “guys” outside of lab.

This past year I have worked extensively with Wei-Chien Hung, Joy Yang, and Kostas Konstantopoulos on the cell migration project. Thank-you Wei-Chien for having so much patience with me and willing to deliver endless amount of samples to the lab. Joy Yang has contributed a large part in the discussion of the cell migration manuscript and I want to thank Joy for always being available and open to any discussion.

Next I want to express my gratitude to my boyfriend Sean Cho for being the most patient, loving and helpful person through everything. No words can express how grateful I am to have met such an intelligent and selfless person. Sean is always willing to listen to my practice talks and somehow is able to pick up on what exactly I'm talking about even when he works in a completely different area of research than me. He always asks the right questions to make sure I have done all the controls for my experiments and have prepared answers to questions that others may ask about my projects. Thank-you for also showing me how to be a more compassionate person, and also see the positive side in frustrating situations.

I also am the luckiest person to be able to have my sister live in the same city and even work at same institution. I'm glad that we've grown closer and are able to be there for each other. I'm sad to be leaving you soon and not having you as a roommate. Thank-you for putting up with my awkwardness and being so supportive in whatever I do.

Lastly, I want to thank my parents for always making sure I am well fed by sending me care-packages full of California-grown produce. Thank-you for caring about my health and helping me find the best medical care for my rheumatoid arthritis. I still remember the day I first moved out from home like it was yesterday. Thank-you for being there for me when I needed someone to talk to during my first year in Baltimore.

Thank-you for supporting me in my decision to study at Johns Hopkins and now dental school at Temple!

Table of Contents

List of Figures

Chapter 1

Introduction

Intracellular signaling and phosphorylation

Our bodies must intrinsically adjust to small and large changes to help us adapt to and survive in new environments. In response to these changes, organs and tissues release signaling molecules such as neurotransmitters, hormones, and polypeptides. Once released, these signaling molecules bind to specific receptors on the cell membrane, initiating a series of intracellular biochemical events that includes the production of second messengers and the modification of the concentrations and activities of downstream target proteins, which function to amplify the initial signals and mediate cellular effects. This series of events, known as intracellular signal transduction, influences a variety of cellular processes, such as cell migration and neuronal differentiation, which are ultimately manifested as physiological responses to environmental changes.

One of the most common ways in which cells modulate protein behavior is through the transfer of a phosphate group from ATP to specific serine, threonine, or tyrosine residues within proteins, a process known as phosphorylation. The first inkling of phosphorylation came during the early 20th century from studies by Phoebus Levene and Carl Alsberg, who observed portions of vitellin, a protein found in egg yolk, that were attached to phosphoric acid via an ester linkage[1]. Similarly, in 1954, Burnett and Kennedy hinted that a liver enzyme could be responsible for adding a phosphate group to casein, yet it remained unclear how or why either of these processes occurred[2].

Meanwhile, in the 1930s, through their research into carbohydrate metabolism, Carl and Gerty Kori characterized glycogen phosphorylase, which initiates the breakdown of glycogen, noting that this enzyme existed in two distinct forms:

phosphorylase a (active) and phosphorylase b (inactive)[3, 4]. In collaboration with Krebs and Fischer, the Koris also discovered the reversibility of phosphorylation through enzymes known as protein phosphatases[5]. From this work, they were able to correlate the two forms of phosphorylase to the phosphorylated/dephosphorylated state of the protein. Krebs and Fischer further demonstrated that the phosphorylation of glycogen phosphorylase required the presence of Mg-ATP and an enzyme first identified as phosphorylase kinase. Specifically, phosphorylase kinase activated phosphorylase b by hydrolyzing and transferring the γ-phosphate group of ATP to a specific serine residue on phosphorylase b, converting it to phosphorylase a.

At the same time, Rall and Sutherland showed that phosphorylase levels increased in the liver in response to glucagon and adrenaline. Thanks to the above insights into phosphorylase a activation, it became clear that ATP and phosphorylase kinase were the link between hormones and phosphorylase a. Further studies subsequently showed that hormones such as adrenaline can modulate intracellular processes by inducing the production of cyclic 3',5' adenosine monophosphate (cAMP)[6]. Finally in 1968, Krebs and his group identified the enzyme responsible for phosphorylating casein and phosphorylase kinase as a cAMP-dependent protein kinase, or protein kinase A (PKA), in the skeletal muscle of rabbits[7].

Since the discovery of phosphorylation and PKA, phosphorylation has been shown to play a central role in human physiology and disease. The human genome is now known to encode approximately 518 protein kinases and a third that number of protein phosphatases. Moreover, roughly 200,000 phosphorylation sites have been reported in the human proteome[8, 9]. Phosphorylation has multiple roles that include inducing

conformational changes, or the creation of surfaces with distinct binding properties that influence protein activity, localization and the recruitment of other signaling molecules. The dysregulation of kinases leads to abnormal phosphorylation that has been uncovered and implicated in many human diseases, including cancer, diabetes, hypertension, and neurodegenerative disorders[10]. For example, in the 1990s, Jack Dixon discovered that a major virulence factor of *Yersinia pestis* is a protein tyrosine phosphatase[11]. This class of bacteria causes several serious diseases, including the bubonic plague, which has been responsible for many pandemics over the past millennium; as early as the 12th and 13th centuries, one of the most famous outbreaks of the bubonic plague, the Black Death, was responsible for killing 25% of the population of Europe (42 million people). In addition, a number of naturally occurring toxins and tumor promoters exert their effects by targeting particular protein kinases and phosphatases to alter phosphorylation levels of important proteins[12]. As a result, many protein kinase inhibitors, such as fasudil, rapamycin, Gleevec, and Lapatanib, which target Rho dependent kinase, TOR, and BCR-Abl, and EGFR, respectively, are currently in clinical use to treat various diseases[13]. Given the importance of PKA and other kinases as signaling molecules and given that targeting kinase-mediated signaling has vast therapeutic potential, it is important to understand the molecular mechanisms underlying proper protein phosphorylation[14, 15].

cAMP/PKA signaling pathway

Cells communicate with their extra- and intracellular environments using signal transduction pathways that relay messages into functional responses. As mentioned earlier, Rall and Sutherland first linked hormones, an extracellular signal, to changes in

phosphorylation, which ultimately modifies protein function. Soon afterwards, Sutherland identified the first second messenger, cyclic 3',5' adenosine monophosphate (cAMP), which serves to amplify the extracellular signal and efficiently modulate the function of its downstream targets, known as effector proteins. By regulating its effector proteins, cAMP can regulate numerous cellular functions, including insulin secretion, cell growth and differentiation, muscle contraction, and long-term memory formation. The classical route of cAMP production is initiated when an extracellular stimulus such as a hormone or neurotransmitter binds to a G-protein-coupled receptor (GPCR) on the cell surface and activates the associated heterotrimeric G protein. The inactive trimer consists of a GDP-bound, stimulatory Gα subunit tightly bound to a Gβγ heterodimer. Stimulated GPCRs function as guanine-nucleotide exchange factors (GEFs), causing Gα to release GDP and bind free GTP. GTP-binding causes Gα to undergo a conformational change, leading to its dissociation from Gβγ. Depending on the type of α subunits ($G\alpha_s$, $G\alpha_i$, $G\alpha_{q/11}$, $G\alpha_{12/13}$), G-proteins can further affect intracellular signaling proteins [16]. Specifically, once $G\alpha_s$ dissociates from Gβγ, it associates with and activates transmembrane adenylyl cyclase (tmAC), which catalyzes the conversion of intracellular ATP into cAMP[19, 20] (Fig. 1.1). Once produced, cAMP can activate effector proteins such as PKA and Epac.

PKA was the first discovered cAMP effector and is one of the best characterized protein kinases. The inactive PKA holoenzyme exists as a heterotetrameric enzyme that consists of two regulatory (R) and two catalytic (C) subunits. There are four known isoforms of the R subunit (RIα, RIβ, RIIα, and RIIβ), along with three C subunit isoforms (Cα, β, γ) that are largely identical to each other but exhibit slight differences in tissue-

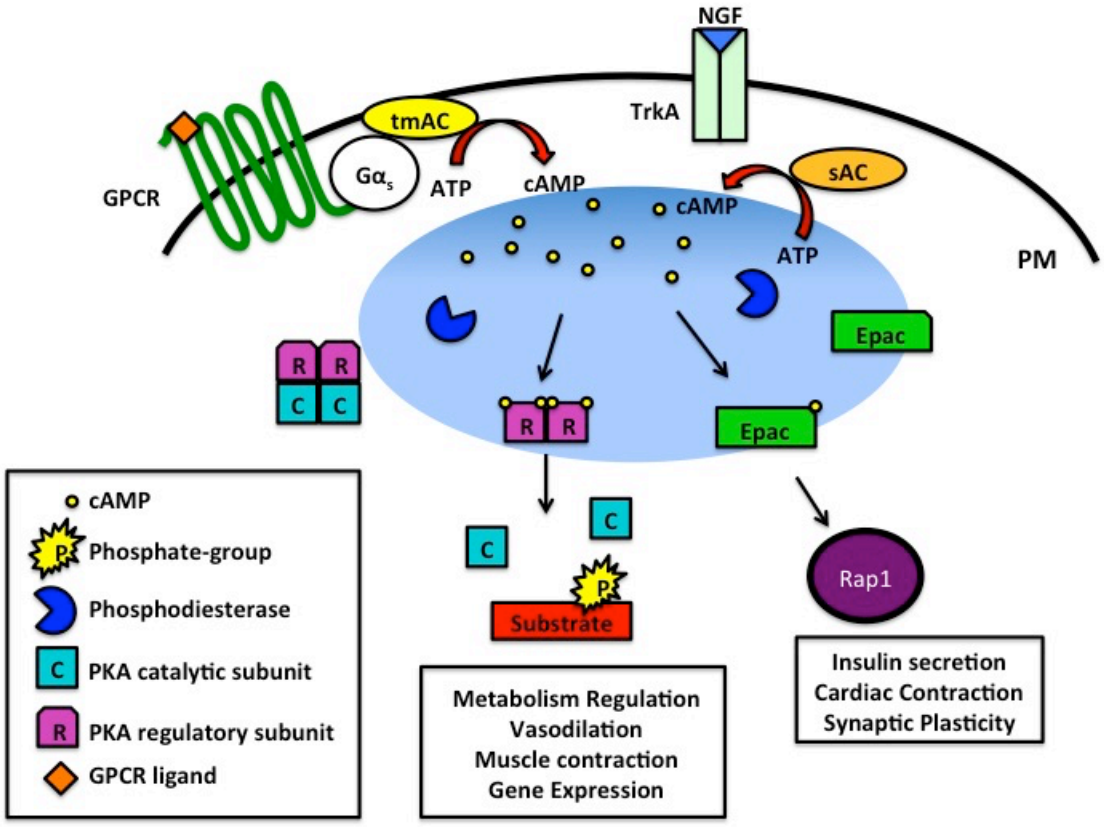

Figure 1.1 The cAMP Signaling Pathway
Following input of an appropriate signal, tmAC and/or sAC is activated to produce cAMP from intracellular ATP. Once produced, cAMP activates its downstream effectors, PKA or Epac. Degredation of cAMP is achieved by phosphodiesterases, which can help to form gradients of cAMP within the cell.

specific expression[17]. The cooperative binding of cAMP to the two R subunits induces a conformational change that leads to the release of active catalytic subunits[18]. The catalytic subunits are responsible for phosphorylating PKA substrates and contain two binding sites, one for the peptide substrate and the other for binding of ATP. Unlike the catalytic subunits, the R subunits (RI, RII) exhibit distinct molecular weights, protein sequences, phosphorylation states, cAMP-binding affinities, tissue distributions, and subcellular localizations. The RII subunits can be phosphorylated by the catalytic subunits, whereas RI subunits cannot[19]. Furthermore, the type I PKA holoenzyme (RIα and RIβ) is predominantly cytoplasmic, whereas the majority of type II PKA (RIIα and RIIβ) associates with cellular structures such as the plasma membrane, cytoskeleton, nuclear membrane, secretory vesicles, and organelles. In addition, the RIα and RIIα subunits are expressed in most tissues while RIβ and RIIβ are selectively expressed in the central nervous system and in reproductive tissues[20]. The distinct, isoform-specific expression patterns of the R subunits allow PKA to effectively phosphorylate specific substrates that are required for many tissue-specific cellular processes, including metabolism, gene expression and muscle contraction.

A more recently discovered cAMP effector, Epac functions as a GEF for Rap1 and Rap2, members of the Ras G-protein family. Upon cAMP binding, Epac is recruited to the plasma membrane and activates Rap by exchanging bound GDP for GTP[21, 22]. Epac has two main domains, a regulatory domain and a catalytic domain, each of which consists of a series of smaller functional units. The regulatory region contains the cAMP-binding domain (cNBD) and a Dishevelled, Egl-10, Pleckstrin (DEP) domain, which is involved in membrane localization. The catalytic domain consists of a Ras-exchange

motif (REM), a Ras-association (RA) domain and CDC25-homology domain (CDC25-HD). There are two Epac isoforms, Epac1 and Epac2: Epac1 has only one cNBD and is expressed in all tissues. Epac2, on the other hand, is expressed mainly in adrenal, pancreatic and neuronal tissues and has two cNBDs. cNBD1, located at the N-terminus of Epac2, exhibits a lower cAMP binding affinity (K_d=87μM) than cNBD2 (K_d =1.2 μM)[23]. Despite these differences, the DEP, REM, RA, and CDC25-HD domains are conversed between both Epac isoforms. Prior to cAMP binding, Epac exists in a closed conformation wherein the protein folds onto itself such that the regulatory and catalytic domains interact with one another. This conformation is held together by an ionic interaction ("ionic latch") between the CDC25-HD and the N-terminal helical bundle of the cNBD, along with a "hinge-region" located between the cNBD and the REM domain. This closed conformation prevents members of the Ras family of GTPases, such as Rap, from interacting with the catalytic domain. Upon cAMP binding to the cNBD, the ionic interaction is disrupted and the cNBD rotates away via the "hinge region" of the regulatory domain, creating an open conformation that exposes the CDC25-HD to GDP-bound Rap1[24-26].

Compared with PKA, Epac binds cAMP with much lower affinity. Furthermore, although Epac and PKA can act independently, given their common upstream regulation, there is often overlap between these two signaling pathways. Many cAMP-mediated effects that were previously thought to act through PKA alone may also be transduced by Epac. Extensive studies have established that Epac proteins are involved in a host of cAMP-related cellular functions such as cell adhesion, cell-cell junction, exocytosis/secretion, cell differentiation and proliferation, gene expression, apoptosis,

cardiac hypertrophy and phagocytosis[27-29].Therefore, there is a need to develop small molecules that can act as Epac- or PKA-specific inhibitors and activators[30-32]. In addition, due to the tissue and cell-type specificity of Epac, the role of Epac2 in diabetes-related diseases, hypertrophy, and Alzheimer's has generated considerable interest[33-35].

Spatiotemporal Compartmentalization of the cAMP/PKA Signaling Pathway

The cAMP signaling pathway controls a wide range of cellular processes in response to specific stimuli. However, as cAMP signaling became associated with more and more cellular functions, scientists found themselves at a loss to explain how PKA "knew" which targets to phosphorylate in response to which stimuli. In cardiac muscles, for example, it was thought that increases in cAMP would lead to overall activation of PKA, and the subsequent phosphorylation of phosphoryase kinase and glycogen synthase to stimulate glycogenolysis to facilitate cardiac contraction. However, it was shown that upon prostaglandin (PGE1) stimulation in rat hearts, these PKA substrates were inactive even though cAMP concentration increased[36]. Meanwhile isoproterenol, which causes similar effects as PGE1 in rat and guinea pig hearts, did lead to the activation of glycogen phosphorylase. Additional studies also revealed that cAMP, PKA, and PKA substrates were bound in varying amounts to particular sites within cardiac tissues[37]. Similarly, later studies also demonstrated that specific adenylyl cyclases, were activated by specific receptors. Altogether, these studies demonstrated how specific external stimuli could increase cAMP in specific intracellular spaces. Thus, despite some initial skepticism, the idea that cAMP signaling is dependent on subcellular compartmentalization emerged. Since these pioneering studies, various factors have been found to directly contribute to

the compartmentalization of cAMP/PKA signaling at level of the receptor, at the level of cAMP production and degradation, and at the effector level.

Receptors and Adenylyl cyclases

One critical factor in the spatiotemporal regulation of cAMP-mediated signaling is the dynamic cellular organization of adenylyl cyclase (AC) localization. Of the ten different AC isoforms in mammals, nine are classified as transmembrane ACs (tmACs). tmAC are localized throughout the plasma membrane, in close proximity to heterotrimeric G proteins that can regulate tmAC activity upon hormone and neurotransmitter binding to GPCRs. Within the plasma membrane, tmACs can be localized in various membrane subdomains to regulate their activity. For instance, tmACs tend to exist throughout the cell membrane, while in certain cell types the β_2-adrenergic receptor (β_2-AR), a $G_{\alpha s}$-coupled GPCR, is known to localize specifically to cholesterol-rich membrane rafts. This spatial restriction in the access of $G_{\alpha s}$ and tmAC to β_2-AR is a mechanism to properly regulate the level of cAMP production from β_2-AR. In addition, tmACs associate with different types of proteins that differentially regulate tmAC activity. For example, whereas the G_α isoform $G_{\alpha s}$ is a stimulator of cAMP production,, another class of G-proteins that consists of $G\alpha_i$ acts as an inhibitor of cAMP production. Acetylcholine is an example of a neurotransmitter that mediates cell signaling through binding to M_2 receptors and activation of $G\alpha_i$[38]. tmACs can also be expressed in different tissues to mediate different cellular processes and signaling events, depending on the localization and type of receptors. For example, AC1 is expressed in neurons and

therefore is involved in memory formation, while AC5 resides in the heart and contributes to cardiac function[39].

In contrast to the nine tmACs, the recently discovered AC10 is classified as a soluble AC (sAC) that is distributed throughout the cell, including in discrete compartments such as the nucleus, mitochondria, centrioles or cilia [40, 41]. The discrete localization of sAC to subcellular compartments allows it to regulate specific downstream targets of cAMP. Unlike tmACs, sACs are specifically activated by bicarbonate and Ca^{2+}, with the former allowing sAC to function as a general bicarbonate/CO_2 or pH sensor for metabolic reactions[42]. It has been found that sAC are highly expressed in sperm cells, consistent with the role of AC activity in sperm maturation, motility, capacitation, and in the acrosome reaction. Moreover, the bicarbonate concentration at which recombinant sAC is activated is well within the concentration range found in epididymal fluid[43].

Phosphodiesterases

While cAMP/PKA signaling can be regulated as early as the production of cAMP, it can also be regulated through the degradation of cAMP by phosphodiesterases (PDEs). PDEs are a group of enzymes that degrade cAMP to AMP by hydrolyzing the phosphodiester bond between the phosphate group and AMP. Given that cAMP can rapidly diffuse throughout the cell following its production by ACs, PDEs play a critical role in restricting the aberrant dispersion of cAMP and generating localized pools or gradients within the cell to target specific groups of effector molecules. The first hint of PDE-regulated cAMP microdomains came from studies in cardio myocytes by Hohl and Li in the early 1990s[44]. They found that the cytosolic and particulate pools of cAMP

responded differently to same cAMP-elevating reagents. Based on the presence of various types of PDEs expressed in cardiac tissue, they and other groups speculated that PDEs were responsible for generating this non-uniform intracellular distribution of cAMP. Since then, accumulating evidence has shown that PDEs are vital to compartmentalized cAMP/PKA signaling by controlling the localization, duration, and amplitude of cyclic nucleotide signaling within subcellular domains.

cAMP/PKA signaling is differentially regulated by various PDE isoforms. There are eleven families of PDEs which contain multiple isozymes with subcellular, cell type-, and tissue-specific distributions and effects. While the carboxy-terminal catalytic domain of each PDE is highly conserved, the amino-terminal regions of these proteins are highly diverse, being responsible for the unique regulation and targeting of individual PDEs to strategic subcellular sites[45]. The specific localization of PDEs confers their particular functions in regulating specific cAMP pools. For example, PDE3 has been shown to be important in the spatial compartmentalization of growth factor-stimulated PKA activity to the plasma membrane of PC12 cells[46]. In addition, PDE1C2 isoforms, which are highly localized in olfactory epithelium of the brain, are thought to play an important role in the rapid regulation of cAMP responses to odorants[47].

PDEs themselves can also be regulated by diverse biochemical mechanisms including phosphorylation/dephosphorylation. For instance, PDE3 can also be regulated via phosphorylation by PKA in response to hormonal stimulation in several cell types[48]. Phosphorylation enhances PDE3 activity and constitutes a negative feedback loop to ensure that cAMP levels are properly maintained.

While ACs release cAMP in a particular region in response to change in the extracellular environment, sequestered PDEs help sculpt localized cAMP gradients, by setting the 'gate' for activation of associated effector systems, as well as by protecting them from inappropriate activation by fluctuations in basal cAMP levels. The coordinated action of PDEs and ACs help finely tune the level and persistence of the cAMP/PKA signaling at that particular spatial locale to efficiently adjust specific physiological processes.

A-Kinase Anchoring Proteins (AKAPs)

Another critical component in the formation of localized cAMP-mediated signaling networks are A-kinase anchoring proteins (AKAPs), which act as scaffolding proteins to specifically tether PKA to dedicated PKA substrates such as GPCRs, tyrosine kinase receptors, and ion channels. In a sense, AKAPs help facilitate rapid, efficient, and enhanced signal transmission in local environments through substrate phosphorylation. Currently, more than 70 diverse AKAPs are known to be expressed in a cell- and organelle-specific fashion[49].

AKAPs interact with PKA through direct binding between amphipathic 14–18 amino-acid long α-helical region of the AKAP and the N-terminal docking/ dimerization (D/D) domain formed by the first forty-five amino acids of the R subunit[50]. The majority of AKAPs specifically interact with RII subunits; however, a handful of AKAPs that interact with the RI subunit have also been discovered. Some of these RI-interacting AKAPs are dual-specificity AKAPs such as ezrin, D-AKAP1, D-AKAP2, merlin, and AKAP220[51]. Generally in dual-specificity AKAPs, the affinity for RI subunits is lower

than that for RII subunits[51]. To date, known RI-specific AKAPs include, sphingosine kinase interacting protein (SKIP), which is found in heart tissue, and the RI-specific interaction is believed to be mediated by aromatic residues in the SKIP helix that are missing from both RII- and dual-specificity AKAPs, and integrins[52-54].

With unique targeting domains, AKAPs are able to sequester PKA to subcellular regions where PKA substrates are in close proximity for efficient modulation by PKA,. AKAPs are able to sequester PKA to subcellular regions where PKA substrates are in close proximity for efficient modulation by PKA, due to unique targeting domains within AKAPs. For example, members of the S-AKAP84/D-AKAP1 family contain a consensus sequence for targeting to the outer mitochondrial membrane. Similarly, AKAP15/18 is targeted to the plasma membrane through lipid modifications, namely, myristoylation and palmitoylation. mAKAP, a muscle-selective anchoring protein, was also shown to be targeted to the perinuclear location through a sequence region that contains spectrin-like repeats.

In addition to PKA, AKAPs can bind to key cAMP-regulating enzymes, namely, ACs and PDEs, to dictate the level and persistence of the cAMP signal and to subsequently regulate PKA activity at that particular spatial locale. Moreover, some AKAPs can bind additional signaling molecules such as protein kinases, phosphatases, GTPases and adaptor proteins so as to provide additional regulatory components and integrate different signaling pathways into these compartmentalized complexes. Disruption of these AKAP-mediated interactions can lead to aberrant PKA activity and therefore diseases such as cardiac hypertrophy and heart failure[55]. Hence, AKAPs help

add another layer of complexity by forming a network that synchronizes multi-protein signaling that is required for tightly regulating specific cellular processes.

Crosstalk between cAMP/PKA and other signaling pathways

As an added level of complexity in signal transduction regulation, many canonical signal transduction cascades are subject to crosstalk, wherein the signaling status of one pathway alters the state of another. For instance, as mentioned above, AKAPs facilitate crosstalk between the cAMP/PKA pathway and other signaling pathways through their interactions with various types of signaling molecules. This allows cells to tailor the cAMP signaling network to control specific cellular process. In particular, the cAMP/PKA pathway engages in extensive crosstalk with the calcium signaling pathway, as well as with other kinase signaling pathways, including the MAPK/ERK and PI3K/Akt signaling pathways.

Calcium Signaling

Calcium (Ca^{2+}) is another ubiquitous second messenger that is associated with multiple cellular processes, including neurotransmission, muscle contraction, gene expression, cell proliferation, and cell death. The versatility of calcium signaling in various specific biological processes is attributed to its ability to interact with a wide variety of molecules that modulate its concentration to create different spatial and temporal profiles.

The Ca^{2+} and cAMP pathways are very tightly regulated by mutual crosstalk, with each messenger able to regulate the levels of the other. For example, Ca^{2+} signals can modulate both the production and degradation of cAMP by regulating AC and PDE

activity in signaling hubs and microdomains. In general, AC1, AC3 and AC8 are each activated, whereas AC5 and AC6 are both inhibited, by physiological increases in Ca^{2+} concentrations. Ca^{2+} can also regulate ACs indirectly through PKC and Ca^{2+}/calmodulin protein kinase CaMKII, such as AC2, 4, and 7 [56]. ACs are also known to be recruited to microdomains in close proximity to Ca^{2+} channels such as ryanodine receptors (RyR), L-type Ca^{2+} channels and SERCA pumps through interactions with AKAPs. Similarly, PDE1 family members are positively regulated by the binding of Ca^{2+}/calmodulin to two N-terminal calmodulin-binding domains, which activates PDE1 by relieving autoinhibition. Conversely, PKA can modulate the release of Ca^{2+} from intracellular stores by phosphorylating and activating calcium transporters such as the IP_3R and RyR located on the ER surface. Furthermore, AKAP15 has been shown to be responsible for recruiting PKA to voltage-gated calcium channels (VGCCs) to regulate their activity. This crosstalk between Ca^{2+} and PKA provides a mechanism for achieving efficient and specific control of cellular processes such as exocytotic insulin release and cell migration[57, 58].

Crosstalk with other kinase signaling pathways

In general, PKA can crossregulate with a slew of kinases. One of the most well-studied signaling pathway interactions is between the PKA and MAPK/ERK pathways. MAPK cascades are typically initiated by the binding of growth factors to a receptor tyrosine kinase (RTK) on the cell surface. This binding event induces autophosphorylation of the RTK and promotes the recruitment and binding of adaptor proteins to the RTK. This ultimately activates a small GTPase which subsequently

activates the first of three kinases in the MAPK cascade. In the case of ERK signaling, the GTPase Ras or Rap1 activates the first kinase in the cascade, Raf, which phosphorylates and activates MEK1/2, which then phosphorylates and activates ERK1/2. Studies have shown that PKA can differentially regulate ERK through the Raf isoforms B-Raf or Raf1, which are activated and inhibited, respectively, by PKA. Therefore, depending on the expression levels of these Raf isoforms, PKA can either inhibit or activate ERK activity. Furthermore, while both Raf isoforms are activated by Ras, only B-Raf is activated by Rap1; thus, the effect of PKA on ERK activity is also dependent on the expression levels of Ras and Rap1.

The PKA and MAPK/ERK crosstalk has been shown to play a critical role in regulating cell fates. Traditionally in PC12 cells, a cell line derived from a pheochromocytoma of the rat adrenal medulla, ERK activity alone was thought to control the decision between differentiation and proliferation in these cells. Specifically, transient ERK activity induced by epidermal growth factor (EGF) binding to its cell surface receptor, the epidermal growth factor receptor (EGFR), induces proliferation, whereas sustained ERK activity induced by the binding of nerve growth factor (NGF) to TrkA causes cell differentiation[59]. As further evidence of the crosstalk between cAMP/PKA and ERK signaling, however, PKA and PDE3 were shown to regulate both the onset and duration of GF-stimulated ERK activity. When PDE3 was inhibited and the spatiotemporal regulation of PKA disrupted, PC12 cells treated with EGF displayed prolonged nuclear ERK activity. A separate study using HEK293 cells, also found that KSR-1, a scaffold for proteins involved in the MAPK signaling pathway, and AKAP-Lbc form the core of a larger ERK network that incorporates PKA and integrates signals from

cAMP [60]. With the recruitment of PKA to the MAPK signaling complex, PKA can phosphorylate KSR-1 to promote sustained ERK activity. AKAP-Lbc is responsible for recruiting PKA to this signaling complex by directly binding to three different Raf isoforms involved in the MAPK pathway[61]. As proper regulation of MAPK activity is involved in coordinating numerous cellular functions, including the regulation of cell growth and proliferation, the stress response, and apoptosis, an enhanced understanding of the spatiotemporal regulation of this pathway, including the cross-regulation by cAMP-mediated signaling, is necessary.

Similarly, recent studies have also implicated PKA-Akt crosstalk in regulating cell differentiation in other cell types such as ovarian granulosa cells[62]. Moreover, this PKA-Akt crosstalk was shown to be mediated by an AKAP, GAB2. However, there are far fewer examples of PKA-Akt crosstalk in the literature, and the mechanism and function behind this interaction remains unclear. The studies presented in Chapter 3 provide new insights into the regulation of Akt activity by cAMP/PKA signaling and vice versa.

Methods for studying signal transduction pathways

As eluded to above, signal transduction pathways are subject to spatial and temporal modulation through a variety of complex molecular mechanisms. Disrupting the spatiotemporal regulation of signal transduction affects numerous processes, such as differentiation and migration that are vital to the survival of cells and organisms. Dissecting the mechanisms that govern signal specificity and developing a comprehensive understanding of the functional roles of these regulatory molecules in

various dynamic processes depends on the ability to study signal transduction in the native context of living cells, tissues, or organisms, wherein these processes are maintained intact. Furthermore, with an increasing numbers of studies highlighting the heterogeneity of cells within a tissue, there is a growing emphasis on studying single-cell behaviors[63, 64]. However, traditional methods to study signal transduction in cells rely heavily on biochemical techniques, including immuno-based assays, which often involve cell fixation or lysis and are utilize cell populations, thus leading to the loss of critical spatial and temoral information. For instance, these population-based assays often fail to capture biologically relevant dynamics such as oscillatory signaling and bistability[65, 66], instead providing only static snapshots of signal transduction cascades. To alleviate many of these constraints, a number of tools have been developed to directly visualize and quantify specific signaling events with high spatial and temporal resolution within the native cellular context.

Visualization of signal transduction pathways

Genetically encoded reporters have existed for close to two decades and allow the tracking of signal transduction events in real time with high spatiotemporal resolution. Being genetically encodable, these fluorescent reporters can be non-destructively introduced into living systems in the form of plasmid DNA, taking advantage of the intracellular machinery to synthesize the functional biosensor. Fluorescent biosensors have been utilized to monitor pH, Ca^{2+} levels, membrane potential, post-translational modifications, second messenger accumulation/degradation, and enzyme activity[67-71]. Moreover, these biosensors can be targeted to specific cells or subcellular locations to

monitor local signaling dynamics[72-74]. The ongoing development of biosensors capable of detecting new target molecules will continue to lead to discoveries in cell signaling. Likewise, the development of novel sensors with enhanced sensitivity will enable the study of signal transduction in new settings[75].

The most diverse and versatile class of genetically encoded fluorescent biosensors are based on fluorescence resonance energy transfer (FRET), which involves the nonradiative transfer of energy from an excited donor fluorophore to an acceptor fluorophore. Efficient energy transfer requires the two fluorophones to be close together (e.g., less than 10 nm apart) and to exhibit sufficient overlap between the donor emission spectrum and the acceptor excitation spectrum. FRET-based reporters are engineered to undergo a conformational change in response to a given biochemical event, such as phosphorylation, second messenger binding, or protein-protein interaction, which alters the distance and orientation between the two fluorophores. The module that undergoes conformational changes is known as the molecular switch. Therefore the readout for change in a signaling event is the change in FRET. Most commonly in FRET-based reporters, the two FPs are cyan fluorescent protein (CFP), which acts as the donor, and yellow fluorescent protein (YFP), which acts as the acceptor.

Kinase activity reporters

Kinase-activity reporters (KARs) are a class of FRET-based biosensors that report on the dynamics of phosphorylation mediated by kinases. The general design of FRET-based KARs consists of four components: the FRET donor (e.g., CFP), a kinase-specific substrate domain, a phosphoamino acid binding domain (PAABD), and a FRET acceptor

(e.g., YFP). Phosphorylation of the substrate domain induces the binding of the PAABD to the phosphopeptide, thus causing a conformational change that alters the distance and/or orientation between the FPs to produce a change in FRET. Following attenuation of signaling, for example, by internalization of the receptor or removal of the stimulus, phosphatases dephosphorylate the substrate domain, reversing the FRET change[76]. This general design has been applied to develop biosensors for a variety of kinases, including PKA, PKC, Akt/PKB, MAPKs, AMP-activated protein kinase (AMPK), and Proto-oncogene tyrosine-protein kinase (Src). Furthermore, the modular design of KARs has enabled the creation of many new reporters through the substitution of one kinase-specific substrate and/or PAABD for another (Fig. 1.2A).

An alternative strategy to designing kinase activity reporters is utilizing a naturally existing conformationally responsive element as the molecular switch. For example, TORCAR, a FRET-based mTORC1 activity biosensor, utilizes full-length 4EBP1 (elF4E binding protein 1) as the molecular switch. Upon phosphorylation of 4EBP1, a conformational change is induced leading to a change in FRET. In this case, this design strategy worked better than the molecular switch that consists of a short peptides substrate and PAABD[77]. Therefore, for TORCAR, the mTOR1 activity is detected as a decrease in FRET response. Depending on the type of conformational change that takes place, the FRET response can either increase or decrease upon kinase activation.

Second messenger biosensors

Second messengers can take the form of small molecules, lipids, or ions, that relay signals received at receptors on the cell surface and amplify a physiological signal

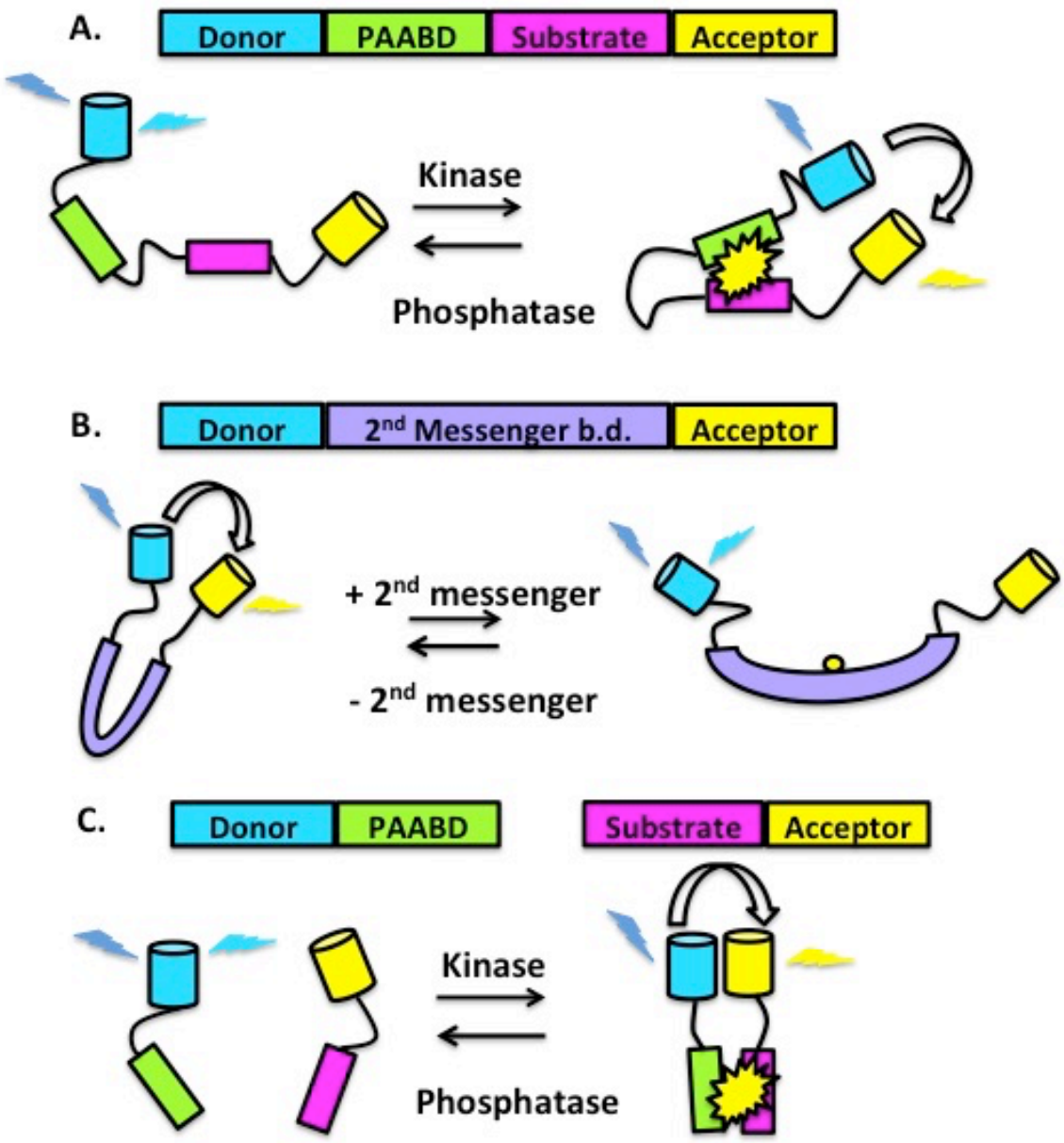

Figure 1.2: Genetically encoded FRET-based biosensors
(A) General design of a KAR that increases in FRET in response to endogenous kinase activation. (B) General design of a FRET-based second messenger biosensor that decreases in FRET upon second messenger accumulation. (C) General design of BimKARs

by regulating kinase activity. Well-studied second messengers include cyclic nucleotide monophosphates (cAMP and cGMP), diacylglycerol (DAG), phophstidylinositol 2,4,5-triphosphate (PIP_3), and Ca^{2+}. Changes in second messenger concentrations are tightly regulated both spatially and temporally under physiological conditions, and this regulation is coupled to spatiotemporal control of its effector proteins. Currently, there are many FRET-based biosensors for detecting second messenger dynamics, including cAMP, Ca^{2+}, cGMP, DAG, phosphoinositides, and nitric oxide[78-81]. As with KARs, second messenger biosensors contain molecular switches that often are the second messenger effector proteins because they undergo conformational change upon second messenger binding. For example, the FRET-based cAMP biosensor, *i*ndicator of *c*AMP *u*sing *E*pac (ICUE), consists of Epac1 as the sensing domain, sandwiched between two fluorescent proteins, CFP and YFP. Prior to cAMP, Epac1 exists in a closed conformation, causing the FP to be in close proximity with one another. In presence of cAMP, Epac1 undergoes a conformational change that pulls the two FP apart. Therefore, upon increase in cAMP, the readout is a decrease in FRET (Fig. 1.2B).

Development and improvement of genetically encoded biosensors

The design and use of genetically encoded FRET-based biosensors has rapidly expanded our molecular understanding of numerous signaling pathways in a variety of biological systems. KARs are invaluable tools for studying kinase activity dynamics, but their utility may be restricted by a limited dynamic range, which can hinder the detection of minute yet physiologically relevant changes in kinase activity or for use in high-throughput compound screens. Most traditional KARs are based on a unimolecular design. However, the relatively small separation of the FPs in the basal state may restrict

the maximum possible FRET change that can be achieved. Therefore, efforts to further improve the responses of kinase biosensors led to the generation of bimolecular KARs (bimKARs) that utilize a kinase-inducible bimolecular switch[75, 82]. BimKARs contain the same components as unimolecular KARs; however, the substrate and PAABD are encoded by two separate polypeptides (Fig. 1.2C). One potential advantage of this design stems from its tendency to exhibit an increased dynamic range compared to unimolecular KARs. This effect is frequently attributed to greater separation of the FPs in the off state.

Similarly, biosensors that use bioluminescent proteins (BPs) in place of FPs have been developed to detect small changes in both a low- and high-throughput fashion in a number of different contexts, such as in cell lysates, in single cells and in living animals. Bioluminescence is the emission of light by living organisms, mainly marine vertebrates and invertebrates, caused by an enzymatic reaction. One class of BPs, commonly referred to as luciferases, catalyzes the oxidation of specific substrates known as luciferins to form oxyluciferin, along with the concurrent emission of a photon. Many variants of luciferase have been described and are characterized by differences in their substrates, the required cofactors, the specific wavelength emitted, and the kinetics of emission. However, the luciferases most commonly used in the laboratory are derived from the firefly *Photinus pyralis* (FLuc) and the sea pansy *Renilla reniformis* (RLuc). Free from the need for exogenous illumination, bioluminescence-based assays are not subject to interference from autofluorescence[83-85]. Therefore, luciferases have been exploited and incorporated in biosensors that function similarly to FRET-based reporters. Similar to FRET, when a luciferase is located in close proximity and with the proper orientation to a fluorophore with appropriate spectral overlap, the luminescence generated by luciferase is used to

excite the acceptor fluorophore in a phenomenon known as bioluminescence resonance energy transfer (BRET). A number of biosensors have been designed that utilize BRET to detect various signaling processes, including GPCR and β-arrestin interactions, PKA activation, and Ca^{2+} and cAMP dynamics[86-88]. The continued development of bioluminescence-based assays, which can capture the spatiotemporal patterns of signaling events, will expand the molecular toolkit for detecting signaling dynamics and facilitate the study of signal transduction in a greater number of settings such as imaging in tissue and animal models or high-throughput drug screens.

Significance

Throughout this chapter, it has been stressed that the spatiotemporal regulation of signaling pathways is important for the proper propagation of specific cellular processes. Accumulating evidence has shown that dysregulation of signal transduction pathways can lead to some of the most common diseases. In order to tease out the molecular mechanisms underlying specificity in signal transduction, applying tools that can capture these dynamic events in their native context is necessary. FRET-based reporters have become extremely useful tools in detecting various signaling molecules with high spatiotemporal resolution, and elucidating new regulatory mechanisms. With this molecular understanding, new approaches can be taken in developing new therapeutic strategies for treating diseases such as diabetes, cancer, hypertension and neurological disorders. The first part of the work described herein focuses on the role of compartmentalized PKA activity in integrating crosstalk with other signaling pathways to regulate specific cell processes. We first elucidate a novel molecular mechanism that governs efficient cell migration in confined environment that involves the intricate

regulation of PKA activity by both calcium and myosin II signaling pathways. Then, we investigate the crosstalk between PKA and Akt at the plasma membrane of PC12 cells to decipher how cells regulate the decision to undergo proliferation or differentiation. The second portion then describes our efforts to improve genetically encoded biosensors for use in drug-screening applications to search for small molecule kinase inhibitors that can be utilized to develop new treatments for the diseases mentioned above. Along these same lines, the third part of the work details the generation of a more sensitive FRET-based cAMP probe (ICUE4) to detect small but dynamic changes in cAMP concentrations.

Chapter 2

Confinement-sensing and signal optimization mediated by PKA and myosin II

INTRODUCTION

Cells optimize their migratory potential by altering migration modes as they encounter different physical microenvironments [89-91]. Cells migrating in a mesenchymal mode share the typical hallmarks of two-dimensional (2D) planar migration, including actin-based membrane protrusion, integrin-dependent adhesion and myosin II-mediated retraction. Alternatively, cells can migrate in an amoeboid mode and squeeze through narrow channel-like tracks formed between collagen bundles [89] or crawl along linear collagen fibers [92]. To cope with the physical confinement imposed by these channel- and fiber-like tracks, cells adopt mechanisms distinct from those used for locomotion on unconfined 2D substratum [89, 90, 93, 94].

Using microfabricated devices and substrate-printing methods that mimic earmarks of the channel- and fiber-like tracks encountered *in vivo*, researchers have identified several key mechanisms that are crucial for cell motility under confinement [95-98]. One of the mechanisms involves the RhoA/myosin II signaling axis [90, 94, 96]. In contrast to Rac1-dependent migration of many cell types on unconfined 2D surfaces, confined migration does not require Rac1-mediated protrusive activities, but instead depends on myosin II-driven contractility [90, 94]. The contractile forces generated by an actomyosin network propel cell locomotion under physical confinement via several strategies [93, 99, 100]. For efficient migration, cells tune the signaling input in different ways to achieve a balance between Rac1 and RhoA/myosin II, which leads to a strong Rac1 output by unconfined cells and a strong myosin II output by confined cells [94]. One unresolved question is how cells differentially regulate Rac1 and RhoA/myosin II in response to different degrees of confinement. Another important unresolved question is what the

underlying mechanosensing mechanism is that allows the cells to respond to physical confinement.

Using an α4 integrin-expressing CHO cell model (referred to as CHO-α4WT cells) that recapitulates aspects of the motile activities of invasive melanoma cells, we have reported that CHO-α4WT cells respond to physical confinement by tuning Rac1 and RhoA/myosin II activities to optimize cell motility [94]. Intriguingly, the Rac1 activity in CHO-α4WT cells is tightly regulated by cAMP-dependent protein kinase A (PKA), which phosphorylates the α4 integrin cytoplasmic tail [101]. PKA, a regulator of a wide array of physiological functions [102], is also known to play an important role in the migration of carcinoma cells and in the regulation of RhoA and Rac1 functions in several cooperative pathways [103], These studies, however, have largely focused on cell migration on unconfined 2D surfaces. Little is known about how PKA modulates cell migration through physically confined spaces.

To investigate the role of PKA in confinement-induced mechanosensing and signaling optimization, we employed well-established Förster resonance energy transfer (FRET)-based PKA activity reporters in conjunction with microfabrication and substrate printing technologies to explore the real-time modulation of PKA activity and its interaction with relevant signaling networks in response to physical confinement. We also examined changes in cell mechanics in response to confinement using atomic force microscopy. We demonstrate that efficient cell migration in confined spaces is achieved by negative feedback interactions between Ca^{2+}/phosphodiesterase 1 (PDE1)/PKA and myosin/Rac1 signaling modules. We also provide evidence for PKA- and myosin II-mediated confinement-sensing mechanisms. These findings provide a novel mechanism

by which cells adapt to different degrees of physical confinement, and optimize their motile activities.

RESULTS

Physical confinement suppresses the phosphorylation levels of α4 integrin in CHO-α4WT cells.

We have reported that α4β1 integrin, ectopically expressed on CHO cells (CHO-α4WT), promotes cell migration through both unconfined and confined microenvironments. This is achieved by an optimized signaling output that favors Rac1 activation in unconfined cells versus myosin II-driven contractility in confined cells. Because phosphorylation of α4 integrin at Ser988 enhances Rac activity [101, 104], we hypothesize that physical confinement negatively regulates α4Ser988 phosphorylation. To test this hypothesis, we monitored the extent of α4Ser988 phosphorylation as a function of the degree of physical confinement, using a microchannel assay. In this assay, CHO-a4WT cells (stably expressing GFP-tagged α4 integrin) were induced to migrate toward a chemoattractant source through fibronectin-coated channels of fixed height (10 μm) and length (200 μm) but with different widths (20 μm, 10 μm, 6 μm, and 3 μm) (Fig. 2.1A). After having migrated into the channels or on an unconfined 2D surface, the cells were fixed, stained with an antibody specific for phosphorylated α4Ser988 (referred to as phospho-α4Ser988), and imaged by confocal microcopy. CHO-α4WT cells migrating on a 2D surface or inside 20 μm-wide channels displayed strong phospho-Ser988 staining. However, the level of α4Ser988 phosphorylation gradually diminished

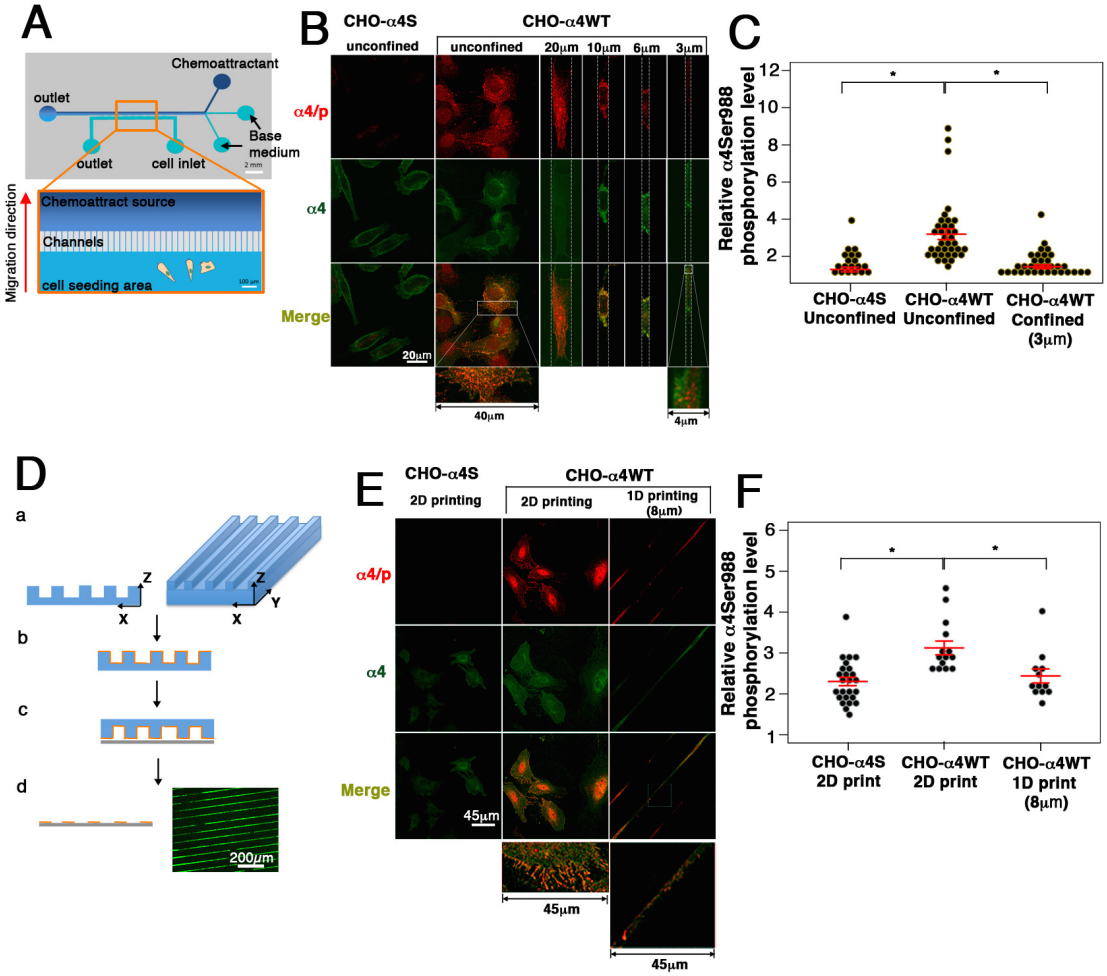

Figure 2.1 Effects of physical confinement on α4 phosphorylation.
(A) Schematic of the microchannel device bounded to glass slide. Also shown below is a close-up detail of channel array. Channels of 50-μm, 20-μm, 10-μm, 6-μm, and 3-μm in width were used in the study. The red arrow (left to the close-up channel array) indicates the direction of migration. (B) CHO-α4WT and CHO-α4S988A cells were seeded in cell seeding area (indicated as unconfined) and then induced to migrate through 20-μm, 10-μm, 6-μm, or 3-μm fibronectin-coated channels. Cells expressing GFP-α4 integrins were stained with phosphorylated α4 (red) and imaged by dual color confocal microcopy. (C) For each designated condition, overall level of α4 phosphorylation is quantified by measuring α4 phosphorylation red fluorescence intensity normalized by GFP-tagged α4 integrin. (D) Schematic representation of microcontact printing. (a and b) PDMS stamp (blue) was coated with fibronectin (orange) to be printed. (c) Fibronectin was transferred by printing onto cover slide (gray) and then examined by fluorescence staining (d). (E) CHO-α4WT and CHO-α4S988A cells placed on either 2D or 1D fibronectin printed cover slide were stained with phosphorylated α4 and imaged by confocal microcopy (F) The overall α4 phosphorylation level was quantified by measuring α4 phosphorylation red fluorescence intensity normalized by GFP-tagged α4 integrin. Data represent means ± SEM. *, $P < 0.05$.

with increasing the degree of confinement and reached nearly background levels in 3 μm-wide channels. As a control, little or no staining was detected when α4 integrin was mutated, substituting Ser988 with alanine (the cells are referred to as CHO-α4S988A, also tagged with GFP) (Fig. 2.1B, 1C). In addition to reduced overall phospho-α4Ser988 levels, the spatial staining pattern of phospho-α4Ser988 was also altered, and became bipolar as the channel width decreased from 20 μm to 10 μm or less (Fig. 2.1B).

Cells utilize myosin IIA to promote efficient migration on 1D printed lines[98]. This mechanism shares similarities with migration inside narrow microchannels[94]. Thus, we examined the change of α4Ser988 phosphorylation levels in response to lateral confinement resulting from adhesion/spreading constraints, by generating 1D 8μm-wide fibronectin-printed lines where cells were allowed to attach and assume an elongated morphology (Fig. 2.1D, E). Similar observations with respect to α4Ser988 phosphorylation were noted between cells on 1D printed lines and inside narrow channels. Specifically, CHO-α4WT cells on 1D fibronectin-coated lines exhibited significantly lower α4Ser988 phosphorylation levels than cells on 2D fibronectin-coated surface (Fig. 2.1E, F). These data reveal that physical confinement down-regulates α4Ser988 phosphorylation in CHO-α4WT cells. Taken together, the cells are capable of modulating their α4Ser988 phosphorylation levels in response to confinement.

Differential modulation of PKA activity is required for optimized migration of CHO-α4WT cells through unconfined versus confined spaces

α4Ser988 is phosphorylated by PKA[101]. Because confinement alters α4Ser988 phosphorylation levels in CHO-α4WT cells, we hypothesize that PKA activity is

differentially regulated in unconfined versus confined cells in order to optimize their migration in distinct microenvironments. As a first step, we examined the effects of a PKA inducer, forskolin, and a PKA inhibitor, Rp-cAMPs, on cell migration as a function of the degree of physical confinement, using our microchannel assay. CHO-α4WT cells treated with forskolin (50 μM) migrated as efficiently as vehicle controls in wide (50 or 20 μm) channels, but displayed a markedly reduced velocity in narrow (10, 6 or 3 μm) channels. In contrast to forskolin, PKA inhibition using Rp-cAMPs (50μM) had the opposite effect. Cells migrated efficiently in narrow channels but with significantly lower velocity relative to vehicle control in wide channel (Fig. 2.2A, B). Because α4Ser988 phosphorylation is suppressed in CHO-α4WT cells when confined in narrow channels or on narrow 1D printed lines, we next tested the effects of PKA modulation on CHO-α4WT cells migrating on 8 μm-wide fibronectin-coated lines compared to those on 2D fibronectin-coated surfaces. In accord with our microchannel data, induction of PKA activity using forskolin (50 μM) suppressed both the velocity and instantaneous speed in cells migrating on 1D fibronectin-printed lines. In contrast, inhibition of PKA activity using Rp-cAMP enhanced 1D cell migration (Fig. 2.2C-E). Using forskolin and Rp-cAMP, we also demonstrate that PKA activity inhibits myosin II-dependent assembly of stress fibers and focal adhesion density but enhances Rac1-dependent cell spreading in both CHO-α4WT and parental CHO cells (Fig. 2.3). Taken together, low PKA activity is required for optimal migration of CHO-α4WT cells in confined spaces, whereas high PKA activity is necessary for efficient cell migration in unconfined microenvironments. We propose that the cells are capable of tuning the level of PKA activity in response to different degree of physical confinement.

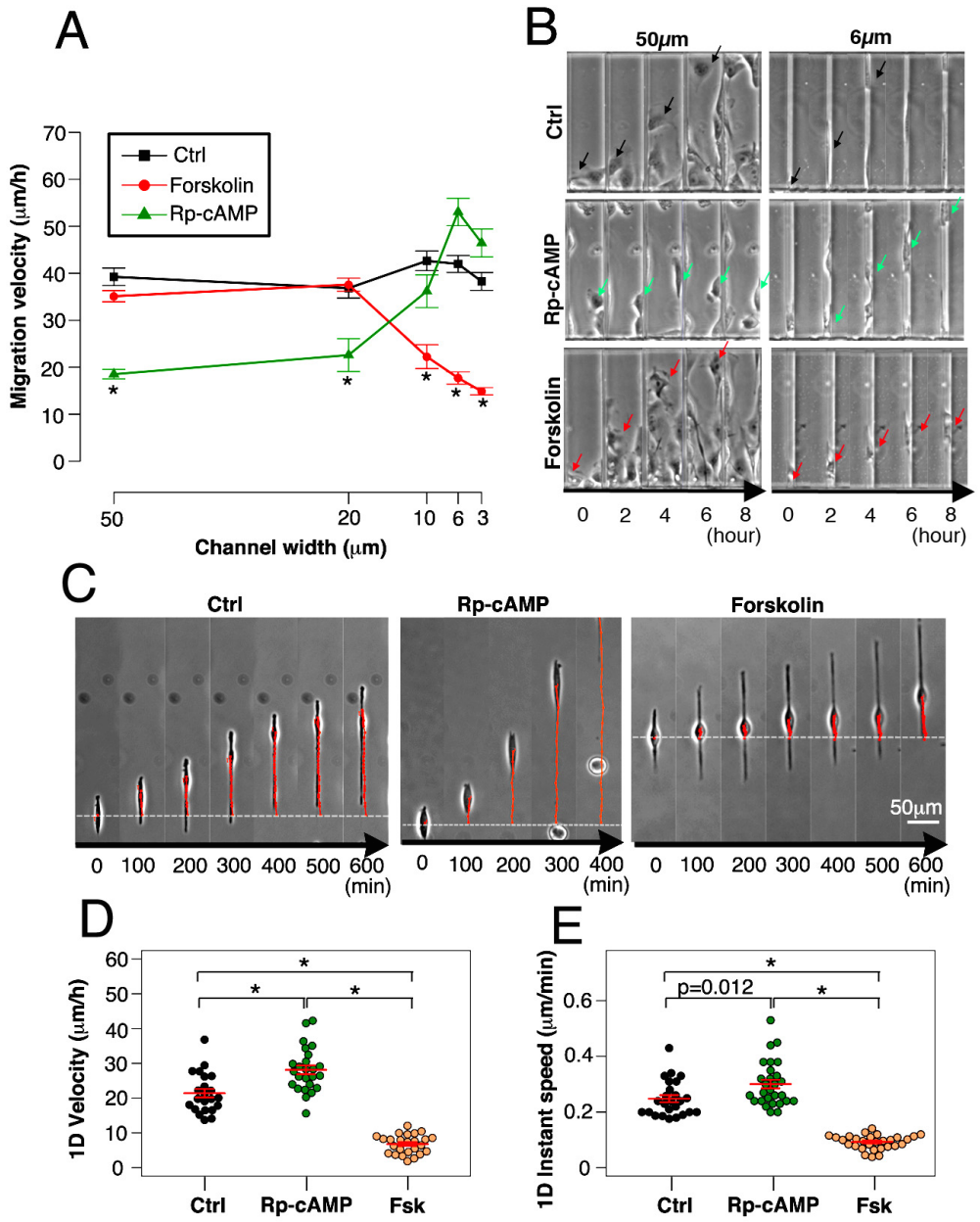

Figure 2.2 Effects of inhibiting or enhancing PKA activity on confined migration and 1D migration of CHO-α4WT cells.
CHO-α4WT cells were treated with either PKA enhancer forskolin, PKA inhibitor Rp-cAMPs, or vehicle control and allowed to migrate inside of fibronectin-coated channel (A and B) or on fibronectin printed 8μm wide 1D pattern (C, D, and E). Their migration velocities (A and D) and instantaneous speed (E) were quantified. The time-lapse images of migrating cells in designated channel widths (B) and 1D pattern (C) are shown. Data represent means ± SEM. *, $P < 0.005$.

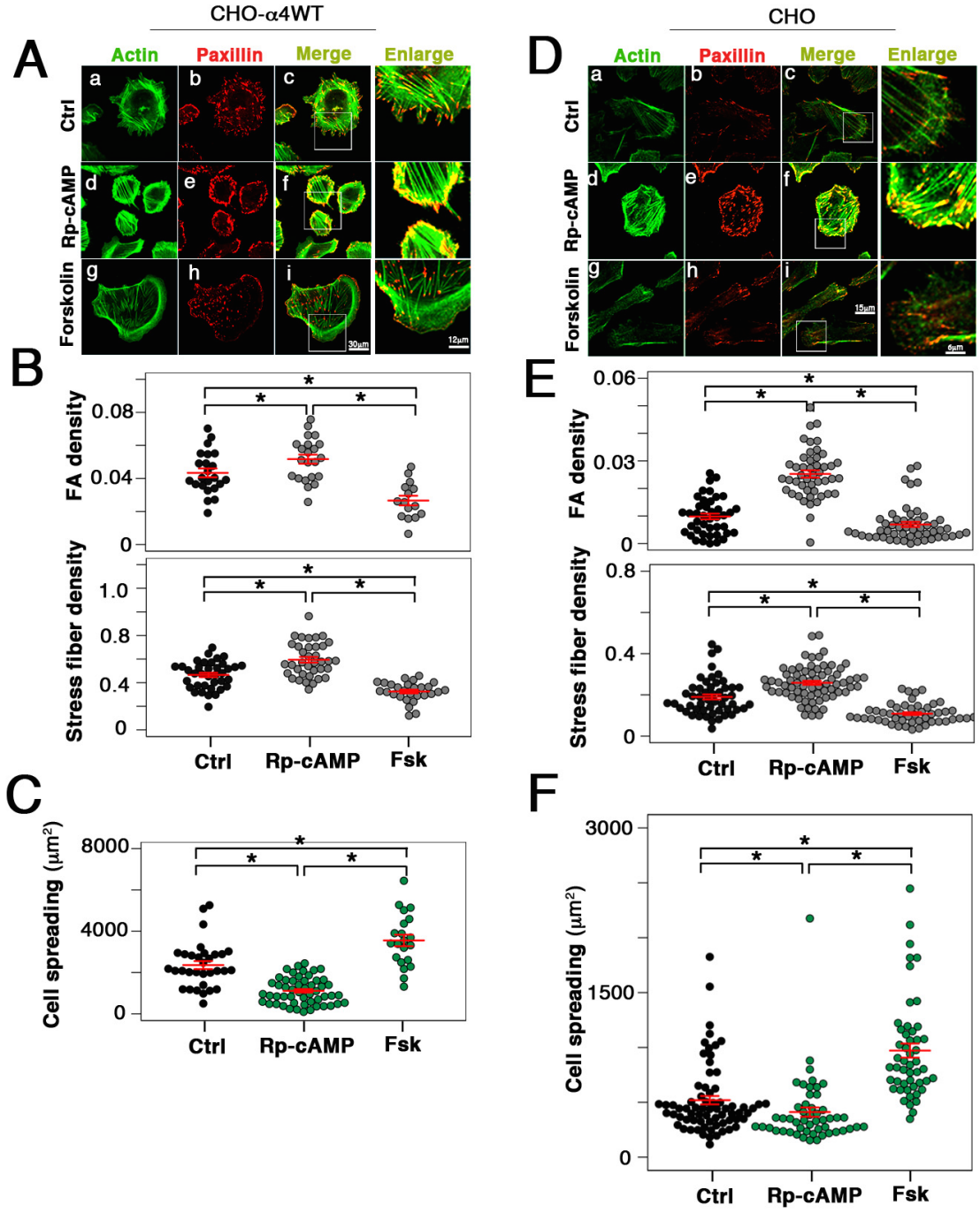
CHO-α4WT
CHO
A
D
Actin
Paxillin
Merge
Enlarge
Ctrl
Rp-cAMP
Forskolin
B
E
FA density
Stress fiber density
C
F
Cell spreading (μm²)
Ctrl
Rp-cAMP
Fsk

Figure 2.3 Effects of modulation of PKA activity on focal adhesion and stress fiber densities and spreading of CHO-α4WT and CHO cells. CHO-α4WT or CHO cells were plated on fibronectin-coated coverslips in presence of vehicle control, the PKA inhibitor Rp-cAMPs, or the PKA inducer forskolin. (A and D) Cells stained with phalloidin (green) and with an antibody specific for paxillin (red) were imaged by confocal microcopy. To evaluate myosin II activity, focal adhesion densities were quantified as the ratio of the total area of focal adhesions to the cell spreading area. Stress fiber densities were also quantified as the ratio of the total area of stress fibers to the cell spreading area (B and E). Cell spreading (C and F) was also quantified by image processing. Data represent mean±SEM. *, $P < 0.05$.

Physical confinement suppresses PKA activity

To test the hypothesis that PKA activity is differentially regulated in unconfined versus confined spaces, we utilized a FRET-based PKA activity biosensor (AKAR4) to measure PKA activity levels in unconfined and confined CHO-α4WT cells. PKA activity is detect as an increase in FRET ratio (yellow-to-cyan emission upon CFP excitation) due to PKA phosphorylation0induced conformational change of the sensor. To assess plasma membrane-localized PKA activity we used a plasma membrane-targeted version of AKAR4, AKAR4-Kras[72] (Fig. 2.4A). AKAR4-Kras was transiently transfected into CHO-α4WT cells, and the initial FRET ratio (yellow-to-cyan emission ratio) prior to drug treatments was obtained to quantify the basal levels of plasma-membrane PKA activity (referred to as PKA activity hereafter). Unconfined cells exhibited higher initial FRET ratio compared to confined cells (Fig. 2.4B, E), indicating that confined cells had lower basal PKA activity than unconfined cells. As a control, we showed that the FRET ratio did not significantly correlate with transfection efficiency (Fig. 2.4F). To substantiate the reduction of PKA activity observed in confined cells, we quantified the effects of the PKA inhibitor H89 (10 μM) in unconfined and confined CHO-α4WT cells. A smaller reduction of FRET ratio is indicative of a lower basal PKA activity. Indeed, after 30 min of cell treatment with H89, unconfined cells exhibited a pronounced reduction (20.6±4.2%) in FRET ratio whereas only a modest decrease (7.0±1.2%) was detected in confined cells (Fig. 2.4B-C). Taken together, these data indicate that confined CHO-α4WT cells possess lower basal PKA activity levels than unconfined cells. Along these lines, a decrease in PKA activity levels is observed as cells

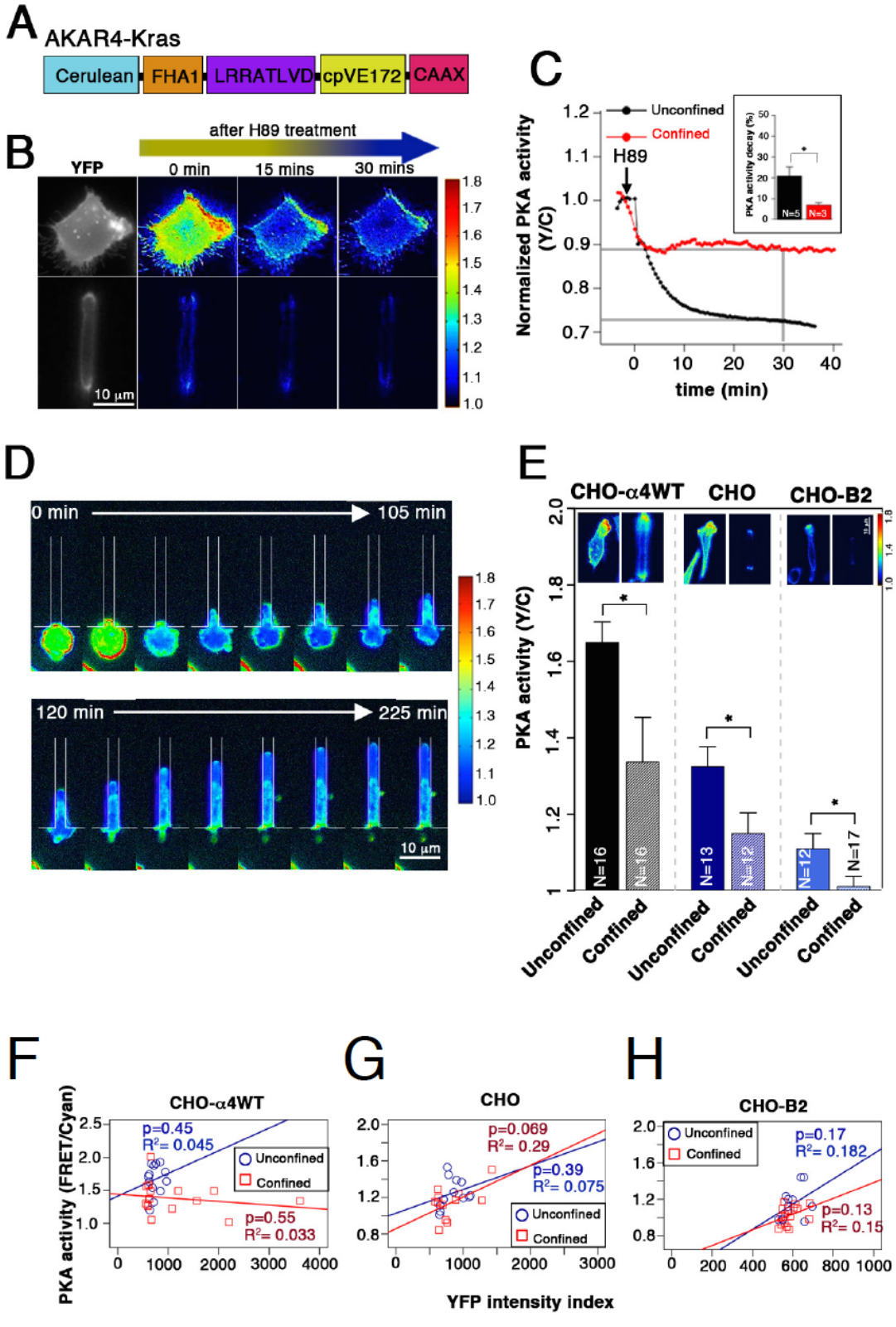
A
AKAR4-Kras
Cerulean
FHA1
LRRATLVD
cpVE172
CAAX
B
after H89 treatment
YFP
0 min
15 mins
30 mins
10 μm
C
Unconfined
Confined
H89
Normalized PKA activity (Y/C)
time (min)
PKA activity decay (%)
N=5
N=3
D
0 min
105 min
120 min
225 min
10 μm
E
CHO-α4WT
CHO
CHO-B2
PKA activity (Y/C)
N=16
N=16
N=13
N=12
N=17
Unconfined
Confined
F
CHO-α4WT
PKA activity (FRET/Cyan)
p=0.45
R²= 0.045
p=0.55
R²= 0.033
G
CHO
p=0.069
R²= 0.29
p=0.39
R²= 0.075
YFP intensity index
H
CHO-B2
p=0.17
R²= 0.182
p=0.13
R²= 0.15

Figure 2.4 Confinement suppresses PKA activity.
(A) Schematic diagram of AKAR4-Kras biosensor. The biosensor is composed of a substrate peptide, cpVE172 and the phosphoamino-binding domain (FHA1), each tagged with a fluorescent protein, and the membrane targeting motif CAAX. (B) CHO-α4WT cells expressing AKAR4-Kras were plated on unconfined spaces or induced to migrate into 3μm channel to experience confinement. YFP and FRET ratiometric images of confined and unconfined cells before the PKA inhibitor H89 was added (0 min) and at 15 and 30 min after the addition. (C) Representative curves of normalized PKA activity of CHO-α4WT cells in confined or unconfined microchannels after addition of H89. Bar graph represents the percentage of decay of PKA activity at 30 min after addition of H89. (D) Time-lapse FRET ratiometric images of a CHO-α4WT cell expressing AKAR4-KRAS, as the cell is migrating from an unconfined area into a 3μm channel. (E) The basal PKA activities of confined and unconfined CHO-α4WT, CHO, and CHO-B2 cells. The basal PKA activities (Y/C) of CHO-α4WT (F), CHO (G), and CHO-B2 (H) cells were plotted against YFP intensity index, which represents the transfection efficiency of AKAR4-Kras. Linear regression was performed to evaluate the correlation of PKA activity and YFP intensity index in confined and unconfined cells. P-value and R-squared values are indicated. Data in the bar graphs in C and E represent the mean±SEM. *, $p<0.05$.

transition from an unconfined two-dimensional surface to a narrow (3 μm in width) channel (Fig. 2.4D).

We have previously shown that an invasive melanoma cell line, A375-SM, responds to confinement in a similar manner as CHO-α4WT cells [94]. Both cell types optimize cell motility by modulating Rac1 and myosin II in unconfined and confined spaces [94]. Along these lines, we found that A375-SM cells tune PKA activity similarly to CHO-α4WT cells for efficient migration in unconfined and confined spaces (Fig. 2.5).

α4 and α5 integrins have been reported to play important roles in the spatiotemporal regulation of PKA in order to stimulate CHO cell migration on 2D substrates[105]. We thus investigated if the reduced PKA activity in confinement is mediated by α4 and/or α5 integrins. To this end, we quantified the basal PKA activity levels in three cell lines: CHO-α4WT that expresses both α4 and α5 integrins, parental CHO that only expresses α5 integrin and CHO-B2 that lacks α4 and α5 integrins[106, 107]. Interestingly, physical confinement significantly suppresses PKA activity in all three cell lines (Fig. 2.4E), suggesting that α4 and α5 integrins are not required for the differential levels of PKA activity in unconfined versus confined cells. As a control again, we also showed that the FRET ratio did not significantly correlate with transfection efficiency (Fig. 2.4G-H). However, it is noteworthy that the expression of α4 and α5 integrins elevates the basal levels of PKA activity in both unconfined and confined cells. Collectively, these results indicate that although α4 and α5 integrins enhance the overall PKA activity, they are not required for the cells to sense and respond to physical confinement.

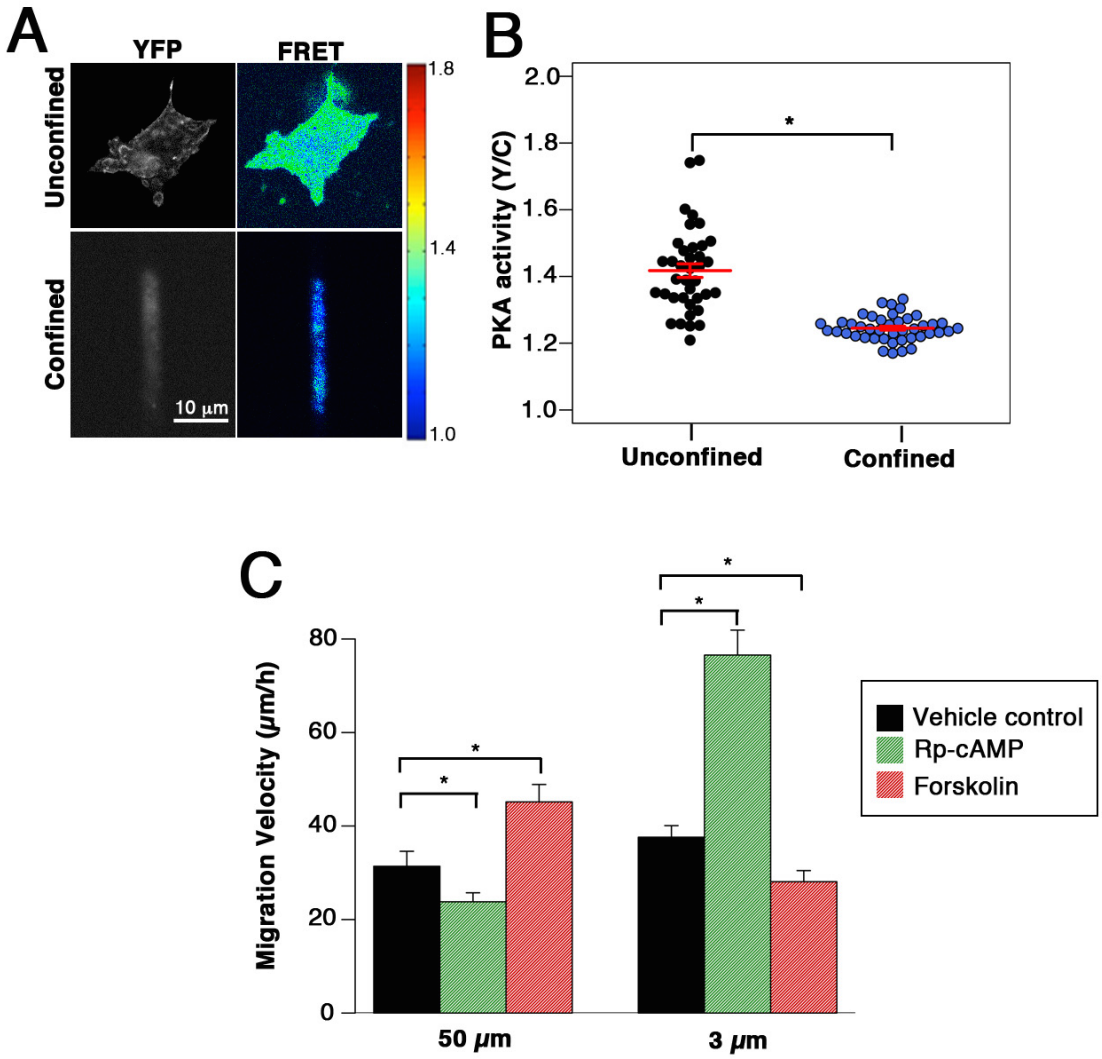

Figure 2.5 Effects of confinement on PKA-modulated migration of A375-SM melanoma cells. (A) YFP and FRET ratiometric images of confined and unconfined A375-SM melanoma cells expressing AKAR4-Kras. (B) Integrated dot/box plot comparing the basal PKA activities of unconfined and unconfined A375-SM cells. (C) A375-SM cells were treated with either the PKA inhibitor Rp-cAMP or the PKA inducer forskolin or appropriate vehicle control, and induced to migrate inside fibronectin-coated microchannels of 50µm or 3µm in width. Data represent the mean±SEM. *, $p<0.05$.

Elevated intracellular calcium in confined cells negatively regulates PKA via PDE1

In light of prior work showing the role of calcium in cell migration, and the presence of negative crosstalk between calcium and PKA[58], we hypothesize that the changes in PKA activity induced by physical confinement are regulated via Ca^{2+}-dependent signaling mechanisms. To test this, we used a FRET-based Ca^{2+} indicator, Yellow Cameleon 3.6 (YC 3.6) to monitor intracellular Ca^{2+} levels in both unconfined and confined CHO-α4WT cells (Fig. 2.6A)[108]. Upon Ca^{2+}binding, the CaM-M13 molecular switch undergoes a conformational change, thereby resulting in a FRET ratio increase. Confined compared to unconfined CHO-α4WT cells exhibited lower basal Ca^{2+} levels (Fig. 2.6, C). To investigate the potential source of higher basal Ca^{2+} levels in confined cells, we treated CHO-α4WT with the stretch-activated cation channel inhibitor GsMTx4 [109]. This treatment suppressed the Ca^{2+} levels in confined cells down to those of unconfined cells (Fig. 2.6C). Moreover, GsMTx4 failed to alter the Ca^{2+} levels in unconfined cells (Fig. 2.6C). Taken together, these data suggest that physical confinement elevates intracellular Ca^{2+} via stretch-activated ion channels.

To directly assess the effect of Ca^{2+} on PKA, we measured PKA activity in CHO-α4WT cells transfected with AKAR4-Kras in the presence or absence of the Ca^{2+} chelator BAPTA-AM (40 μM). An increase in PKA activity was detected in confined cells following BAPTA treatment (Fig. 2.6D). This response is attributed to the higher intracellular calcium levels in resting confined cells, which greatly suppresses PKA activity. On the other hand, no significant change was noted in unconfined cells under BAPTA treatment (Fig. 2.6D), which is consistent with the unconfined cells having low

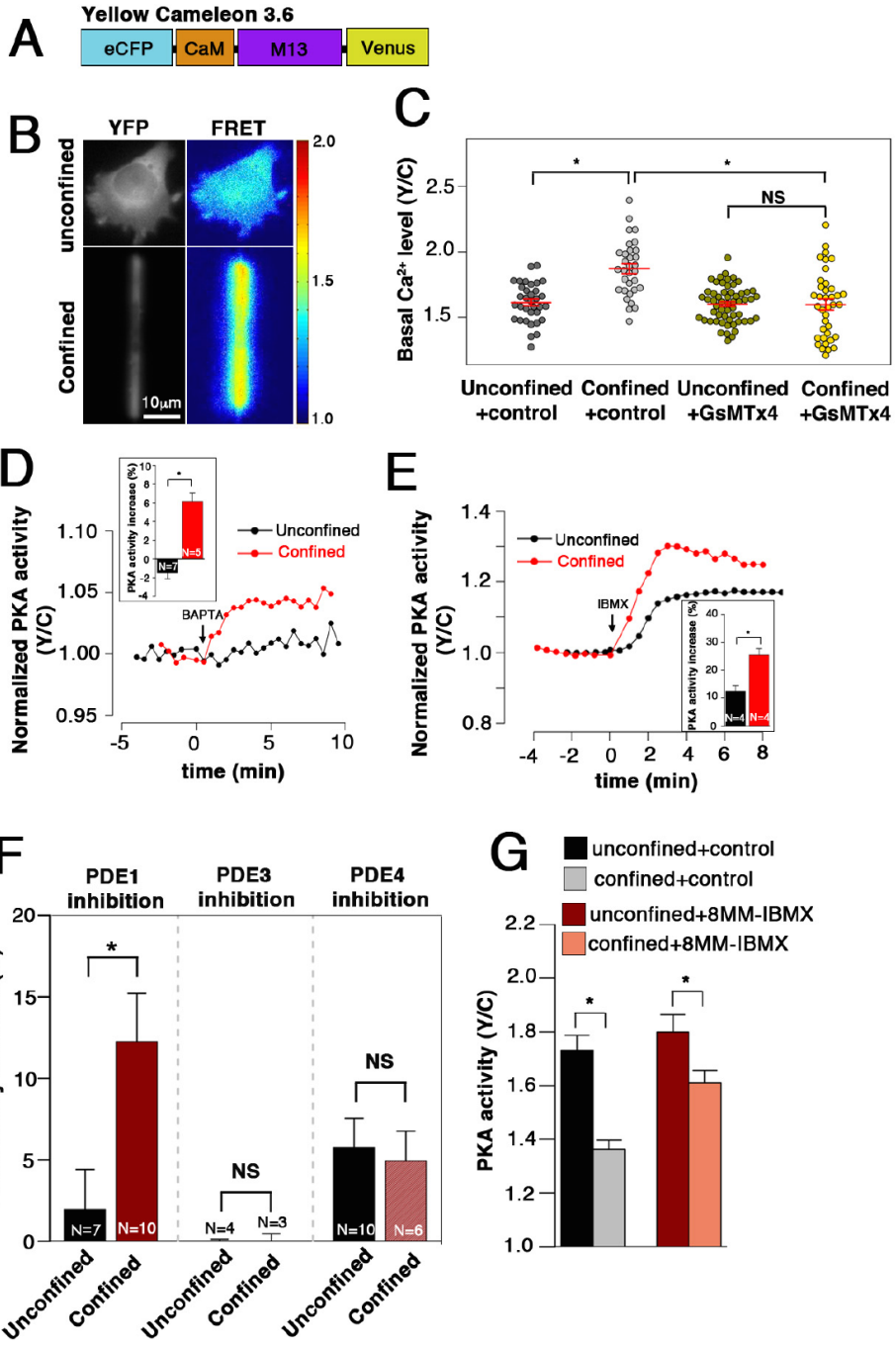
A
Yellow Cameleon 3.6
eCFP
CaM
M13
Venus
B
YFP
FRET
unconfined
Confined
10μm
2.0
1.5
1.0
C
Basal Ca2+ level (Y/C)
2.5
2.0
1.5
*
*
NS
Unconfined +control
Confined +control
Unconfined +GsMTx4
Confined +GsMTx4
D
Normalized PKA activity (Y/C)
1.10
1.05
1.00
0.95
Unconfined
Confined
BAPTA
-5
0
5
10
time (min)
PKA activity increase (%)
N=7
N=5
E
Normalized PKA activity (Y/C)
1.4
1.2
1.0
0.8
Unconfined
Confined
IBMX
-4
-2
0
2
4
6
8
time (min)
PKA activity increase (%)
N=4
N=4
F
PDE1 inhibition
PDE3 inhibition
PDE4 inhibition
PKA activity increase (%)
20
15
10
5
0
*
NS
NS
N=7
N=10
N=4
N=3
N=10
N=6
Unconfined
Confined
Unconfined
Confined
Unconfined
Confined
G
unconfined+control
confined+control
unconfined+8MM-IBMX
confined+8MM-IBMX
PKA activity (Y/C)
2.2
2.0
1.8
1.6
1.4
1.2
1.0
*
*

Figure 2.6 Calcium modulates PKA activity via PDE1
(A) Schematic diagram of FRET-based Calcium indicator, Yellow Cameleon (YC3.6) (B) YFP and FRET ratiometric images of confined and unconfined CHO-α4WTcells expressing YC3.6. (C) The basal Calcium levels of confined or unconfined CHO-α4WT cell treated with either the stretch-activated ion channels inhibitor GsMTx4 (10 μM) or vehicle control are quantified by measuring the initial FRET (i.e. yellow-to-cyan ratio). (D) Representative curves of normalized PKA activity in unconfined (N=7) and confined (N=5) CHO-α4WT expressing AKAR4-KRAS, treated with BAPTA at time 0 min. Corresponding bar graph shows the increase of PKA activity after 5 min of drug treatment. (E) Representative curves of normalized PKA activity in unconfined and confined CHO-α4WT expressing AKAR4-KRAS, treated with IBMX. Corresponding bar graph shows the increase of PKA activity after 5 min of drug treatment. (F) Changes in PKA activity in unconfined and confined CHO-α4WT cells after treatment with PDE1, PDE3, and PDE4 inhibitors, respectively. (G) CHO-α4WT cells treated with the PDE1 inhibitor or vehicle control were compared for differential PKA activities in unconfined versus confined spaces. $N > 25$ for each condition and data represent the mean±SEM. *, $p<0.05$.

basal intracellular calcium levels. Along these lines, treatment of CHO-α4WT cells with the stretch-activated cation channel inhibitor GsMTx4 suppressed the high Ca^{2+} level in confined cells down to that of unconfined cells (Fig. 2.6C). Moreover, GsMTx4 failed to alter the Ca^{2+} level in unconfined cells. Taken together, these data reveal that physical confinement elevates intracellular calcium via stretch-activated ion channels, to suppress PKA activity. To delineate the mechanism underlying Ca^{2+}-mediated suppression of PKA activity in confined cells, we investigated the potential contribution of PDEs, which are enzymes that down-regulate PKA by hydrolyzing cAMP. As a first step, cells transfected with AKAR4-Kras were treated with a general PDE inhibitor 3-isobutyl-1-methylxanthine (IBMX; 100 μM)[46]. Both unconfined and confined cells treated with IBMX displayed an increase in PKA activity (Fig. 2.6E), thereby demonstrating the presence of basal PDE activity in CHO-α4WT cells and the inhibitory effect of PDEs on PKA. Notably a significant difference in the amplitude of the AKAR4-Kras response was observed between unconfined and confined cells following treatment with IBMX (Fig. 2.6E, G). The larger increase in PKA activity in confined cells in response to IBMX indicates that confined cells exhibit higher PDE activity than unconfined cells, which contributes to their differential basal PKA activity levels.

We next wished to identify the PDE responsible for regulating Ca^{2+}-mediated suppression of PKA activity in confined cells. Certain PDEs, such as PDE1 and PDE4, are specifically upregulated by Ca^{2+}[110]. The distinguishing feature of PDE1 is its regulation by Ca^{2+}/calmodulin through direct interactions. Another potential Ca^{2+}-mediated regulator of PKA activity is PDE4 due to a phosphorylation-dependent activation by Ca^{2+}/calmodulin-dependent protein kinase II (CaMKII)[111]. Cell treatment

with the PDE4 specific inhibitor rolipram (10 μM) elicited a similar increase in PKA activity in both unconfined and confined cells (Fig. 2.6F). These results indicate that, although PDE4 contributes to the suppression of basal PKA activity, it does not exert a differential effect in response to physical confinement. In contrast, cell treatment with a PDE1 selective inhibitor 8 methoxy methyl IBMX (8MM-IBMX, 100μM) caused a pronounced increase in PKA activity levels in confined cells, whereas only a modest increase was noted in unconfined cells (Fig. 2.6F, G) indicating that PDE1 contributes to the confinement-dependent PKA suppression. As a control, we inhibited a non-Ca^{2+}-dependent PDE, PDE3, with milrinone (1 μM) and monitored the FRET response from AKAR4-Kras. As predicted, there was no detectable enhancement in PKA activity in either unconfined or confined cells, indicating that PDE3 is not involved in regulating PKA activity in response to changes in intracellular Ca^{2+} and physical confinement (Fig. 2.6F). Taken together, our data provide clear evidence that the differential PKA regulation in response to confinement is Ca^{2+}-dependent and proceeds mainly through PDE1.

PKA and myosin II form a double negative feedback loop

Because Rac1 and myosin II play key roles in optimizing cell motility in unconfined and confined spaces [94], we tested if their activities are affected by modulating PKA activity. We found that, in both CHO-α4WT and parental CHO cells, Rp-cAMP enhanced myosin II-dependent assembly of stress fibers and focal adhesion density but reduced Rac1-dependent cell spreading, whereas forskolin had the opposite effects (Fig.

2.3). These data show that Rac1 and myosin II act as downstream effectors of the Ca^{2+}/PDE1/PKA pathway.

Myosin II acts not only as a downstream PKA effector but also as an upstream regulator of PKA. This conclusion is substantiated by data showing that inhibition of myosin II by blebbistatin (50 μM) caused a significant increase in PKA activity of both unconfined and confined CHO-α4WT and parental CHO cells relative to vehicle control (Fig. 2.7A, A', B, and B'). Rac1 is known to activate A-kinase anchoring proteins (AKAPs) that in turn recruit and activate PKA at the leading edge of migrating cells [112, 113]. Due to the interaction between Rac1 and myosin II, myosin II may negatively regulate PKA activity via a Rac1-dependent pathway. To test this possibility, CHO cells were treated concurrently with blebbistatin (50 μM) and the Rac1 inhibitor NSC23766 (20 μM). This dual treatment abolished the enhancing effect of blebbistatin on the PKA activity of both unconfined and confined cells (Fig. 2.7B, C), thereby indicating that myosin II down-regulates PKA activity through a Rac1-dependent pathway.

In view of these data (Fig. 2.7 and 2.3), we propose that PKA modulates the activities of myosin II and Rac1, and myosin II further tunes the activity of PKA via Rac1. These interactions establish a negative feedback loop, which ultimately leads to an optimized balance between Rac1 and myosin II and efficient cell motility in different degree of physical confinement.

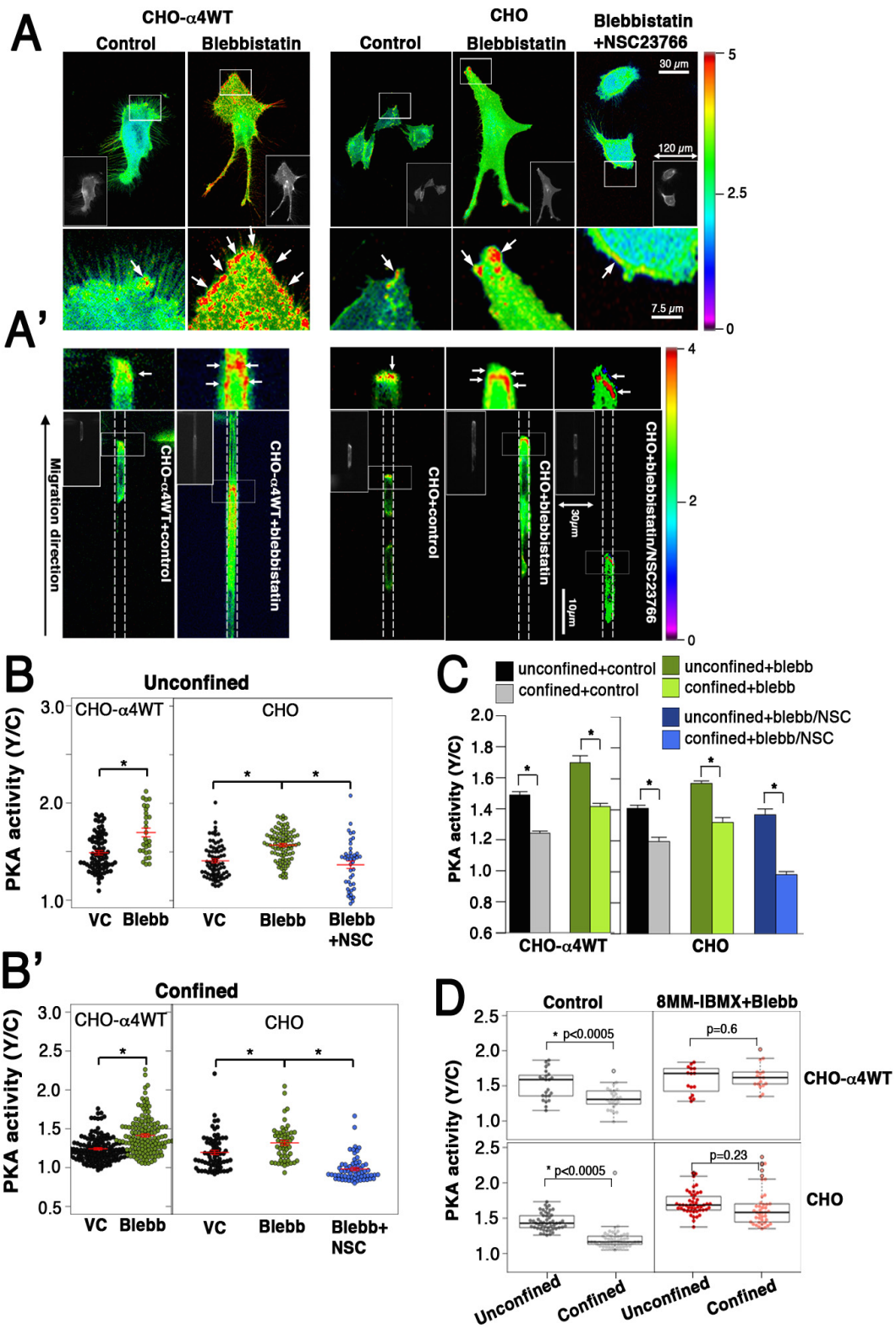
A
CHO-α4WT
Control
Blebbistatin
CHO
Control
Blebbistatin
Blebbistatin +NSC23766
30 μm
120 μm
7.5 μm
5
2.5
0
A'
Migration direction
CHO-α4WT+control
CHO-α4WT+blebbistatin
CHO+control
CHO+blebbistatin
CHO+blebbistatin/NSC23766
30μm
10μm
4
2
0
B
Unconfined
PKA activity (Y/C)
CHO-α4WT
CHO
VC
Blebb
Blebb +NSC
B'
Confined
C
unconfined+control
confined+control
unconfined+blebb
confined+blebb
unconfined+blebb/NSC
confined+blebb/NSC
D
Control
8MM-IBMX+Blebb
* p<0.0005
p=0.6
p=0.23
Unconfined
Confined

Figure 2.7 Myosin II modulates PKA activity via Rac1.
(A and A') Unconfined (A) and confined (A') CHO-α4WT and CHO cells expressing AKAR4-Kras were treated with blebbistatin or vehicle control. The arrows indicate the high PKA activity at the leading edge of cells. (B and B'). The PKA activities in unconfined (B), and confined (B') CHO-α4WT and CHO cells with each indicated treatments were quantified and graphed. (C) Untreated CHO-α4WT or CHO cells were compared with cells under designated drug treatments for changes in PKA activity in response to confinement. (D) Integrated dot/box plots for comparing the basal PKA activities in unconfined versus confined CHO-α4WT or CHO cells in the presence or absence of concurrent treatment with blebbistatin and 8MM-IBMX. Data represent the mean±SEM. *, $p<0.05$.

PDE1 and myosin II inhibitors synergistically abrogate confinement-induced PKA suppression

Our finding that elevation of intracellular Ca^{2+} in response to confinement depends on stretch-activated ion channels implicates a confinement-sensing pathway mediated by the Ca^{2+}/PDE1/PKA signaling module. We reasoned that, if Ca^{2+}/PDE1/PKA is the sole confinement-sensing mediator, then inhibition of PDE1 should abrogate the differential PKA activity in unconfined versus confined cells. However, treating CHO-α4WT cells with the PDE1-selective inhibitor 8MM-IMBX suppressed but failed to abolish the confinement-induced differential PKA activity (Figure 2.6G), suggesting that cells can sense confinement via an alternative pathway independent of PDE1.

External forces have been reported to induce assembly of myosin II bi-polar filaments and actomyosin bundles [114, 115]. This force-sensitive activity of myosin II led us to hypothesize that myosin II may also mediate confinement-sensing, thereby leading to a cascade of signaling events that ultimately suppress PKA. To test this possibility, we treated CHO-α4WT cells with blebbistatin alone or with blebbistatin and the Rac1 inhibitor NSC23766. These treatments failed to abolish the difference in the PKA activity of unconfined versus confined cells (Fig. 2.7C), indicating that the myosin II/Rac1 pathway is dispensable for confinement-induced PKA suppression. However, simultaneous treatment with blebbistatin and the PDE1 inhibitor 8MM-IBMX effectively abrogated the confinement-induced suppression of PKA activity in both CHO-α4WT and parental CHO Cells (Fig. 2.7E). The synergistic effect of this dual inhibition reveals the existence of two confinement-sensing pathways, one is mediated by the Ca^{2+}/PDE1/PKA

pathway, and the other by the myosin II/Rac1 pathway. Each of these confinement-sensing pathways can act independently in the absence of the other.

PDE1 and myosin II inhibitors synergistically abrogate confinement-induced enhancement of cell stiffness

To further understand how cells respond to physical confinement, we also evaluated the ability of cells to resist deformation (referred to as cell stiffness) in response to confinement simulated using 1D fibronectin-coated lines. Specifically, we employed atomic force microscopy to measure the elastic modulus by indenting a cell with an AFM cantilever tip. The applied force was calculated from the degree of bending (deflection) of the cantilever as a function of indentation position of the AFM tip, using the Sneddon/Hertz model [116] (Fig. 2.8A,B). We investigated the effects of confinement on the stiffness of CHO-α4WT and parental CHO cells plated on fibronectin-coated 2D unconfined surfaces and narrow 1D fibronectin-printed lines (Fig. 2.8B). The results indicate that cells on 1D lines displayed a markedly higher stiffness compared to cells on a 2D surface (Fig. 2.8C).

Remarkably, perturbing either myosin II or the optimally tuned activity of PKA significantly affected cell stiffness (Fig. 2.8D): inhibition of myosin II activity using blebbistatin suppressed cell stiffness (Fig. 2.8C), whereas inhibition of PKA using Rp-cAMPs or induction of it via forskolin enhanced or repressed cell stiffness, respectively (Fig. 2.8D). These results indicate that cell stiffness is regulated by PKA and myosin II. Next, we asked if the PKA- and myosin II-dependent pathways contribute to the sensing capability of the cells that allow the cells to differentially regulate the stiffness in

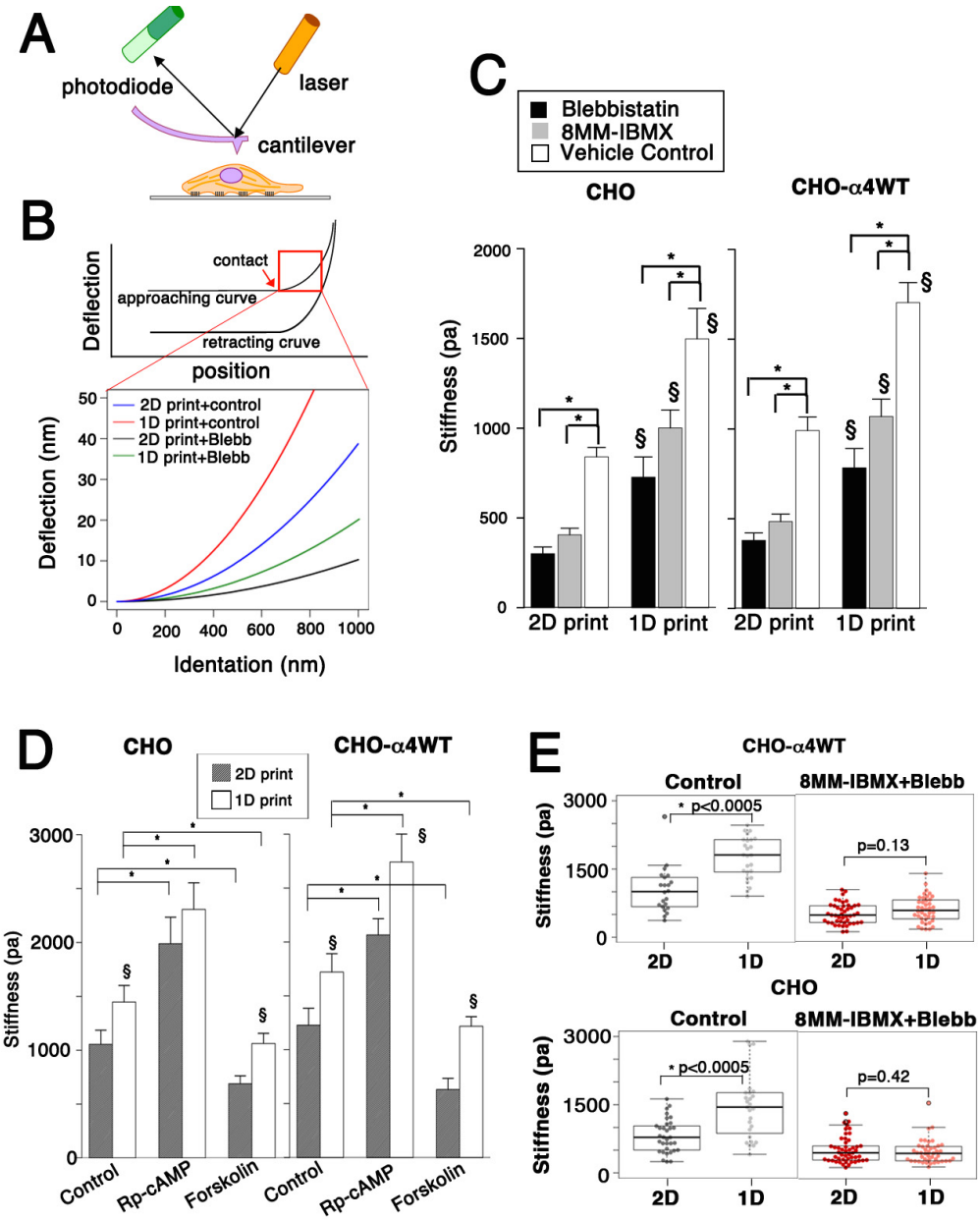

Figure 2.8 Confinement enhances cell stiffness.
(A) Schematic diagram of atomic force microscopy (AFM) technique used for measuring cell stiffness. (B) Representative approach curves from parental CHO cells cultured on 2D or 1D fibronectin-printed surfaces showing deflection (degree bending of AFM cantilever) as a function of indented position. (C, D) Bar graphs represent the elastic modulus (stiffness) of parental CHO and CHO-α4WT cells for each designated condition, calculated from the approach curves. Data represent the mean±SEM for n>35 cells for each condition. *, $p<0.05$. (E) Integrated dot/box plots comparing stiffness of the cells plated on 1D versus 2D fibronectin-printed patterns in the presence or absence of concurrent treatment with blebbistatin and 8MM-IMBX.

response to confinement. While perturbing PKA, PDE1 or myosin II alone did not abolish confinement-induced enhancement of cell stiffness on 1D compared to 2D printed lines (Fig. 2.8C,D), dual inhibition of myosin II and PDE1 effectively abrogated the difference in cell stiffness between the two conditions (Fig. 2.8E). These data support the existence of two independent confinement-sensing mechanisms mediated by the Ca^{2+}/PDE1/PKA and myosin II/Rac1 signaling modules, respectively.

DISCUSSION

Combining FRET-based biosensors, a microfabricated device, and AFM, we delineated the mechanism by which physical confinement is sensed and responded to by CHO-α4WT cells. Based on our current data and those reported in the literature, we propose a new model where confinement signals sensed by two separate pathways are integrated through a double-negative feedback loop, resulting in optimal circuit activity for efficient cell migration (Figure 2.8).

There are two independent confinement-sensing mechanisms

We show that confinement-induced suppression of PKA and enhancement of cell stiffness are not abolished when cells are treated with a PDE1 inhibitor or blebbistatin alone, but treating the cells simultaneously with both inhibitors abrogates the confinement-induced effects. Therefore, there are two confinement-sensing mechanisms, one is mediated by the Ca^{2+}/PDE1/PKA pathway, and the other by the myosin II/Rac1 pathway; each pathway can elicit cell responses to confinement. Having two sensing

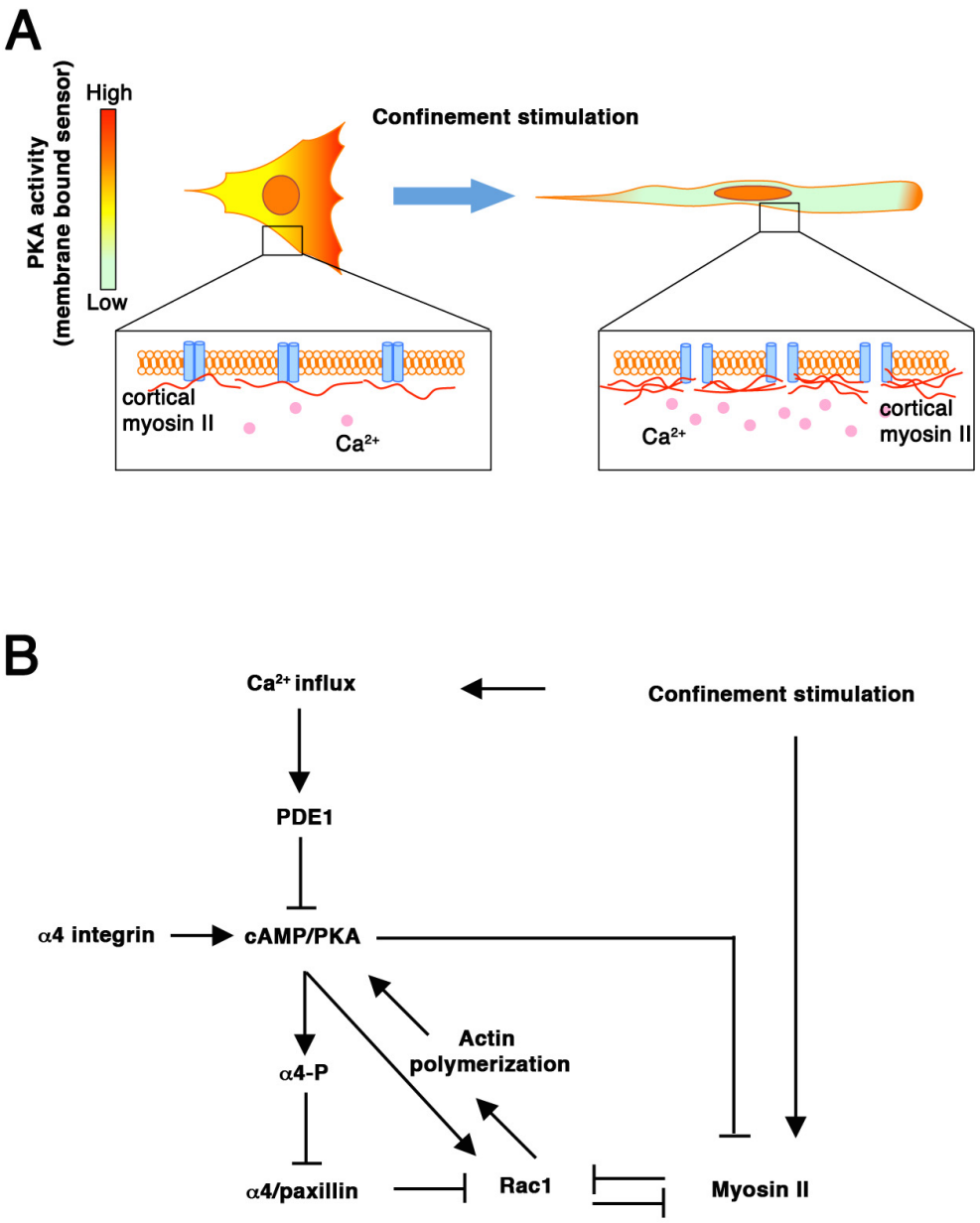

Figure 2.9 Proposed negative feedback signaling loop that promotes migration of CHO-α4WT cells in response to physical confinement.

mechanisms could enhance the sensitivity of the cells to confinement and increase the range of confinement signals to be sensed. Because myosin II senses confinement signal and also directly contributes to migratory activities, it "short-cuts" the mechanotransduction circuit, which may fasten the response of the cells to confinement.

It is known that integrins play a pivotal role in mechanosensing [117]. However, we show that α4 and α5 integrins are dispensable for cells to sense confinement and suppress PKA activity. In addition, synergy and compensation are not observed between α4 integrin and PDE1 or myosin II. These observations are consistent with the notion that in confined environment integrin-mediated cell adhesion becomes less important for cell motility [97, 118], and confined migration favors low adhesion [90]. We show that, although not contributing to confinement-sensing, α4 integrins do participate in PKA regulation in a confinement-independent manner, which supports the AKAP function of α4 integrins as reported in the literature [54].

Collectively, our data reveal that the Ca^{2+}/PDE1/PKA and myosin II/Rac1 signaling modules, but not α4 integrins, act as mediators for confinement-sensing. Further studies are necessary to elucidate the confinement-sensing mechanisms. We show that, when treated with a stretch-activated cation channel (SAC) blocker, cells fail to increase their intracellular Ca^{2+} level in response to confinement. This finding implicates SACs in confinement-sensing. When cells are compressed by confinement, SACs could be activated by tension generated by deformation of the lipid bilayer and the stretching force from cortical actomyosin network. But, given that cells can sense confinement when myosin II is inhibited, SACs could be activated via both myosin II-dependent and independent mechanisms. Besides SACs, myosin II may also act as a mechanosensor by

facilitating force-sensitive assembly of myosin II bi-polar filaments [114, 115]. Myosin II may also mediate confinement-sensing by activating cytoskeletal mechanosensors [119]. Future work should be directed toward determining if these mechanisms facilitate confinement sensing.

PKA and Myosin II amplifies circuit activity via a double negative feedback system

We demonstrate that, in response to confinement, PKA and myosin II form a double negative feedback loop. In CHO-α4WT cells, confinement-induced suppression of PKA leads to decreased PKA-dependent phosphorylation of α4 integrin, which promotes the formation of an α4/paxillin/GIT1 complex that inhibits Rac1, thus enhancing myosin II activity [94, 120]. In parental CHO cells, PKA also regulates Rac1 and myosin II independent of α4 integrin, which is likely due to direct inhibitory effects of PKA on RhoA and Rho-GEF [121, 122]. Our data indicate that, myosin II acts not only as a downstream PKA effector, but also as an upstream regulator that suppresses PKA activity. The suppression depends on Rac1. Several Rac1 effectors, including WAVE1 and WAVE2, function as AKAPs that recruit and activate PKA at the cell cortex proximal to the plasma membrane [112, 113]. Therefore, the activity of membrane-associated PKA could be affected by inhibition of the Rac1/WAVEs pathways. Thus, PKA and myosin II/Rac1 form a double negative feedback loop. Because it is known that calcium may directly enhance myosin II via calmodulin-mediated pathways [123], and myosin II-driven contractility plays a key role in activation of stretch-activated ion channels [124], the signaling circuit could be more complex. The presence of double-negative feedback may allow this circuit system to respond to physical confinement with ultrasensitivity and

even exhibit switch-like behaviors. As a consequence, small changes in the physical environment may flip the PKA-Myosin II switch, leading to a new balance between Myosin II and Rac1 activities, thereby optimizing the efficiency of cell motility. This double negative feedback mechanism provides a novel strategy for signal optimization.

We extended our observations by demonstrating confinement-induced suppression of PKA activity in an invasive melanoma cell line, A375-SM. Optimal modulation of PKA activity is necessary for A375-SM cells to migrate efficiently in unconfined and confined spaces. These results are consistent with our previous findings showing that A375-SM cells modulate Rac1 and myosin II in response to physical confinement in a similar manner as CHO-α4WT cells [94]. Therefore, the mechanotransduction signaling mechanism uncovered in this work provides novel insights into how cells sense and adapt to microenvironments with different degrees of physical confinement, and optimize their motile activities.

MATERIALS AND METHODS

Cell culture, pharmacological inhibitors, plasmids and transfection

CHO-α4WT and CHO-α4S988A cell lines were generated by stably transfecting CHO cells with pQN4G and pQN4S988AG plasmids, respectively, in which wild-type or mutant α4 integrin cDNA was tagged with GFP by inserting into a PGBI25-fN1 GFP vector [125, 126]. The CHO-α4WT cells were maintained in Ham's F12 (Cellgro). CHO and CHO-B2 (ref: Schreiner) cells were maintained in DMEM (high glucose, Life technology) and minimal essential medium (Invitrogen), respectively. Media were supplemented with 10% fetal bovine serum (FBS, Gibco) and 1 μg/ml

penicillin/streptomycin. For studies with pharmacological agents, 50 μM forskolin (Santa Cruz), 50 μM Rp-cAMPs (Santa Cruz), or appropriate vehicle controls were added to the cells seeded in serum-free medium near microchannel entrances. For PKA study, 3-isobutyl-1-methylxanthine (IBMX), 8 methoxy methyl IBMX (8MM-IBMX) rolipram (Cayman Chemical), and milrinone (Enzo Life Sciences) were used to probe basal PKA activity. Transient transfection was performed using Lipofectamine 2000 (Life Technologies) according to the manufacturer's protocol.

Microfluidic-based microchannel assay

PDMS microchannels were fabricated using standard replica molding. Masks to generate the microchannel design were drawn using Adobe Illustrator CS2 and printed onto a transparency by a 5080 dpi printer (Pageworks) or transferred to a chrome-on-glass photolithography mask (Advance Reproductions Corp.). To prepare masters, SU-8 2010 and SU-8 2025 epoxy negative photoresists (Microchem Corp.) were applied by spin coating (Laurell Technologies Corp.) onto silicon wafers (Montco Silicon Technologies Inc.) in two steps. SU-8 2010 was first spread at 600 rpm for 20 s and then at 4000 rpm for 60 s to a final thickness of 8-10 μm. The photoresist was prebaked at 60 °C for 1 min, exposed to UV (350−450 nm) radiation through appropriate masks for 40 s, postbaked at 115 °C for 8 min, and subsequently developed using SU-8 developer (Microchem Corp.). This step was used for generating the microchannels present in the final device. The second feature of the microfluidic-based microchannel master consisted of the cell seeding line and the FBS gradient generation line, and was fabricated using the following steps: SU-8 2025 was first spread at 500 rpm for 10 s and then at 4000 rpm for 30 s to a final thickness of 50 μm. The photoresist was prebaked at 80 °C for 3 min and at 110 °C

for 6 min, cooled, and exposed to UV (350−450 nm) radiation for 30 s through a mask aligned with the previously fabricated microchannels. The photoresist was then exposed for 8 min at 110 °C and developed as before. PDMS stamps were obtained by mixing Sylgard 184 prepolymer with cross-linker (Dow Corning) in a 10:1 ratio (by weight), degassing in a vacuum, and curing at 80 °C for 1 h. Each PDMS well inlet and outlet was punched out with a diameter of 6 mm. Both the PDMS device and microscope slide (FisherFinest) were cleaned and made hydrophilic using a plasma cleaner for 2 min. The PDMS device was then attached to a glass slide, followed by pre-coating various concentrations of 20µg/ml fibronection at 37 °C for 1 h. The microchannel was washed with PBS (1X) containing calcium/magnesium for 1 min before seeding cells. A total of $1x10^5$ cells in a 50 µl volume were added to the cell inlet port. Chemotactic-driven cell migration was recorded via time-lapse microscopy (inverted Eclipse Ti microscope, Nikon) using software controlled stage automation (Nikon). To calculate migration velocity, the cell center was identified as the midpoint between poles of the cell body, and was tracked for changes in X, Y position at 20-min intervals over a 10 h period.

Fabrication of 1D Protein Micropatterns

Standard lithography was used to create a silicon wafer with an array of features that are 50µm wide, 5µm tall, and 20mm long, with 8µm in between adjacent features. Replica molding was used to create a PDMS stamp bearing the inverse of these features. PDMS stamps were sonicated in ethanol and dried under an air stream. Stamps were functionalized with 100µg/mL Fibronectin (Sigma-Aldrich, F-0895) in Dulbecco's Phosphate Buffered Saline (PBS) (Life Technologies, 14190-144). After one hour at

room temperature, this solution was removed and the stamps were again dried under an air stream. Stamps were then inverted onto tissue culture dishes (Falcon, 353002) under steady pressure. After 30 minutes, the stamps were removed and the dish was backfilled with 2.5%wt Bovine Serum Albumin (Sigma-Aldrich, A9647) in PBS to prevent cell adhesion outside of the fibronectin-patterned areas. After one hour the BSA solution was removed and the stamps were rinsed three times with PBS. 2D areas were created using a flat PDMS stamp according to the same procedure.

AKAR4-Kras, Yellow Cameleon 3.6 (YC 3.6), and PKA activity Imaging

Cells transfected with biosensors, AKAR4-Kras or Yellow Cameleom were washed twice with Hanks' balanced salt solution buffer and maintained in the dark at room temperature. Transfected cells were imaged on a Zeiss Axiovert 200M microscope with a cooled charge-coupled device camera (MicroMAX BFT512, Roper Scientific, Trenton, NJ) controlled by METAFLUOR 6.2 software (Universal Imaging, Downingtown, PA). Dual cyan/yellow emission ratio imaging used a 420DF20 excitation filter, a 450DRLP dichroic mirror, and two emission filters [475DF40 for CFP and 535DF25 for YFP]. These filters were alternated by a filter-changer Lambda 10–2(Sutter Instruments, Novato, CA). Exposure time was 50–500 ms, and images were taken every 10–30 s. Fluorescence images were background-corrected by subtracting the fluorescence intensity of background with no cells from the emission intensities of cells expressing fluorescent reporters. The ratios of yellow/cyan emissions were then calculated at different time points. The values of all time courses were normalized by dividing each by the average basal value before drug addition,

Atomic force microscopy and stiffness measurement

Force spectroscopy experiments were conducted using a Molecular Force Probe (MFP-1D; Asylum Research, Santa Barbara, CA). Using thermal oscillation method, a triangular cantilever (nominal spring constants of 10 pN/nm) was calibrated, with its deflection (degree of bending) measured by laser reflection onto a split photodetector[127, 128]. CHO-α4WT or CHO cells were seed on the glass slide patterned with 8μm fibronectin line or uniform fibronectin 2D surface. Cells were cultured in serum-free desired medium solution with 50μM blebbistatin, 50μM forskolin, 50μM Rp-cAMPs or appropriate vehicle control. The cantilever height was adjusted such that each approach cycle generated a slight force (~1–2 nN) onto the cell surface before reproach. For each run, reproach velocity was 25 mm/s, and the dwell time was set to 20 ms. Stiffness was analyzed and quantified as previously described[116]. Briefly, the point of contact between the AFM tip and the cell surface was identified by a custom MATLAB program. The positions of the AFM tip were measured during the approach and retraction cycle and recorded by a photodiode. The approaching curve (deflection as a function of indented position) was then fitted by Hertz model for corresponding tip geometry,. The Sneddon model of indentation force was used to calculate the elastic modulus (i.e. the stiffness) of the cell from the shape of this curve.

Statistical analysis

Data are expressed as mean ± SEM. Statistical significance of differences between means was determined by Student's *t*-test or one-way ANOVA followed by the Tukey test for multiple comparisons, where appropriate.

Chapter 3

PKA regulates subcellular Akt activity in PC12 cells

INTRODUCTION

The PC12 cell line was derived from a rat pheochromocytoma, a tumor arising from chromaffin cells of the adrenal medulla. A unique feature of PC12 cells is their distinct responses to different growth factors. Specifically, NGF signaling through the receptor tyrosine kinase (RTK), TrkA, causes differentiation, while another RTK activated by EGF can stimulate proliferation. Although the responses to both NGF and EGF require ERK activation, when stimulated with EGF, ERK exhibits a rapid and transient activity pattern mediated by both Ras and Rap1, while NGF stimulation of ERK leads to both rapid and sustained signaling through Rap1 alone. PC12 cells have since become a model system for studying cell differentiation, as well as how different signaling dynamics can lead to distinct biological outcomes.

RTKs are known to recruit and activate a host of downstream signaling molecules, including additional docking proteins[129], and a variety of signaling pathways have been shown to interact with components of the MAPK/ERK pathway, which may provide a possible mechanism for these specific growth-factor induced cellular processes. For example, PKA can activate Rap1, B-Raf and subsequently ERK via tyrosine kinase Src[130]. Others have shown that cAMP signals via both Epac and PKA to tune ERK activity and thus the cellular response[21, 29]. Furthermore, other studies have focused on the cross-talk between ERK signaling and other neuronal second-messenger systems. Certain Ras- and Rap-GEFs were found to be activated by direct binding to second messengers such as calcium and DAG[131]. Additionally, PKC inhibition resulted in transient Erk1/2 activation after NGF treatment, which is more characteristic of EGF stimulation, and resulted in proliferation of PC12 cells[132]. However, despite growing

evidence that other signaling pathways can modulate ERK activity, the exact mechanism by which NGF and EGF achieve signaling specificity in PC12 cells remains elusive.

Rather than honing in on the convergence of signaling pathways at a single point, such as ERK, recent studies suggest that multiple pathways could be working in parallel and that the balance between these different pathways dictates cell fates. Interestingly, Jia-Yun Chen *et al*. suggest that crosstalk between the PI3K and Ras pathways via the activation of the multifunctional protein kinases ERK and Akt, important downstream targets of Ras and PI3K signaling respectively, determines the fate of PC12 cells treated with NGF. In addition, they identified a feedback link between these two pathways: Rasa 2 is a late NGF-induced PI3K-related RasGAP that connects PI3K to Ras signaling via negative feedback. We were therefore interested in further characterizing the role of PI3K/Akt signaling in PC12 cell proliferation and differentiation.In addition, we previously found that PKA regulates ERK signaling in PC12 cells in response to both EGF and NGF. Various studies have also revealed associations between cAMP-dependent signaling and the PI3K/PKB/AKT pathway, indicating that PKA operates upstream of Akt and can modulate its activity. However, the effects of PKA on Akt activity are cell type-specific and complicate our understanding of PKA-Akt cross-regulation. In COS7 and HEK293 cells, for example, PKA can indirectly inhibit or activate Akt by affecting Akt translocation to the plasma membrane and activating or inhibiting kinases and phosphatases that control Akt phosphorylation. On the other hand, in granulosa cells, PKA enhances Akt activation by promoting phosphorylation of insulin receptor substrate-1 (IRS-1) to promote proliferation, differentiation, survival, and enhanced mRNA translation. Interestingly, in primary cortical neurons, AKAP150

coordinates PKA and Epac-mediated Akt phosphorylation. More importantly, these two cAMP-dependent effectors were shown to exert reciprocal effects on neuronal Akt signaling. These results provide strong evidence of a link between PKA and Akt signaling in cell-fate determination, leading us to also investigate the effect of PKA, an upstream regulator of ERK, on Akt activity in PC12 proliferation and differentiation.

RESULTS

Spatial differences in Akt activity dynamics in PC12 cells

We first characterize Akt activity in response to EGF and NGF in PC12 cells. Given that the plasma membrane is the site of activation for the PI3K/Akt pathway and because Akt activity has been shown to differ between plasma membrane raft and non-raft regions in NIH3T3 cells, we utilized the raft and non-raft targeted FRET-based reporter Akt activity reporters, Lyn-AktAR2 and AktAR2-KRAS, respectively, to monitor Akt dynamics (Fig. 3.1A,B). AktAR2 contains a molecular switch that consists of FHA1 as the PAABD and an Akt substrate domain derived from the sequence surrounding Thr-24 of FOXO1 sandwiched between Cer and cpVenE172[133]. Interestingly, upon NGF stimulation, which is known to induce sustained ERK activity and drive the neuron-like differentiation of PC12 cells, we observed sustained Akt activity in both raft and non-raft regions. Furthermore, when the cells were exposed to EGF, which normally induces transient ERK activity and PC12 cell proliferation, we also observed transient Akt activity in both of these plasma membrane regions (Fig. 3.1C,D). Noticeable differences were observed in Akt activity when PC12 cells responded to EGF and NGF. The first difference is in the amplitude of the FRET response upon growth

factor stimulation. Upon EGF stimulation, both raft- and non-raft-localized Akt exhibited similar FRET responses (14.8 ± 1.1%, n=14 and 14.04 ± 0.56%, n=28, respectively). In contrast, when treated with NGF, raft-localized AktAR showed a weaker response than non-raft-localized AktAR (9.4 ± 0.84%, n=10 and 16.32 ± 0.87%, n=22, respectively) (Fig. 3.1D).

In addition, we compared the kinetic differences between Akt activity in these different microdomains induced by the different growth factor treatments. To quantify these differences, we employed the Sustained Activity Metric (SAM), defined as follows:

$$SAM = \frac{R_{30} - R_0}{R_p - R_0}$$

where R_0 and R_{30} are the response amplitudes at 0 and 30 minutes, respectively, and R_p is the maximum response measured between 0 and 30 minutes. Thus, higher SAM values generally correspond to more sustained responses, with a SAM value of 1 indicating that the response is completely sustained, whereas a SAM value of 0 corresponds to a fully adapted, transient response. In general, EGF induced more transient Akt activity and NGF induced more sustained activity. However, raft-localized Akt activity was more sustained that non-raft-localized Akt activity in response to EGF treatment (SAM values: 0.38 ± 0.03 and 0.22 ± 0.03, respectively) (Fig. 3.1E). Under NGF treatment, Akt in the raft regions showed more transient activity that non-raft Akt (SAM values: 0.69 ± 0.06 and 0.92 ± 0.03, respectively) (Fig. 3.1E).

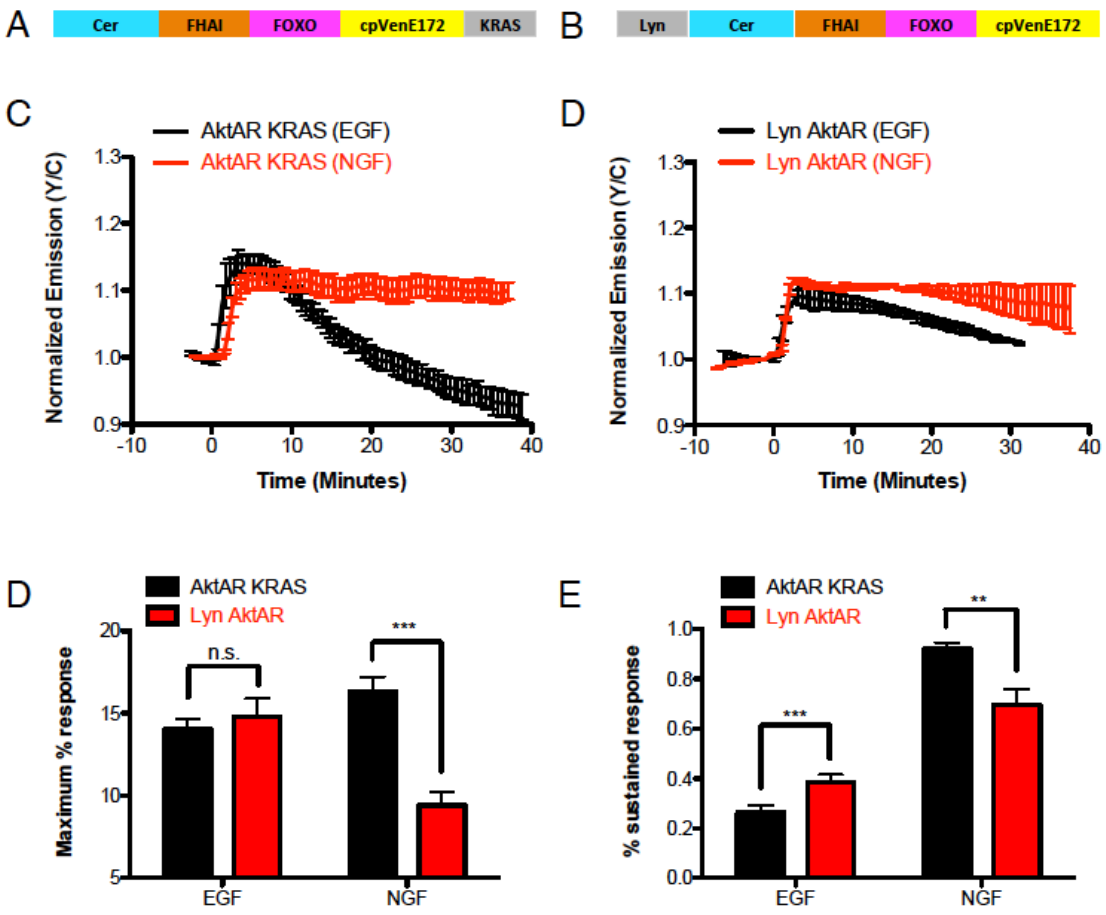

Figure 3.1 Growth-factor induced Akt activity in plasma membrane microdomains
(A) Representative time course plot of PC12 cells expressing AktAR KRAS and (B) Lyn AktAR with EGF (n=28) and NGF (n=22). (C) Bar graph comparing maximum % response from AktAR KRAS and Lyn AktAR in response to EGF (n=14) and NGF (n=12). (D) Bar graph depicting difference in SAM or % sustained response values of AktAR KRAS and Lyn AktAR under EGF and NGF treatments.

Other than the plasma membrane, Akt activity has been known exist in other subcellular regions. Once activated, Akt can translocate to various subcellular compartments, including the endoplasmic reticulum, mitochondria, Golgi and nucleus, where it phosphorylates substrates or interacts with other cell components[134]. Therefore, we next examined if the unique temporal dynamics of Akt activity specifically induced by each growth factor also extended to other regions of the cell in which Akt activity has been detected. We were able to detect Golgi-localized Akt activity. Interestingly, both EGF and NGF stimulated transient Akt responses at this region, with maximum responses of 4.0 ± 0.34% (n=11) and 6.8 ± 0.6% (n=10), respectively (Fig. 3.2A). The addition of either EGF or NGF induced only a minute, transient Akt responses in the cytosol, as measured using AktAR NES, with an average maximum FRET ratio changes of 2.2 ± 0.23% (n=21) and 1.8 ± 0.15% (n=16) for EGF and NGF, respectively (Fig. 3.2B). In the nucleus, Akt has been reported to phosphorylate the FOXO family of transcription factors, as well as the transcriptional coactivator p300[135]. In addition, other studies have shown that NGF elicits Akt translocation into the nucleus[136]. Surprisingly, we observed no detectable nuclear Akt activity upon EGF or NGF stimulation. In addition, other subcellular regions such as the mitochondria and endoplasmic reticulum showed no Akt activity upon EGF and NGF treatment (Fig. 3.2C-E).

PKA regulation of subcellular Akt activity

In order to decipher the mechanism underlying these different spatiotemporal Akt activity dynamics in presence of EGF and NGF, we looked towards other signaling

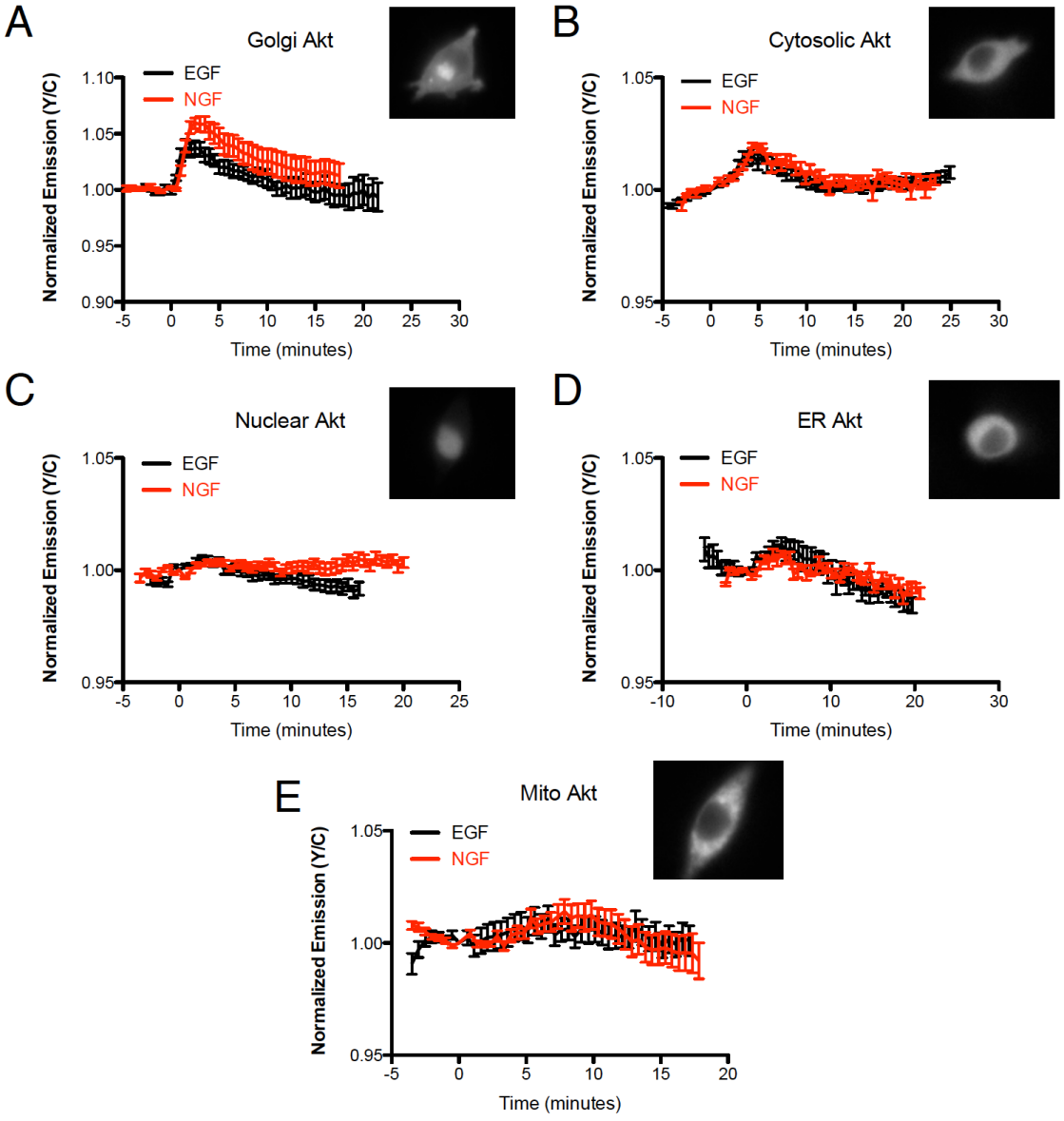

Figure 3.2 Subcellular growth-factor induced Akt activity
(A) Golgi (B) Cytosol (C) Nuclear (D) Endoplasmic reticulum (E) Mitochondrial Akt activities in response to EGF (100ng/mL) and NGF (200ng/mL), (n=4-10).

molecules that could regulate GF-induced Akt activity. Previously, Herbst et al. showed that non-raft localized PKA could be activated by EGF and NGF to regulate cell proliferation and differentiation, and other studies have implicated PKA in the regulation of Akt activity[46]. Therefore, we set out to investigate the role of PKA in regulating the spatiotemporal dynamics of Akt activity in PC12 cells.

To test the effect of PKA on Akt activity, we pretreated cells with either a PKA inhibitor, H89 (10 μM), or a potent cAMP-elevating cocktail containing both the general PDE inhibitor IBMX and the AC activator Forskolin (Fsk) for 10 minutes prior to stimulation with either EGF or NGF. Using non-raft-localized AktAR, PKA inhibition was found to promote a more sustained EGF-induced Akt response (Fig. 3.3A,B) and a more transient NGF-induced response (Fig. 3.3C,D) versus treatment with either GF alone. These kinetic changes were also quantified using SAM values and compared to those from the GF-alone treatments. H89 pretreatment doubled the SAM value of EGF treatment while reducing the SAM value of NGF treatment by more than half. On the other hand, upregulating PKA activity led to a more transient EGF-induced Akt response (Fig. 3.3A,B) and had no discernible effect on the kinetics of the NGF-induced response (Fig. 3.3C,D). These results suggest that PKA does not function as a simple inhibitor or stimulator of Akt and that a more complex regulatory interaction is involved in tuning subcellular Akt activity patterns.

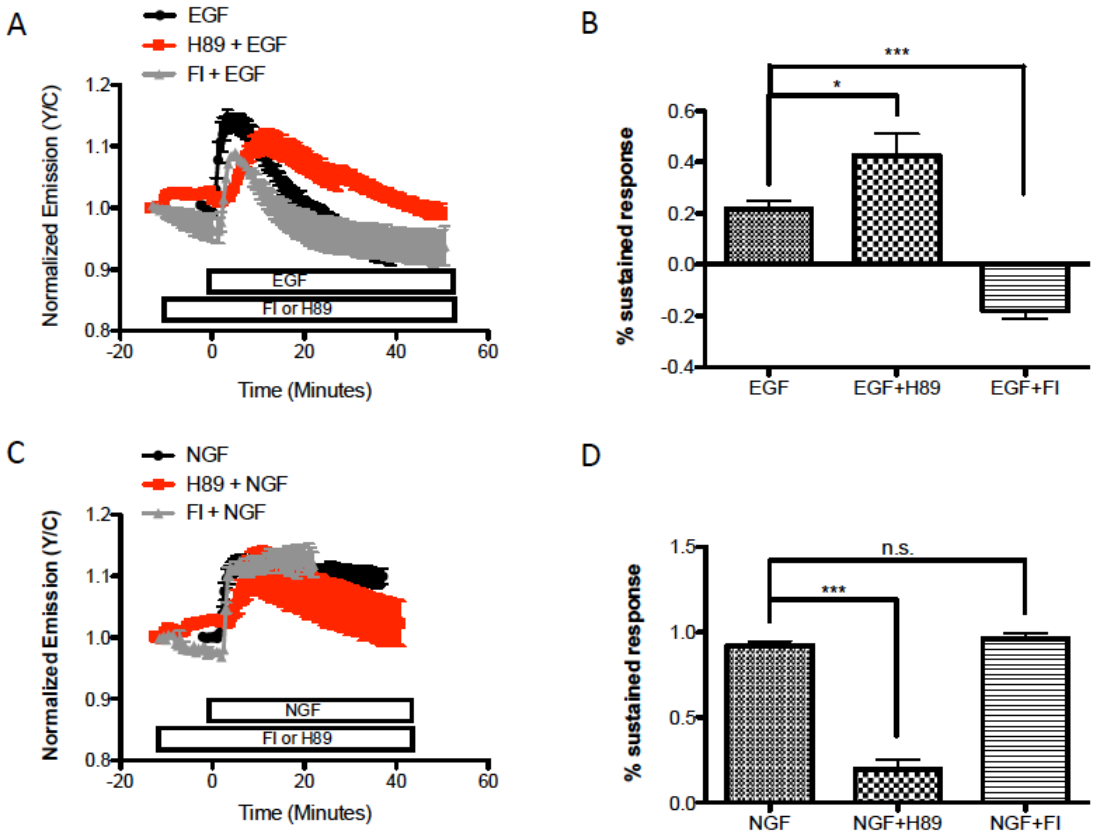

Figure 3.3 PKA modulates growth-factor induced Akt activity at the plasma membrane

(A) Representative curves of AktAR KRAS responses treated with EGF (n=28), 10μM H89 and EGF (n=11), and Fsk (50μM)/IBMX (100μM) and EGF (n=11). (B) Bar graphs depicting the SAM values for the EGF-related treatments. (C) Representative curves of AktAR KRAS responses treated with NGF (n=22), 10μM H89 and NGF (n=12), and Fsk (50μM)/IBMX (100μM) and NGF (n=4). (D) Bar graphs depicting the SAM values for the NGF-related treatments.

Tuning of PKA activity via negative feedback from PI3K/Akt signaling

Given the complex regulation of Akt by PKA in presence of EGF and NGF, we looked into additional mechanisms that could contribute to this complex PKA-Akt crosstalk. Cellular signaling cascades are complex systems embedded with non-linearities in the form of feedback loops. Therefore, to gain an understanding of plasma membrane PKA-Akt crosstalk, we investigated the possible existence of negative feedback from Akt to PKA in non-raft regions. To determine if Akt can modulate PKA activity, PC12 cells expressing AKAR4-Kras, a non-raft-targeted FRET-based PKA activity reporter, were treated with 20 μM LY294002, a PI3K inhibitor. Treatment with LY294002 alone led to a robust, 17.6 ± 3.4% (n=18) increase in the AKAR4-KRAS FRET ratio (Fig. 3.4A,B), and subsequent treatment with either EGF or NGF failed to elicit any additional PKA response. Previously, we showed that both EGF and NGF are capable of inducing a noticeable increase in PKA activity at the plasma membrane. However, because maximally elevating PKA activity using Fsk and IBMX treatment leads to a maximum FRET response of 22.6 ± 1.4% (n=5) in AKAR4-KRAS-expressing PC12 cells, the lack of a further response from growth factor treatment after LY294002 pretreatment suggests that LY294002-induced PKA activity has already saturated the response range of the reporter. Along the same lines, LY294002 treatment following a 10-min treatment with either EGF or NGF led to additional increase in PKA activity. As with ERK and Akt, we have also shown that PKA exhibits differential activity patterns, being transient in response to EGF and sustained in response to NGF. However, regardless of whether cells were first treated with EGF or NGF, subsequent stimulation with LY294002 invariably led to sustained PKA activity (Fig. 3.4C,D). Taken together, these data suggest that Akt

activity has a strong inhibitory effect on PKA at the plasma membrane. Interestingly, in the cytoplasm, PKA activity only increased by 1.2 ± 0.7% upon Akt inhibition (Fig. 3.4E). Subsequent treatment with Fsk and IBMX led to a dramatic increase in PKA activity, indicating that that lack of a significant response to LY294002 treatment was not due to malfunctioning of the reporter. Given that GF stimulation was also unable to induce significant changes in cytosolic Akt activity, the apparent lack of any Akt effect on cytosolic PKA could be due to low basal PI3K or Akt activity in this subcellular region.

To further elucidate the mechanism behind the negative regulation of PKA by Akt at the plasma membrane, we next investigated the involvement of known negative regulators of PKA activity, such as PDEs, that may be regulated by PI3K or Akt. Previously, PDE3 was shown to specifically regulate PKA activity at the plasma membrane in PC12 cells, thereby preventing active PKA from diffusing into the cytoplasm. Therefore, we transfected cells with diffusible ICUE3, a FRET-based cAMP reporter, and treated these cells with LY294002. Following LY294002 treatment, we detected a larger response from ICUE3 than with either EGF or NGF alone, signifying that PI3K may inhibit PKA activity by negatively regulating cAMP levels (Fig. 3.5F).

Determining the role of PKA-Akt crosstalk in PC12 cell differentiation

To test if the PKA-Akt crosstalk has implications in growth-factor induced neurite extension, we treated PC12 cells with various treatments for 3 days and monitored the

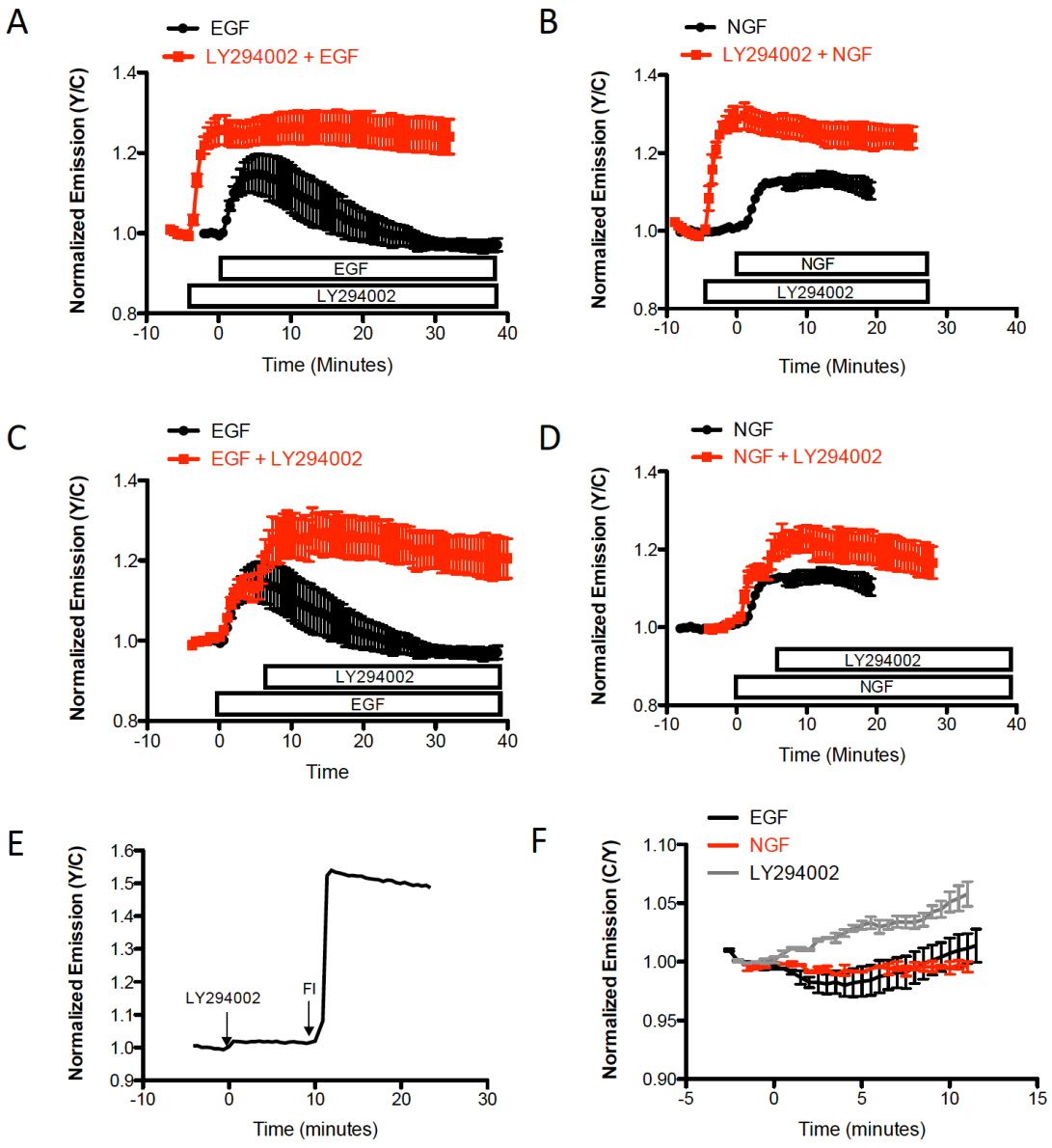

Figure 3.4 Akt regulation of PKA activity at the plasma membrane
(A-D) Time course plots of AKAR4-KRAS with indicated treatments. (E) Time course plot of AKAR-NES with indicated drug treatments (n=2). (F) Time course plot of ICUE3 with either EGF (n=6), NGF (n=6), or LY294002 (n=4).

effects on neurite outgrowth using membrane-targeted YFP to highlight the cell membrane and facilitate the quantification of neurite length. Consistent with previous reports, we found that NGF induces significant neurite outgrowth (neurites were defined as processes with lengths greater than or equal to the length of the cell body), whereas EGF treatment does not. Also in agreement with our previous observations, treatment with both EGF and Fsk also induced neurite outgrowth, although the effect on neurite outgrowth was not as robust as that of NGF treatment in terms of the number of neurites or neurite length[46, 137]. Interestingly, upon treatment with Fsk, alone, the cells exhibited a substrantial amount of neurite extension, more than what was observed in the presence of EGF. Since PI3K suppresses PKA activity, we predicted that additional treatment with LY294002 would further increase the percentage of differentiating cells, possibly to a level that more closely resembles NGF treatment. However, LY294002 treatment in presence of either EGF or Fsk failed to further enhance the neurite extension exhibited by cells treated with EGF and Fsk (Fig. 3.5). To simplify our understanding of these results, we removed EGF from the treatment conditions and observed the functional outcome. Upon treatment with Fsk alone, the cells exhibited a substantial amount of neurite extension, more than what was observed in the presence of EGF. PC12 cells were then treated with a combination of Fsk and LY294002. Even without EGF, however, we again observed less neurite extension than expected. This effect may be due to the toxicity of LY294002 treatment, as a large portion of the cells died over course of the 2-day treatment.

Other approaches to test the relationship between PKA and Akt in the functional assay involve using lower doses of LY294002 to prevent cell death over the course of the

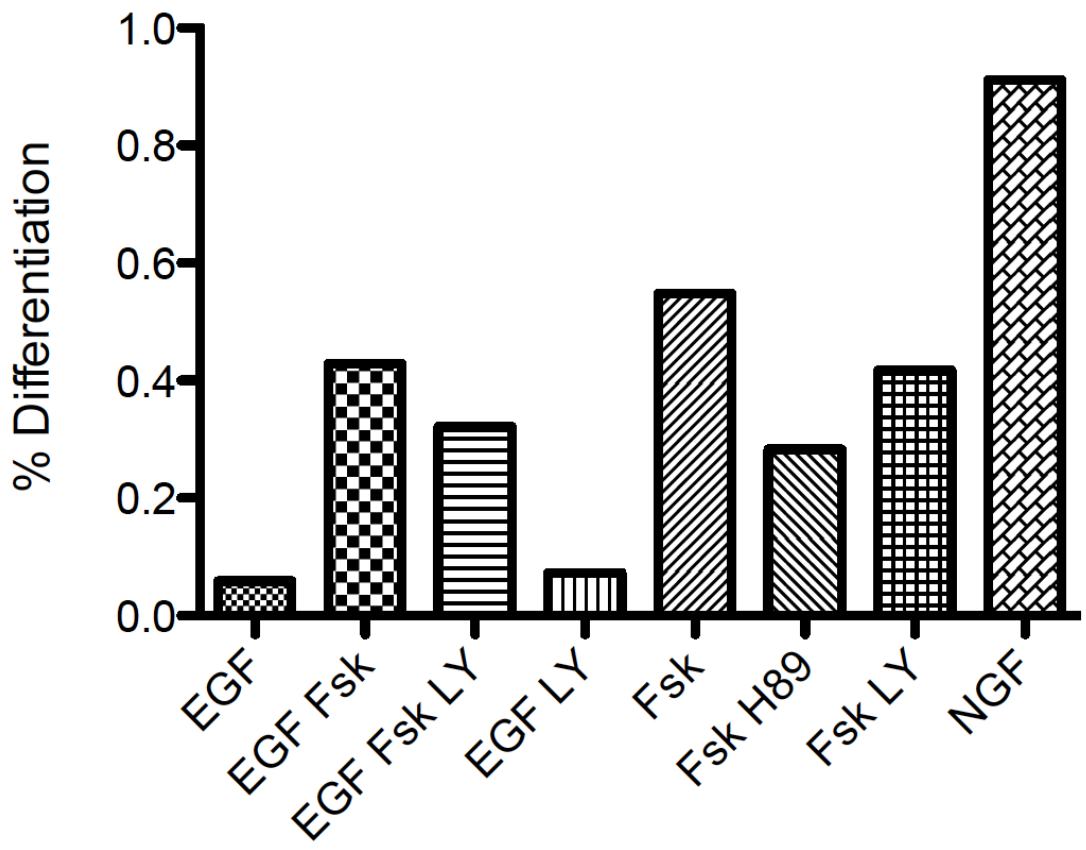

Figure 3.5 PC12 Differentiation Assay
PC12 cells expressing a plasma membrane-targeted YFP were treated for 3 days as indicated, and the number of cells expressing neurites (defined as a cellular extension longer than the length of the cell body) was quantified. *n* = 50 to 130 cells per treatment.

assay or, alternatively, implementing the Akt-specific inhibitor SH-5. Furthermore, to address the role of the differential spatiotemporal regulation of GF-induced Akt in PC12 cell proliferation and differentiation, we plan to incorporate a targetable peptide-based Akt inhibitor in the functional assay. This inhibitor will be targeted to different subcellular localizations and the importance of their activities will be determined by how the functional output differs from the canonical GF treatments. Furthermore, we will combine Akt-specific inhibition with growth factor treatment, as well as with PKA inhibition and activation, to further characterize the role of PKA-Akt crosstalk in GF-induced proliferation and differentiation in PC12 cells.

DISCUSSION

Traditionally, the temporal pattern of ERK activity has been thought to influence whether PC12 cells choose to proliferate or differentiation; transient ERK activity leads to proliferation while sustained ERK activity leads to differentiation. Various groups have found other signaling molecules that could modulate ERK activity and demonstrated ways to perturb the temporal dynamics of ERK, but do not provide a complete mechanism to allow full understanding of how cells decide to proliferate or differentiate. Therefore, instead of honing in on ways in which ERK can be regulated to achieve specific cellular processes, another approach to understanding how cells decide to proliferate or differentiate is to investigate other signaling pathways that work in parallel with ERK.

In this study, we investigated Akt signaling in PC12 cells, as this signaling pathway has been demonstrated to play a role in cell differentiation in other cell types

and to work concomitantly with ERK to regulate PC12 proliferation and differentiation.

Utilizing FRET-based biosensors to observe spatially compartmentalized Akt activity in PC12 cells, we found that upon EGF and NGF stimulation, Akt is predominantly active at the plasma membrane, where it is known to be activated by PI3K and PDK1. Specifically, EGF induces transient Akt activity, while NGF induces sustained Akt activity. Interestingly, their responses mirror the temporal dynamics of EGF- and NGF-stimulated ERK activity. We also showed that these two stimuli result in completely different spatial patterns of Akt signaling in other subcellular regions. EGF stimulation results in consistently transient ERK activity in various sub-cellular organelles; however, NGF stimulation results in a range of Akt activity profiles – from sustained activity in the plasma membrane to transient activity in the cytosol and Golgi – suggesting that these growth factors may engage widely differing signaling mechanisms in different subcellular locations. Phosphorylation is the result of a dynamic balance between the kinase and cognate phosphatase actions. Spatial gradients in phosphorylation have been predicted to occur through differences in the relative concentrations of kinase and phosphatase at different locations. This could be attributed to differences in subcellular concentrations of phosphatase activity, such as PP1A[138]. In regions such as the cytosol or Golgi, there may be a higher concentration of phosphatases, thus leading to more transient NGF-induced Akt activity, compared to NGF-induced Akt activity at the plasma membrane. At other subcellular regions, including the nucleus, and at mitochondrial and ER membranes, we were unable to detect Akt activity, even though previous studies have reported the existence of active nuclear Akt in PC12 cells, along with the implication of Akt activity in anti-apoptotic processes. Of note, these specifically targeted Akt activity biosensors have been shown to be functional in NIH3T3 cells (Zhou etal, unpublished).

These results could indicate the relatively low levels of Akt activity exist in these subcellular regions. Future experiments involving subcellular fraction of PC12 cells and western blots will help confirm these imaging results.

Since the cAMP/PKA pathway has been shown to modulate the temporal dynamics of GF-induced ERK activity at the non-raft region of the plasma membrane, we suspected that the cAMP/PKA pathway could have a similar effect on Akt activity. The cAMP/PKA pathway stimulates Akt in some cells and inhibits it in others. Here, we demonstrated that either inhibiting or upregulating PKA activity does not simply inhibit or activate Akt, but instead alters the temporal dynamics of Akt at the plasma membrane. As a results PKA most likely indirectly modulates Akt activity possibly through upstream regulators of Akt in the PI3K/Akt pathway, such as PI3K. While PI3K is one of the components involved in Akt activation, PI3K has also been shown to be directly phosphorylated by PKA at the regulatory subunit on Ser-83, leading to its activation[139, 140]. On the other hand, downstream regulators of PKA can modulate Akt activity. For example, other studies have shown that Rap1, a downstream target of PKA and Epac, can inhibit Akt activity [141]. To further decipher this complex interplay between Akt and PKA, we also investigated the presence of a feedback mechanism from Akt to PKA. Surprisingly, we found that Akt has a strong negative effect on PKA activity at the plasma membrane through the downregulation of cAMP levels, possibly through the upregulation of PDE3 activity[142]. However, we have yet to directly test whether PDE3 is involved in this regulatory pathway.

We then attempted to show the importance of Akt-PKA crosstalk in PC12 cell proliferation and differentiation. Since upregulating PKA with Fsk causes resting PC12

cells to differentiate to a certain extent, we hypothesized that further upregulating PKA by blocking Akt at the same time would have a similar or enhanced effect on PC12 differentiation. However, the toxicity of LY294002 interfered with the differentiation assay. Therefore, using lower doses of LY294002 would be beneficial. Moreover, LY294002 inhibits the upstream PI3k activity and may have broader effects. Therefore, utilizing SH-5, a specific Akt inhibitor could have a less detrimental effect on cells. Moreover, the Akt-PKA cross-regulation appears to be predominantly occur at the plasma membrane in PC12 cells. As a result, we can specifically inhibit this pool of Akt activity determine the functional role of plasma membrane Akt activity in cell differentiation.

MATERIALS AND METHODS

Materials

EGF, IBMX were purchase from Signm-Aldrich (St. Louis, MO). NGF was purchased from Harlan Laboratories. H89 was purchased from Cayman Chemical. Forskolin and LY294002 were acquired from LC Labs.

Cellular transfection, imaging and analysis.

PC12 cells were plated on sterilized glass coverslips in 35-mm dishes, and then they were grown to 70% confluence in DMEM (10% fetal bovine serum) at 37°C with 5% CO_2. Cells were transfected with Lipofectamine 2000 (Invitrogen). For imaging, PC12 cells were washed with Hanks' balanced salt solution buffer and imaged in. For imaging, cells were washed once and then imaged in Hanks' balanced salt solution in the dark at 37°C,

on a Zeiss Axiovert 200 M microscope with a cooled charge-coupled-device camera (MicroMAX BFT512; Roper Scientific, Trenton, NJ) controlled by METAFLUOR software (Molecular Devices, Sunnyvale, CA). Dual emission ratio imaging was performed using a 420DF20 excitation filter and a 450DRLP dichroic mirror and appropriate emission filters, 475DF40 for cyan fluorescent protein (CFP) and 535DF25 for yellow fluorescent protein (YFP). Exposure time was 50–500 ms. Images were taken every 20–30 s. Imaging data were analyzed with MetaFluor 6.2 software (Molecular Devices, Sunnyvale, CA). Cells were treated with drug as indicated, and images were analyzed using ImageJ software (NIH). Fluorescence images were background corrected by deducting the background (regions with no cells) from the emission intensities of CFP or YFP. Traces were normalized by taking the emission ratio before addition of drugs as 1

Chapter 4

Development of improved bioluminescence-based kinase activity reporters

INTRODUCTION

Protein phosphorylation/dephosphorylation is an important way by which cellular proteins are posttranslationally modified to modulate their function. In many cases, spatial microcompartmentation of protein kinase and phosphatase activities is required to achieve specific and optimized modulation in signaling events and therefore diverse physiological responses. Dysregulation of kinase activities and phosphorylation events has been implicated in a wide array of pathological diseases[10]. Therefore, efforts have been made to study different kinase activities by engineering biosensors to detect specific endogenous kinase activities. FRET-based biosensors have proven to be extremely useful tools in detecting and visualizing this spatiotemporal regulation of kinase dynamics. Being genetically encoded entails the introduction of a fluorescent reporter into living systems at the DNA level, followed by de novo synthesis, and subcellular targeting by the endogenous cellular machinery. However, as a result of the exogenous illumination, there are limitations to the usage of FRET-based biosensors. First, exogenous illumination can lead to high background noise resulting from direct excitation of the acceptor or photobleaching. Second, FRET-based reporters are incompatible with non-invasive deep tissue imaging of whole organisms and other applications where the cellular substrate or drug compounds are autofluorescent. Third, experimental problems also arise when additional external illumination is required, such as for optogenetic tools, which prevents simultaneous use of fluorescence imaging. Finally, the general light intensity required for external illumination sometimes causes phototoxic effects, which alter cellular behavior and ultimately leads to cell death.

To overcome some of the limitations, bioluminescence resonance energy transfer-based biosensors have been developed to monitor cell signaling[75, 143, 144]. In BRET-based readouts, the Cerulean in the FRET-based reporters is replaced with the enhanced variant of Renilla luciferase, RLuc8. When situated with proper distance and orientation to a suitable acceptor fluorophore, such as a yellow fluorescent protein (YFP). the energy produced by the enzymatic oxidation of benzyl-coelenterazine by RLuc8 can be transferred to the acceptor fluorophore, such as a yellow fluorescent protein (YFP)[145]. As a result, no exogenous illumination is required. Moreover, by avoiding the background formed by autofluorescence signals, BRET-based biosensors allow for sensitive imaging in tissues. With FRET-based biosensors, the blue-shifted illumination required for optogenetic tools interferes with the CFP excitation wavelength. In contrast, BRET avoids interference from fluorescent compounds. Without the need for exogenous illumination, BRET-based reporters can be effectively utilized with optogenetic tools to perturb protein activity with high specificity and monitor changes in cell signaling at the same time. Novel BRET-based biosensors have been generated to monitor protein-protein interaction between G-protein coupled receptors (GPCRs) and their binding partners, and second messengers such as calcium and cyclic-AMP (cAMP)[146-149]. However, only one BRET-based kinase activity reporter has been developed, a BRET-based sensor for extracellular signal-regulated kinase (Erk) activity called REV [150]. Here we present a generalizable design based on the bimolecular version of FRET-based kinase activity reporters for the development of sensitive BRET-based sensors to monitor the spatiotemporal dynamics of kinase activities, known as Bim-BRET-KARs[75, 151]. With

these new tools, we aim to demonstrate the applicability of these reporters in presence of fluorescent compounds and in combination with recently developed optogenetic tools.

RESULTS

Bim-BRET-KARs for PKA, Akt, JNK, and AMPK

Using our kinase-dependent bimolecular switch, we redesigned the FRET-based Bim-KARs by replacing the CFP with RLuc8, an RLuc variant with enhanced luminescent properties, to generate the bimolecular BRET-based kinase activity reporters, Bim-BRET-KARs (Fig. 4.1)[75, 82, 151, 152]. Traditionally our kinase activity biosensors are designed as unimolecular constructs. However, by separating the two portions of the molecular switch, the basal BRET is decreased, leading to an enhancement in the dynamic range. As a result, we first generated a sensor to specifically detect protein kinase A (PKA) activity by pairing the RLuc8-FHA1 fusion peptide with a YPet peptide containing the PKA-specific substrate from Bim AKAR[72] (Fig. 4.2A). Upon PKA activation, the PKA-specific substrate is phosphorylated and causes the FHA1 to bind to the phosphorylated site. The interaction between the phosphorylated PKA substrate and FHA1 brings the two portions of the reporting unit, Rluc8 and YPet in close proximity to allow BRET to occur. When expressed in HEK293 cells, the resulting biosensor, Bim-BRET-AKAR, produced a yellow-over-RLuc8 emission ratio increase of 23 ± 6.3% (n = 18) in response to treatment with a cAMP-elevating cocktail of the adenylyl cyclase activator forskolin (Fsk) and the general phosphodiesterase inhibitor 3-isobutyl-1-methylxanthine (IBMX) [46] (Fig. 4.2E,I). In contrast, the Bim-BRET-AKAR T/A mutant biosensor, where the target threonine residue is mutated to alanine, showed a

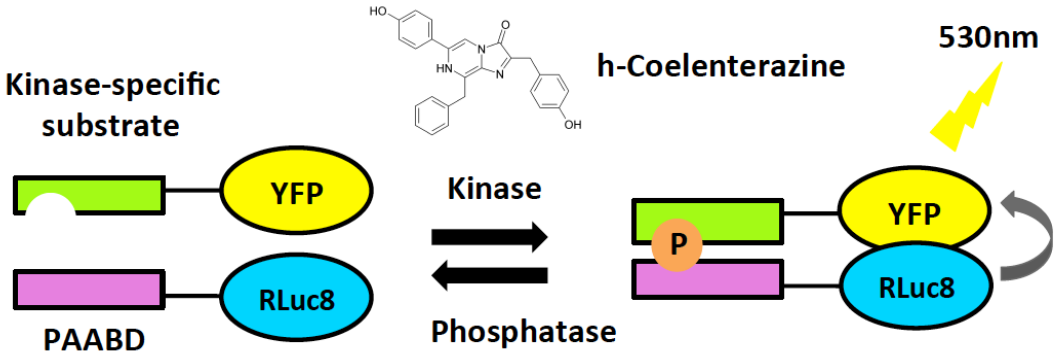

Figure 4.1 Schematic of Bim-BRET-KARs design
Bim-BRET KARS consists of two portions: kinase-specific substrate attached to YFP and phosphoamino binding domain (PAABD) attached to RLuc8. In presence of h-Coelenterazine and upon kinase activation, RLuc8 can emit luminescence and the PAABD can bind the phosphorylated substrate bringing YFP and RLuc8 in close proximity to thus allow BRET to occur.

negligible response of 2.4 ± 4.3% (n=15) to the same treatment, indicating that Bim-BRET-AKAR can be used to detect PKA activity in living cells with BRET-based readout (Fig. 4.4 A-D). Here we did not test H89, a PKA inhibitor, because of its interference with RLuc8[143].

To test the generalizability of this design, we developed additional Bim-BRET reporters for other kinases, Akt, JNK, and AMPK. These kinases have been extensively studied due to their roles in tumorigenesis, from cell growth and proliferation to survival and motility, responding to cytokines and environmental stress signals, and cell metabolism, respectively. Moreover, FRET-based reporters were previously developed to detect Akt, JNK, and AMPK activity and have successfully unveiled new molecular mechanisms in the regulation of these kinases in response to different stimuli[133 153-155]. With the Bim-BRET Akt reporter, we utilized RLuc8 and cpVenE172, an enhanced version of Venus as the BRET reporting unit (Fig. 4.2B). After the addition of 50 ng platelet-derived growth factor (PDGF) in NIH3T3 cells, the BRET change of Bim-BRET-AktAR increased by 15.8 ± 7.3% (n=6). Conversely, treating cells with a PI3K inhibitor, LY294002, caused a subsequent inhibition of Akt as demonstrated by the lack of BRET change (Fig. 4.2N). Similar to Bim-BRET-AKAR, RLuc8 and YPet were used as the BRET pair for Bim-BRET-JNKAR. Upon 5μM Anisomycin treatment, Bim-BRET-JNKAR generated a 23.5 ± 8% (n=30) over a period of 20 to 50 minutes (Fig. 4.2C,G,K). The kinetics of Bim-BRET-JNKAR is consistent with that of the FRET-based JNKAR reporter in HEK293 cells as well[66, 156]. Furthermore, pretreatment with JNK

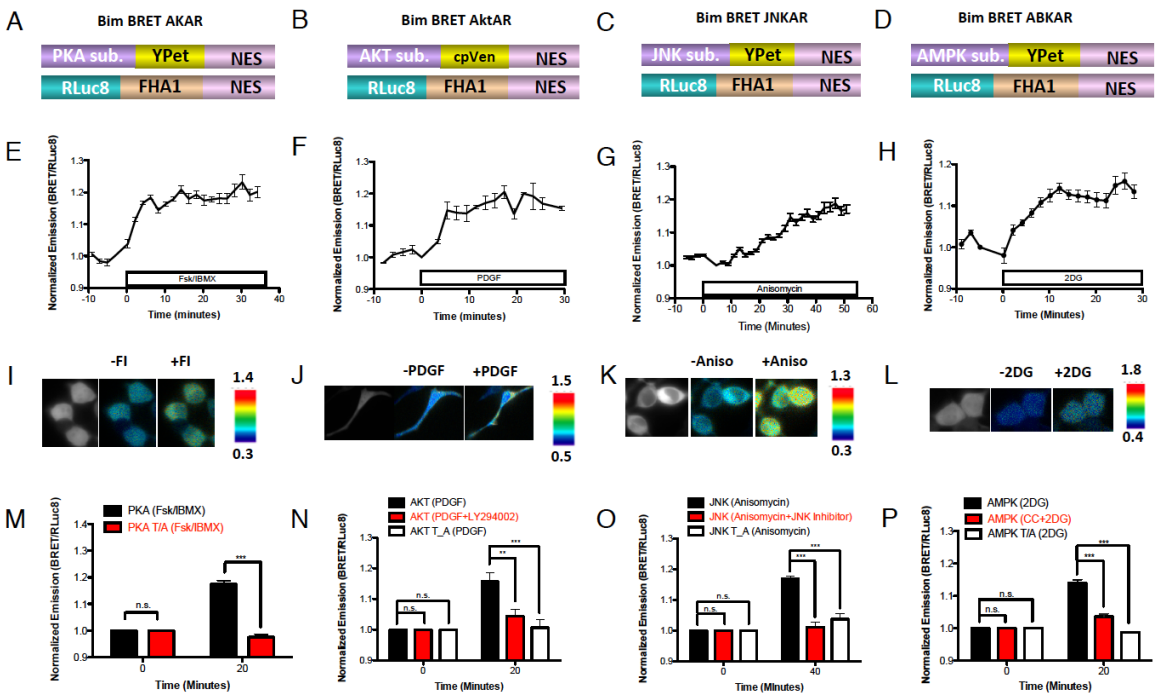

Figure 4.2 Characterization of Bim-BRET-KARs

(A) Schematic of Bim-BRET-AKAR (B) Bim-BRET-AktAR (C) Bim-BRET-JNKAR KRAS (D) Bim-BRET-ABKAR. (E) Representative time course plot of Bim-BRET-AKAR with 50µM Fsk and 100µM IBMX (F) Bim-BRET-AktAR with 100ng PDGF (G) Bim-BRET-JNKAR KRASR with 5µM Anisomycin. (H) Bim-BRET-ABKAR with 20mM 2DG. (I) Representative psuedocolor cell images of cells transfected with Bim-BRET-AKAR before and after Fsk and IBMX treatment (J) Bim-BRET-AktAR before and after 100ng PDGF treatment (K) Bim-BRET-JNKAR with 5µM Anisomycin (L) Bim-BRET-ABKAR with 20mM 2DG. (M) Bar graphs summarizing responses of Bim-BRET-AKAR (Black) and Bim-BRET-AKAR T/A (Red) to Fsk and IBMX, (N) and Bim-BRET-AktAR response to PDGF (Black), combination of PDGF and 20µM LY294002 (Red), and response of Bim-BRET-AktAR T/A to PDGF after 20 minutes (White). (O) Bar graphs summarizing Bim-BRET-JNKAR response to Anisomycin (Black), a combination of Anisomycin and JNK inhibitor VII, (Red), and response of Bim-BRET-JNKAR T/A to Anisomycin (White) after 40 minutes. (P) Bar graphs summarizing Bim-BRET-ABKAR (Black) and Bim-BRET-ABKAR T/A (Red) response to 20mM 2DG.

Inhibitor VIII suppressed the Anisomycin-induced BRET increase (Fig. 4.2O). We then generated and characterized Bim-BRET reporter for detecting AMPK activity in HEK293 cells, by treating cells expressing Bim-BRET-ABKAR with 2-deoxyglucose (2-DG), a non-hydrolyzable glucose analog that inhibits glycolysis and lowers ATP levels, thereby activating AMPK[157] (Fig. 4.2D,H). Bim-BRET-ABKAR generated a yellow-over-RLuc8 emission ratio increase of 13.9 ± 5.9 % (n = 29) after a 20-minute treatment with 20 mM 2-DG (Fig. 4.2H,L,P). In presence of AMPK inhibitor, Compound C, 2DG was unable to elicit a change in BRET from Bim-BRET-ABKAR. Importantly, no change in the yellow-over-RLuc8 emission ratio was observed in cells expressing Bim-BRET-ABKAR T/A (n = 29), confirming that the increase in BRET was caused by reporter phosphorylation (Fig. 4.2P).

Detecting subcellular localized kinase activities with Bim-BRET-KARs

Much of the specificity of cell signaling is attributed to the compartmentalization of signaling components to subcellular regions. This formation of microdomains allow cells to regulate the activity of signaling molecules to elicit distinct cell responses. Therefore, it is important to be able to detect kinase activity in various subcellular regions. One important advantage of genetically-encoded KARs is that they can be targeted, using subcellular localization signals, to distinct cellular compartments where they can detect local kinase activity[158].

Previously a plasma membrane targeted unimolecular FRET reporter, AKAR4-Kras, was developed and revealed the dynamic differences in PKA activity amongst

plasma membrane microdomains[72]. As a result, we also generated a Bim BRET version that consists of the substrate-YPet unit of Bim-BRET-AKAR targeted to the plasma membrane via a CAAX targeting sequence derived from K-Ras, and the RLuc8-FHAI portion that is kept in the cytoplasm (Fig. 4.3A). Specifically, treating cells expressing Bim-BRET-AKAR Kras with a combination of Fsk and IBMX caused a 40.6% ± 2.4% (n = 27) increase in BRET/RLuc8 ratio, whereas the T/A mutant of the reporter showed no BRET change (Fig. 4.3J). DMSO treatment failed to induce PKA activity as well (Fig. 4.3J). Similarly, upon treatment with Fsk and IBMX, cells expressing a nuclear-localized BRET-based PKA reporter, Bim-BRET-AKAR NLS, showed only a small and gradual yellow-over-RLuc8 emission ratio increase of 4.0 ± 0.7% after 30 minutes (n = 18), which is consistent with the time required for the activated PKA catalytic subunit to translocate into the nucleus to phosphorylate its nuclear targets[159] (Fig. 4.3E,H,K). Also, the reporter did not respond to DMSO (Fig. 4.3K). In addition to subcellular PKA activity, we probed the plasma membrane AMPK activity (Fig. 4.3C). 2DG stimulation led to a 23.2 ± 1.4% increase (n=23), while pretreatment with Compound C prevented induction of AMPK activity by 2DG (n=12) (Fig. 4.3F,I,L). To further prove that Bim-BRET-ABKAR KRAS was sensing the inhibitory effect of Compound C, cells were treated with the vehicle control of Compound C, DMSO. Subsequent treated with 2DG led to a large increase in Bim-BRET-ABKAR KRAS response, indicating that the reporter accurately detected the disruption of AMPK activity by Compound C. Together these data indicate that Bim-BRET-AKAR and -ABKAR can sensitively and accurately detect PKA and AMPK activity at subcellular locations, respectively.

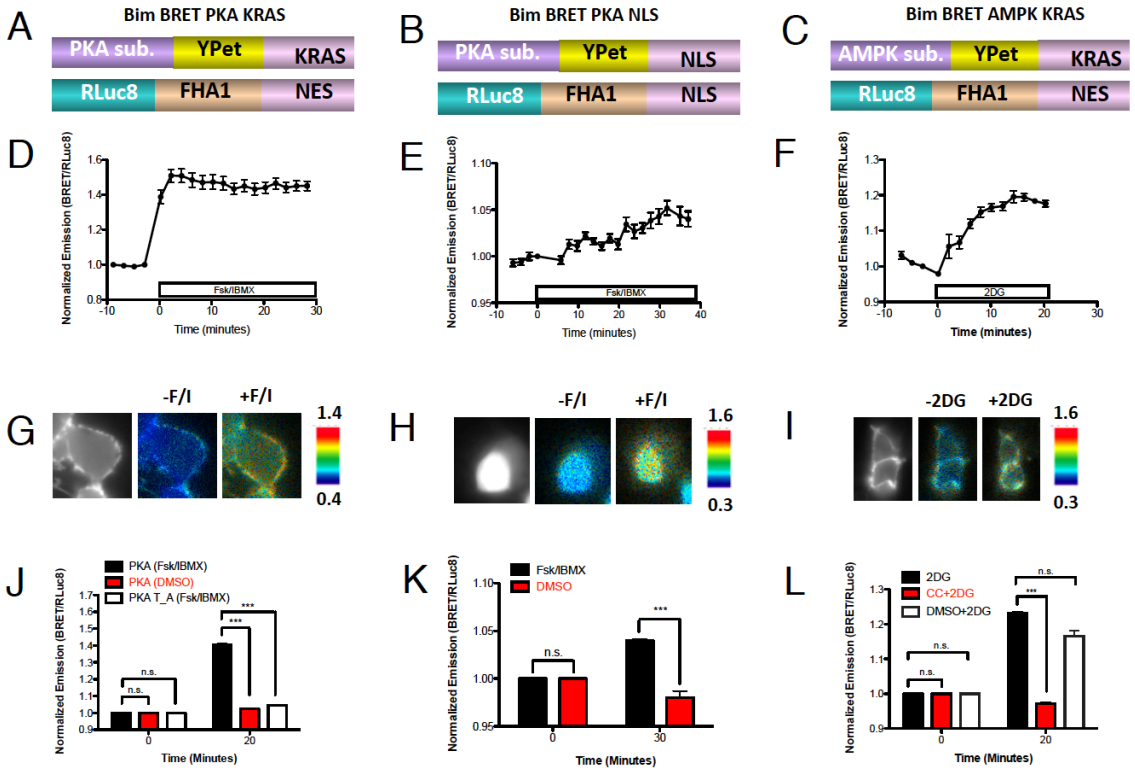

Figure 4.3 Subcellular Bim-BRET-KARs

(A) Schematic of Bim-BRET-AKAR KRAS (B) Bim-BRET-PKA NLS (C) Bim-BRET-ABKAR KRAS. (D) Representative time course plot of Bim-BRET-AKAR KRAS with 50µM Fsk and 100µM IBMX (E) Bim-BRET-AKAR-NLS with Fsk and IBMX (F) Bim-BRET-ABKAR KRASR with 20mM 2DG. (G) Representative psuedocolor cell images of cells transfected with Bim-BRET-AKAR KRAS before and after Fsk and IBMX treatment (H) Bim-BRET-AKAR NLS before and after Fsk and IBMX treatment (I) Bim-BRET-ABKAR with 2DG. (J) Bar graphs summarizing responses of Bim-BRET-AKAR KRAS to Fsk and IBMX (Black), and DMSO (Red), and Bim-BRET-AKAR KRAS T/A response to Fsk and IBMX (White) after 20 minutes. (K) Bar graphs summarizing Bim-BRET-AKAR NLS response to Fsk and IBMX (Black) and DMSO (Red) after 20 minutes. (L) Bar graphs summarizing response of Bim-BRET-ABKAR KRAS to 2DG (Black), Compound C and 2DG (Red), and DMSO and 2DG (White).

A BRET-based sensor design overcomes small molecule fluorescence

When fluorescent compounds are utilized with FRET-based reporters the intrinsic fluorescence properties increase the background, therefore decreasing the sensitivity of the reporters. To demonstrate this, Bim ABKAR, a bimolecular FRET-based AMPK reporter was treated with Compound C, which is autofluorescent. Upon the addition of Compound C, an immediate increase in background of the CFP channel was observed (Fig. 4.4A,B). On the other hand, because Bim-BRET reporters utilize RLuc8 in place of CFP and do not require exogenous illumination, the autofluorescence of Compound C does not appear in the background reading of RLuc8 channel nor does it interfere with the Bim-BRET-ABKAR readout as shown earlier in the chapter (Fig. 4.4C,D).

Previously, in a primary drug screen utilizing a FRET-based PKA reporter, AKAR3, some fluorescent drugs contributed to abnormal fluorescent changes in the FRET readout like Compound C. Since we have shown that Bim-BRET-KARs can overcome this limitation of FRET-based reporters, and detect specific kinase activity, we wanted to test the sensitivity of Bim-BRET-KARs in a high-throughput screening (HTS) format for future use in drug screens[158]. Therefore, we plated HEK293T cells transfected with Bim-BRET-AKAR into a 96-well plate and monitored BRET changes upon drug stimulation. Treatment with Fsk and IBMX generated a 13.1 ± 0.8% increase in PKA activity, which is a stark contrast to the control condition with DMSO treatment. In addition, the BRET response of Bim-BRET-AKAR T/A remained unchanged after Fsk and IBMX stimulation of PKA and with DMSO, the control condition. Similarly, Bim-BRET- AKAR KRAS was tested in the same format. Normally, signals from subcellular

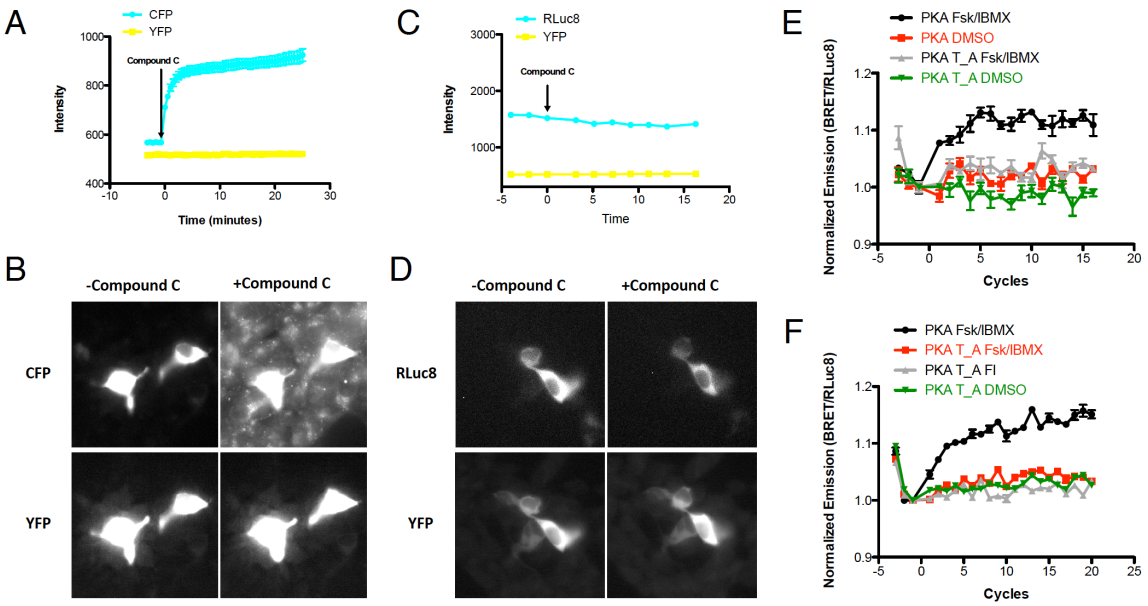

Figure 4.4 Bim-BRET-KARs are ideal for imaging with fluorescent compounds
(A) Representative time course plot of CFP and YFP intensity of cells transfected with Bim ABKAR before and after 20μM Compound C addition (B) Representative CFP and YFP channel images of HEK293 cells transfected with Bim ABKAR before and after Compound C addition. (C) Representative time course plot of RLuc8 and YFP intensity of cells transfected with Bim-BRET-ABKAR before and after 20μM Compound C addition. (D) Representative RLuc8 and YFP channel images of cells transfected with Bim ABKAR before and after Compound C addition. (E) Time course plot of Bim-BRET-AKAR and (F) Bim-BRET-AKAR KRAS in HTS format with indicated treatments and controls.

regions are difficult to detect in high-throughput screening formats because of the low dynamic ranges and the very limited area of detection. However, with the bimolecular design, the dynamic ranges of targeted reporters are significantly enhanced, therefore making imaging in a large cell population possible. Following Fsk and IBMX stimulation, Bim-BRET-AKAR KRAS generated 15.9 ± 0.789% (n=27) BRET change (Fig 4.4E). Conversely, Bim-BRET-AKARKRAS did not show a response to DMSO indicating that response from Fsk and IBMX treatment was due to elevating cAMP levels amongst the cells. Also Bim-BRET-PKA KRAS T/A did not respond to either Fsk and IBMX or DMSO, further demonstrating that Bim-BRET-AKAR KRAS can specifically and robustly detect PKA activity in a HTS setting (Fig 4.4F). Together these data show that Bim-BRET-KARs can be utilized in the presence of fluorescent compounds and has potential accurately detecting kinase activity in HTS setting.

Combining Bim-BRET-KARs with Optogenetic Tools

Currently, an emerging set of popular tools used to perturb signaling pathways with high spatiotemporal resolution to decipher complex biological processes are known as optogenetic tools. They allow one to perturb the biological process by acting directly on a protein and photoinduce a change of its activity. The protein is required to have a light-sensitive module, which may exist within the protein core or be attached, genetically or chemically to the protein of interest. So far, these optogenetic tools have been used to "uncage" an agonist or antagonist of a particular protein, control intracellular concentration of a protein of interest, control protein synthesis, degrade proteins, or relocate proteins to subcellular locations. Some of the commonly used

optogenetic tools that are naturally light-sensitive include azobenes, phytochromes (PHYs), Rhodopsin, and flavorproteins which include light-, oxygen- or voltage-sensing (LOV) proteins, plant light-sensitive cryptocrhome (CRY), and blue light-utilizing flavin (BLUF) proteins[160]. Each protein is sensitive to different wavelength of light.

A recent application of the LOV domain was in the development of a PKA inhibitor whose activity was light dependent, called LOV-PKI[161]. The inhibitor was constructed so that the light-sensitive portion, LOV domain, is fused to a portion of a natural occurring PKA inhibitory peptide, PKI. In the dark, PKI is hidden within the LOVE domain. But upon exposure to blue light, a large conformational changes cause the unfolding of the Jα helix in the LOV domain and exposes the PKI so that it can interact with PKA. Because luminescence imaging can be performed in the absence of external light, Bim-BRET-KARs can be partnered with optogenetic tools, such as LOV-PKI

To demonstrate this, LOV-PKI tagged with mCherry, a red fluorescent protein used as a control, was transfected in HEK293T cells along with Bim-BRET-AKAR KRAS. HEK293T cells were first stimulated with Fsk and IBMX and then we applied a 5 minute exposure to blue light at 435nm to activate LOV-PKI. As expected, a 35.2 $\pm$ 2.1% (n=14) increase was observed from the Fsk and IBMX treatment. However, the subsequent decrease from inhibition of PKA was not observed after the 5 minute light exposure (Fig. 4.5A). Even an additional 5 minute exposure to blue light was not able to induce the PKI effect on Bim-BRET-AKAR KRAS. Furthermore, the relatively long exposure to the blue light rapidly caused a decay in the Rluc8 channel, leading to noisy signals (Fig. 4.5B). In parallel, cells transfected with just Bim-BRET-AKAR KRAS were subjected to the same treatments. Bim-BRET-AKAR KRAS responded as usual to Fsk

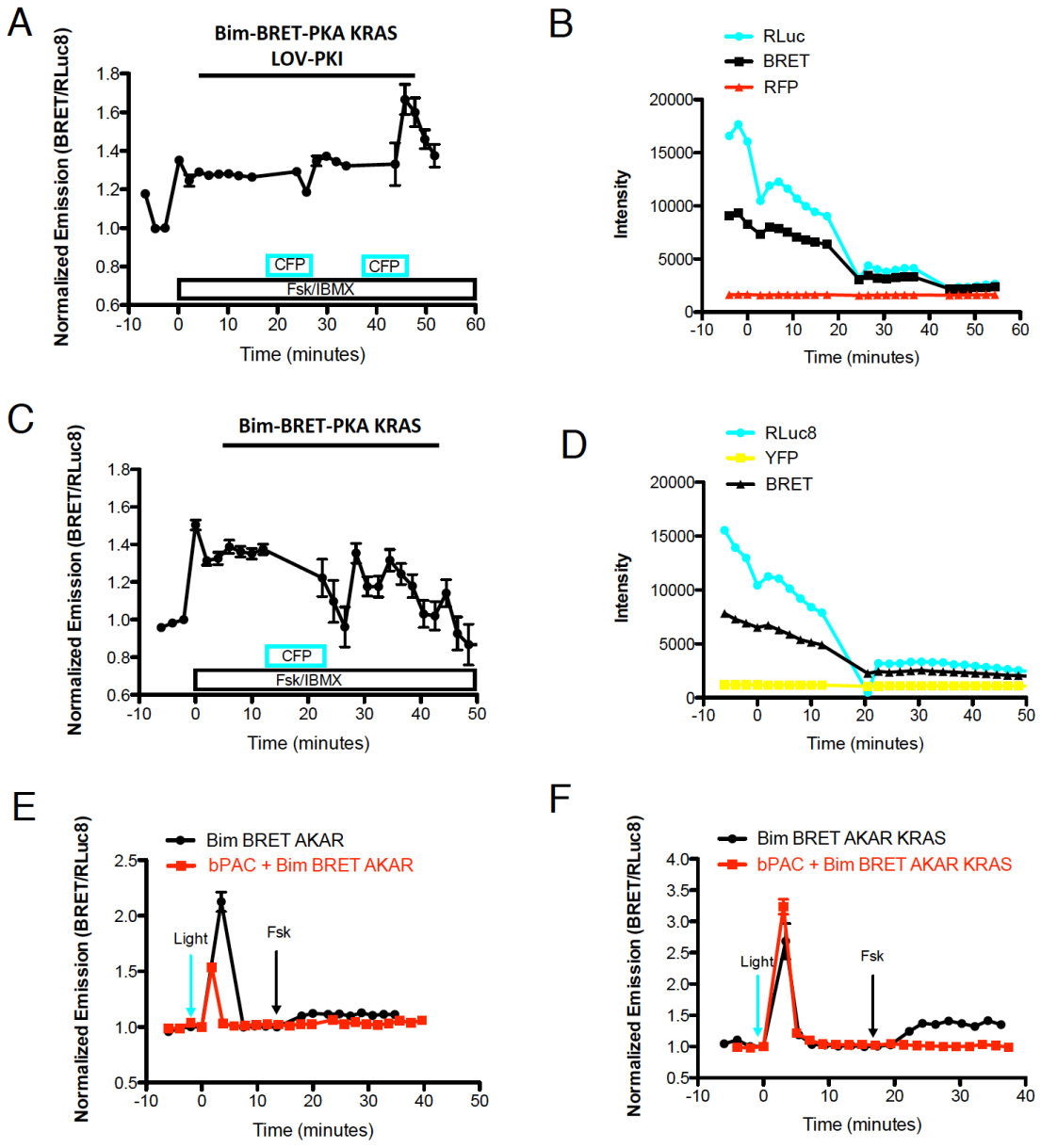

Figure 4.5 Applying optogenetic tools to Bim-BRET AKAR-KRAS
(A) Time course plot of Bim-BRET-AKAR KRAS response to Fsk and IBMX, and LOV-PKI activation. (B) Time course plot of changes in the Rluc, BRET and RFP channel intensities over the course of the experiment. (C) Time course plot of Bim-BRET-AKAR KRAS response to Fsk and IBMX, and LOV-PKI activation. (D) Time course plot of changes in the Rluc, BRET and RFP channel intensities over the course of the experiment. (E) Representative curves of cells transfected with Bim-BRET-AKAR (black), and a combination of Bim-BRET-AKAR and bPAC (red) stimulated with light and subsequently treated with 50µM Forskolin (Fsk). (F) Representative curves of cells treated with the same conditions but transfected with Bim-BRET-AKAR KRAS (black), and a combination of Bim-BRET-AKAR KRAS and BgAC (red).

and IBMX (n=16). Since the sample did not contain LOV-PKI, exposure to blue light should not lead to a decrease in PKA activity. However, we did observe a slight decrease after a 5 minute exposure to blue light (Fig. 4.5C). Again, the Rluc8 channel also showed a rapid decay after the blue light exposure (Fig. 4.5D). These results show inability of LOV-PKI to be activated effectively without damaging the biosensors or even the cells for that matter. Additional tests will be required to determine the right amount of intensity to activate LOV-PKI in cells since the published experiments from Yi *et al*. were performed *in vitro*[161].

Another photoactivatable protein that could be used in conjunction with Bim-BRET-AKAR is the light-gated adenylyl cyclases. Specifically, BLUF (blue light sensor using falvin adenine dinucleotide)-activated adenylyl cyclase (bPAC) has been a useful tool in elevating cAMP levels in neurons, bacteria, and cilia to monitor changes in organism behavior and Ca^{2+} fluctuations from cyclic nucleotide-gated (CNG) channels [162-165]. First we tested the effect of stimulated bPAC on Bim-BRET-AKAR KRAS. HEK293T cells. The cells were transfected with both constructs and stimulated with one minute exposure to blue light. A dramatic transient response was observed, possibly due to the large production of cAMP and the rapid degradation by phosphodiesterases, bringing the BRET response back to baseline. (Fig. 4.5E) To ensure that Bim-BRET-AKAR was still working properly in the presence of bPAC, cells were subsequently stimulated with Fsk. However, Fsk was unable to induce a response from Bim-BRET-AKAR. The same treatments were applied to cells that were only transfected with Bim-BRET-AKAR. Interestingly, exposure to light also caused a large transient PKA activity even though no bPAC was present, and the PKA activity was increased by Fsk treatment as normally

observed. Similar responses were also observed with the same treatments in cells transfected with Bim-BRET AKAR KRAS. These results indicate that the bPAC may not be properly activated. Moreover, the light induction could be interfering with the luminescence, contributing the large transient response observed in cells transfected with and without bPAC. However, the light exposure did not prevent the Bim-BRET-AKAR from working properly because upon Fsk stimulation after light exposure, the diffusible and plasma-membrane targeted probes in control cells still exhibited a difference in the response amplitude, which was observed in previous experiments. As with LOV-PKI, additional experiments will be needed to determine the optimum testing conditions required for these optogenetic tools to work properly in live-cell imaging setting.

DISCUSSION

Protein kinases serve as the key regulators of signal transduction cascades by phosphorylating protein targets in response to various extracellular and intracellular stimuli. In turn, this phosphorylation leads to different effects on protein activity and therefore, the propagation of signal transduction to elicit a desired physiological response. Dynamic tracking of specific kinase activity in living cells has been made possible by a class of genetically encoded reporters based on FRET. It offers sensitive ratiometric fluorescence readout, precise molecular targeting, and high spatiotemporal resolution compared to other fluorescent kinase sensors. A general modular design for such kinase activity reporters based on a phosphorylation-dependent conformational switch has been successfully applied to many serine/threonine and tyrosine kinases. Yet,

there are limitations to the applicability of FRET-based reporters in presence of fluorescent compounds and optogenetic tools.

As a result bioluminescence-based assays, which do not require exogenous illumination and are not susceptible to signal obstruction by autofluorescence, are becoming useful tools for these types of experiment conditions and therefore, can achieve higher sensitivity than fluorescence-based assays[75, 166]. Here we presented a generalizable design for BRET-based kinase activity, Bim-BRET-KARs by demonstrating the functionality and specificity of Bim-BRET-AKAR, Bim-BRET-AktAR, Bim-BRET-JNKAR, and Bim-BRET-ABKAR in detecting PKA, Akt, JNK, and AMPK activity. Additionally, we demonstrated the targetability of these reporters and their ability to detect temporally distinct kinase activity in subcellular regions.

To prove that Bim-BRET-KARs can overcome some of the limitations of FRET-based reporters, we first tested Bim-BRET-KARs with fluorescent compounds, such as Compound C and showed that Bim-BRET-KARs can specifically report on kinase activity without interference from fluorescent compounds. Due to the high signal-to-noise ratio, the lack of exogenous illumination, and applicability with fluorescence compounds, bioluminescence-based reporters are also useful tools to implement in HTS. With Bim-BRET-AKAR and Bim-BRET-AKAR KRAS, we demonstrated that Bim-BRET-KARs can be applied to HTS format. However, since HTS involve averaging the signal amongst a whole cell population, the BRET signal is reduced to about half of the reported value in single-cell imaging, which is what we also observed in our experiments. Consequently, the resolution of the spatiotemporal differences in kinase activity in response to different types of compound treatments may be decreased in HTS format. Therefore, future efforts

to increase the dynamic range of Bim-BRET-KARs are necessary. Some approaches include incorporating brighter luciferases such as a new smaller and brighter luciferase called Nanoluc (Promega)[167].

We also attempted to co-image Bim-BRET-KARs with two optogenetic tools, LOV-PKI and bPAC. However we were unable to do so due to the sensitivity of luminescence to exogenous illumination and the inability to properly activate LOV-PKI and bPAC. Additional characterization of LOV-PKI and bPAC in live-cell imaging is necessary to determine the proper conditions required to activate LOV-PKI and bPAC without generating articfacts in the BRET signals. Moreover, since high intensity light was shown to be detrimental to bioluminescence, finding an alternative optogentic tool that does not require high light intensity to activate will be beneficial. At the same time, incorporating more stable and robust luciferases in Bim-BRET KARS will help counteract the damaging effects of exposure to high intensity illumination.

To further expand the applicability of Bim-BRET-KARs, targeting Bim-BRET reporters to additional important organelles such as the mitochondria, Golgi, ER, and lysosome can be generated to study their functional role. Furthermore, expanding the color variation of BRET-reporters will allow for multiplexed imaging of more that one kinase activity at the same time.

MATERIALS AND METHODS

Construction of Bim BRET KARs

RLuc8-FHA1 was PCR amplified and subcloned into pCDNA3 (Invitrogen) containing the 3'-NES (LPPLERLTL). YPet and cpVenus-E172 were PCR amplified with forward

primers that introduced the PKA-specific substrate (LRRATLVD), JNK-specific substrate (DSVKTPEDEGNPLLEQLEKKGGTGGSEL), Akt-specific substrate (PRPRSCTWPDPRPEF), or AMPK-specific substrate (MRRVATLVD), or the appropriate threonine-to-alanine mutations, and the PCR fragments were subcloned into pCDNA3 containing a 3'-NES, a plasma membrane-targeting sequence derived from K-Ras (KKKKKSKTKCVIM) or NLS sequence (GCIKSKRKDK).

Cell Culture and Transfection

HEK293, COS-7 and NIH3T3 cells were grown in DMEM cell culture media (Gibco) supplemented with 10% FBS and 1% penicillin/streptomycin at 37^{o}C with 5% CO_2. All biosensors were transfected into HEK293T, Cos7, and NIH3T3 cells via Lipofectamine 2000 (Invitrogen) at 60% confluency, according to manufacturer's protocol. For the Bim BRET AktAR reporter, NIH3T3 cells were serum-starved for 24 h. Cells were plated in 35-mm glass-bottom dishes for single-cell imaging experiments and in 10-cm culture dishes for cell-population studies.

BRET Imaging and Analysis

Cells were imaged on a Zeiss Axiovert 200M microscope with a Evolve EM cooled charge-coupled device camera (Photometrics) controlled by METAFLUOR software (Universal Imaging, Downingtown, PA). Cells were maintained in the dark at room temperature and washed with Hank's Balanced Salt Solution (HBSS). Using a 450DRLP dichroic mirror and a 475DF40 emission filter and for luciferase emission and a 535DF25 for BRET emission, images were acquired immediately after 10uM benzyl-coelenterazine

addition. Acquisition time was 90 seconds. Images were acquired every 2-4 minutes. Cells were treated with Phorbol-12-myristate-13-acetate (PMA; Sigma), forskolin (Fsk; Calbiochem), 3-isobutyl-1-methylxanthine (IBMX), ionomycin (Iono; Sigma), platelet-derived growth factor (PDGF), anisomycin (Aniso), and 2-Deoxy-D-glucose (2DG) as indicated. Images were background corrected and processed on Image J software (NIH).

Chapter 5

Developing improved molecular tool for measuring the dynamics of cAMP

INTRODUCTION

Signaling through cAMP influences many biological processes that have been presented in earlier chapters, such as cell migration, proliferation, differentiation, and metabolism. Aberrations in the cAMP signaling pathway have been shown to have implications for clinical conditions such as obesity and type 2 diabetes mellitus, heart disease, and neurological disorders. The classic model of cAMP signaling involves hormone-mediated activation of G-protein coupled receptors (GPCRs) to initiate a cascade of intracellular events involving activation of Gα stimulatory protein and transmembrane adenylyl cyclase (tmAC), which generates cAMP. Many of the cAMP-mediated signaling events that occur to bring about changes to these cellular processes are carried out by cAMP effector proteins, cAMP-dependent protein kinase (PKA), and exchange protein directly activated by cAMP (Epac).

In order to achieve highly specific cellular responses to external stimuli, cells organize components of cAMP signaling into discrete microdomains so that different pools of cAMP can be generated in response to extracellular signals or intrinsic signals. This restriction is partly achieved by phosphodiesterase (PDE), the enzyme responsible for the degradation of cAMP. Furthermore, scaffolding proteins such as AKAPs, help establish distinct environments within subcellular regions by assembling specific signaling complexes. The availability of different pools of cAMP to the local effectors within the same compartments should enhance the specificity and efficiency of cAMP signaling.

To analyze the spatiotemporal dynamics of second messenger signaling, a series of FRET-based cAMP biosensor, represented by Indicator for cAMP Using Epac (ICUE),

was designed by sandwiching full length or truncated Epac proteins, guanine exchange factors for the small GTPase Rap1, between two fluorescent proteins[168, 169]. Upon cAMP binding, the sensing domain undergoes a conformational change resulting in a decrease in FRET. More recently, we developed ICUE3 with an increased dynamic range by changing the FRET acceptor Citrine to a circularly permuted Venus at lysine 194. The large dynamic range of ICUE3 (~100% emission ratio change) makes it suitable for subcellular targeting for detecting local cAMP changes (e.g., plasma membrane and nucleus, primary cilia as addition of subcellular localization tags sometimes leads to decreased response amplitudes[74, 170, 171]. However, since cAMP concentrations vary among different cells, tissues and distinct conditions, the current sets of probes have limited applicability in situations where the intracellular cAMP concentration is too low. For example, ritodrine, a β_2-adrenergic receptor (β_2AR) partial agonist was unable to elicit a response from ICUE3, even though activation of β_2AR are known to induce increase in cAMP levels[168]. In addition, often low cAMP levels are picked up by PKA activity reporters due to their ability to amplify the cAMP signal through PKA phosphorylation activity. For example, in PC12 cells, both EGF and NGF are able to induce PKA activity in the plasma membrane[46]. Since PKA is activated by cAMP, we should be able to utilize the cAMP biosensor to detect changes in cAMP upon growth factor treatment. However, both ICUE3 and Epac1-cAMPs, a cAMP reporter containing only the cAMP-binding domain of Epac1, were unable to detect changes in cAMP levels induced by growth factors[172]. Therefore, since PKA activity reporters indirectly detect cAMP dynamics through PKA activity, generating a more sensitive reporter that directly interacts with cAMP is ideal to accurately detect cAMP levels.

RESULTS

Development and characterization of a more sensitive cAMP biosensor

Between the two cAMP effector proteins, PKA and Epac share a conserved cAMP-binding domain (CNBD). However, the regulatory subunit of PKA has been shown to have higher affinity for cAMP than the cAMP-binding domain within Epac1. Based on sequence alignment of the conserved cAMP-binding region, Epac1 lacks the glutamic acid (Glu) that is necessary for tight binding in PKA. It was proposed that Epac1 and PKA both originally possessed the same Glu residue at this conserved site; however, to avoid being saturated by cAMP at the resting state of the cell and thus incapable of responding to an increase of cellular cAMP, Epac1 evolved away from PKA by acquiring an E270Q mutation[173]. The mutation has resulted in a larger and overall less rigid cAMP-binding pocket in Epac1, leading to a lower affinity for cAMP[173, 174]. As a result, we aimed to revert the residue back to glutamine in Epac1, to mimic the cAMP-binding region within the regulatory subunit of PKA to achieve a more sensitive cAMP-reporter.

We incorporated the Q270E mutation into the CNBD of Epac1 within ICUE3 (Fig. 5.1A). To test whether the mutation enhances the binding of cAMP to ICUE3, we purified both ICUE3 and ICUE3 Q270E from HEK293T cells and took spectrophotometric measurements to compare the emission spectrum of the two reporters. Addition of cAMP decreases yellow emission at 525 nm emission peak, and increases the cyan emission at 485nm emission peak, consistent with reduced FRET change of ICUE reporters. We calibrated these FRET changes to cAMP concentrations, allowing us to measure cAMP responses quantitatively. At 10μM of cAMP, ICUE Q270E elicited

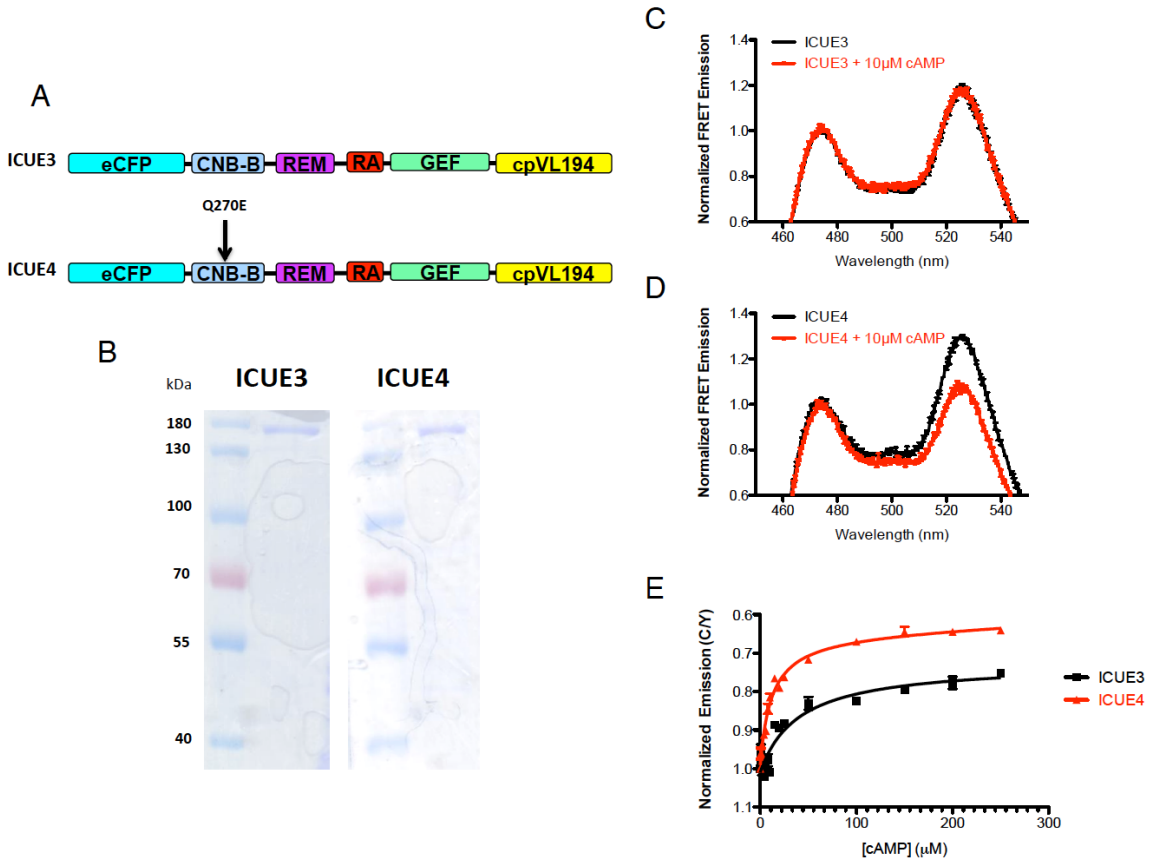

Figure 5.1 *In vitro* characterization of ICUE4
(A) Schematic of ICUE3 and ICUE4 reporters. (B) SDS gel showing purified ICUE3 and ICUE4 at ~152kDa. (C) Spectra of purified ICUE3 and (D) ICUE4 with and without 10μM cAMP. (E) ICUE3 and ICUE4 (5μM) incubated with varying concentrations of cAMP reveal a dose-response relationship of FRET change to cAMP concentrations (n=3) with K_d of 39.8μM and 11.8, respectively.

~18.5% FRET change, while ICUE3 did not show significant difference in FRET (Fig. 5.1C,D). This was also evident in the K_d values that were obtained from the spectrophotometric experiment, 11.8μM for ICUE Q270E and 39.8μM for ICUE3. Moreover, at saturating concentrations of cAMP, ICUE Q270E showed a higher maximum FRET change than ICUE3 (Fig. 5.1E). All together these data confirm that the Q270E does increase the binding affinity of ICUE to cAMP. Therefore, we named this biosensor ICUE4.

We then wanted to test the ability of ICUE4 to sense intracellular cAMP levels in comparison to ICUE3, to further confirm its enhanced binding. HEK293T cells were transiently transfected with either ICUE3 or ICUE4 and then treated with sequential submaximal doses of the general β adrenergic receptor agonist isoporterenol (Iso) in order to elicit low levels of cAMP production[168]. Neither ICUE3- nor ICUE4-expressing cells responded to treatment with 1 nM Iso; however, both probes maximally responded to treatment with a maximal dose of 50 μM Forskolin (Fsk), an adenylyl cyclase agonist, indicating the reporters are functional (Fig. 5.2A). At 40nM Iso, both probes produced clear, transient responses. In addition, clear differences in the amplitude of the FRET change were also apparent between ICUE3 and ICUE4. Whereas ICUE3 showed a modest 48.3 ± 5.2% (n=4) FRET ratio change, ICUE4 showed a 56.6 ± 10.8% (n=5) response (Fig. 5.1B). Increasing Iso concentrations subsequently induced larger responses from ICUE4 than from ICUE3 (Fig. 5.1C-F), suggesting that, in addition to enhancing the cAMP binding affinity of ICUE, the Q270E mutation also improves the dynamic range of the reporter. However,

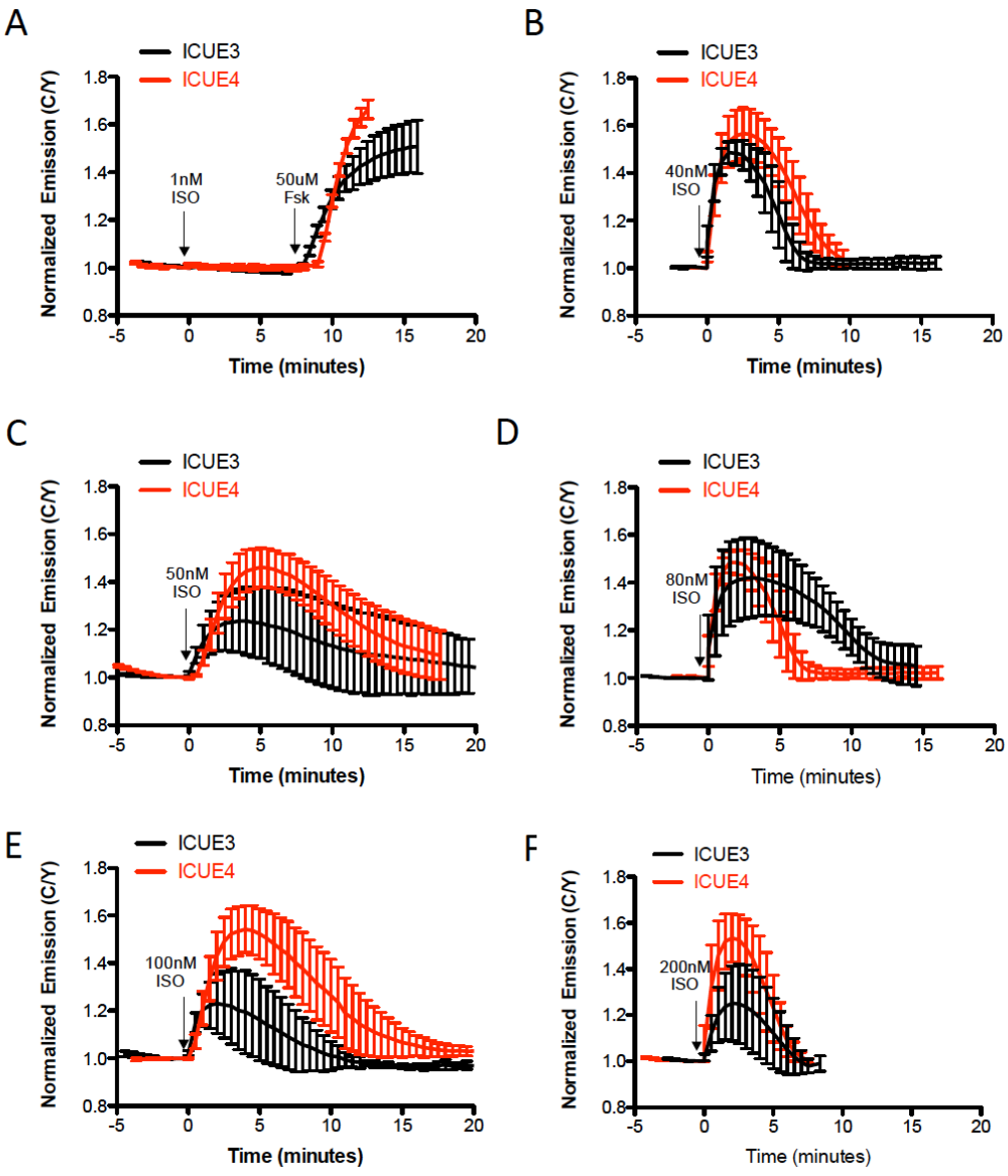

Figure 5.2 Characterization of ICUE4 with Isoproterenol
(A) Comparison of ICUE3 and ICUE4 FRET responses to 1nM (black n=6, red n=4), (B) 40nM (black n=4, red n=5) (C) 50nM (black n=4, red n=7), (D) 80nM (black n=2, red n=5) (E) 100nM (black n=3, red n=4) (F) 200nM Isoproterenol (black n=3, red n=4) (ISO)

we did not detect a clear relationship between the magnitude of the FRET change and the Iso concentration used, either with ICUE4 or with ICUE3. This discrepancy may be due to cell-to-cell variations in receptor expression levels.

Therefore, we next utilized the direct adenylyl cyclase activator forskolin, which is not influenced by receptor expression, in order to reduce cell-to-cell variability in cAMP production. In the presence of a low dose (5 μM) of Fsk, cells expressing ICUE3 produced a 3.7 ± 0.8% (n=3) FRET response, while ICUE4-expressing cells displayed an 11 ± 2.09% (n=3) FRET change (Fig. 5.2A, B). At 10 μM Fsk, ICUE3 started to show a more dramatic difference, with only a 20.97 ± 2.9% (n=5) FRET change compared with 45.2 ± 2.01% (n=5) for ICUE4. At 30 μM and 40 μM Fsk, ICUE4 continued to show a larger response to cAMP than ICUE3. However, whereas the FRET response from ICUE3 continued to increase from 40.2 ± 5.5 % (n=7) to 61.6 ± 6.5% (n=8) for 30 μM and 40 μM Fsk, respectively, ICUE4 displayed similar FRET responses of 75.8 ± 8.0% (n=8) and 77.9 ± 4.0% (n=10) to both treatments (Fig. 5.2A, B). The lack of an additional increase from ICUE4 even though the Fsk concentration was increasing, may indicate that the response from ICUE4 has already saturated at 30 μM Fsk due to the potentially higher binding affinity enabled by the Q270E mutation. Based on these results, ICUE4 detects intracellular cAMP more sensitively than ICUE3. Moreover, the Q270E mutation appears to have increased the dynamic range.

Employing ICUE4 in PC12 cells

The sensitivity of ICUE4 towards low levels of cAMP was tested in a setting where the cAMP levels are nearly undetectable using ICUE3. Previously, it was shown

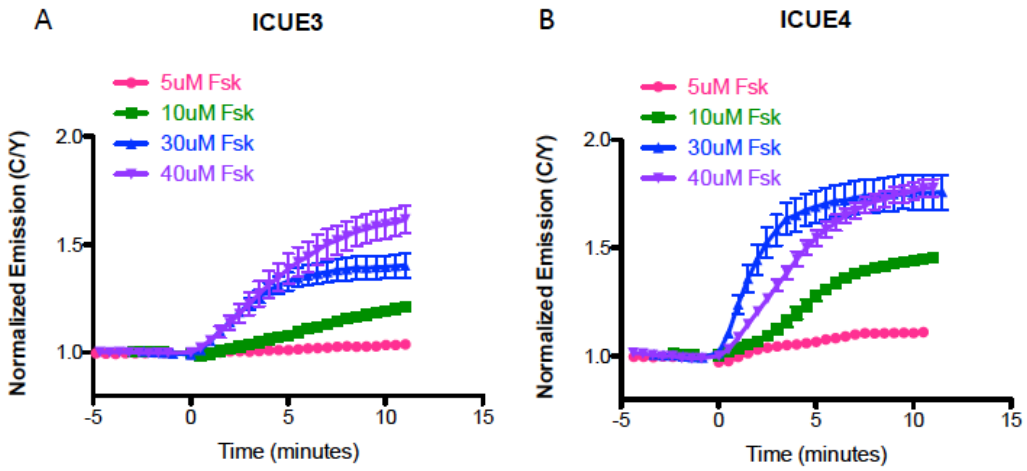

Figure 5.3 ICUE3 vs. ICUE4 responses to increasing Forskolin concentrations
(A) ICUE3 and (B) ICUE4 responses to 5μM, 10μM, 30μM, and 40μM Forskolin (Fsk).

that in PC12 cells, both EGF and NGF were able to induce PKA activity. Since PKA is activated by cAMP, we hypothesized the growth factors could be upregulating PKA activity through cAMP. However, ICUE3 was unable to detect the change in cAMP level. This type of discrepancy between the PKA and cAMP-binding reporters is often due to the ability of the PKA reporter (AKAR) to amplify the cAMP signal through multiple phosphorylation events[72]. We therefore transfected PC12 cells with either ICUE3 or ICUE4 and compared their FRET responses after GF stimulation. After 30 minutes of 100 ng/mL EGF stimulation, ICUE3 showed only a 0.8 ± 1.8% (n=4) FRET response, whereas an identical treatment elicited a 9.4 ± 1.3% FRET (n=11) change from ICUE4 (Fig. 5.4A, B). A similar trend was observed when the PC12 cells were treated with 200 ng/mL NGF, with ICUE3 and ICUE4 displaying average FRET ratio changes of 2.1 ± 1.4% (n=4) and 7.6 ± 2.0% (n=7), respectively (Fig. 5.4C, D).

Additionally, we previously applied ICUE3 to detect LY294002-induced cAMP levels (see Chapter 3). The overall kinetics of the ICUE3 responses were slow, possibly indicating that cAMP levels were again low in PC12 cells. However, unlike the response observed from ICUE3 (4.1 ± 1.1%, n=4), ICUE4 showed a more rapid and robust response to LY294002 treatment (12.0 ± 1.7%, n=5), further demonstrating that ICUE4 is a more sensitive probe that can be utilized to detect small, physiologically relevant changes in cAMP levels (Fig. 5.4E).

DISCUSSION

cAMP is an important second messenger that has a large influence on cell signaling and thus biological processes in response to various types of external stimuli.

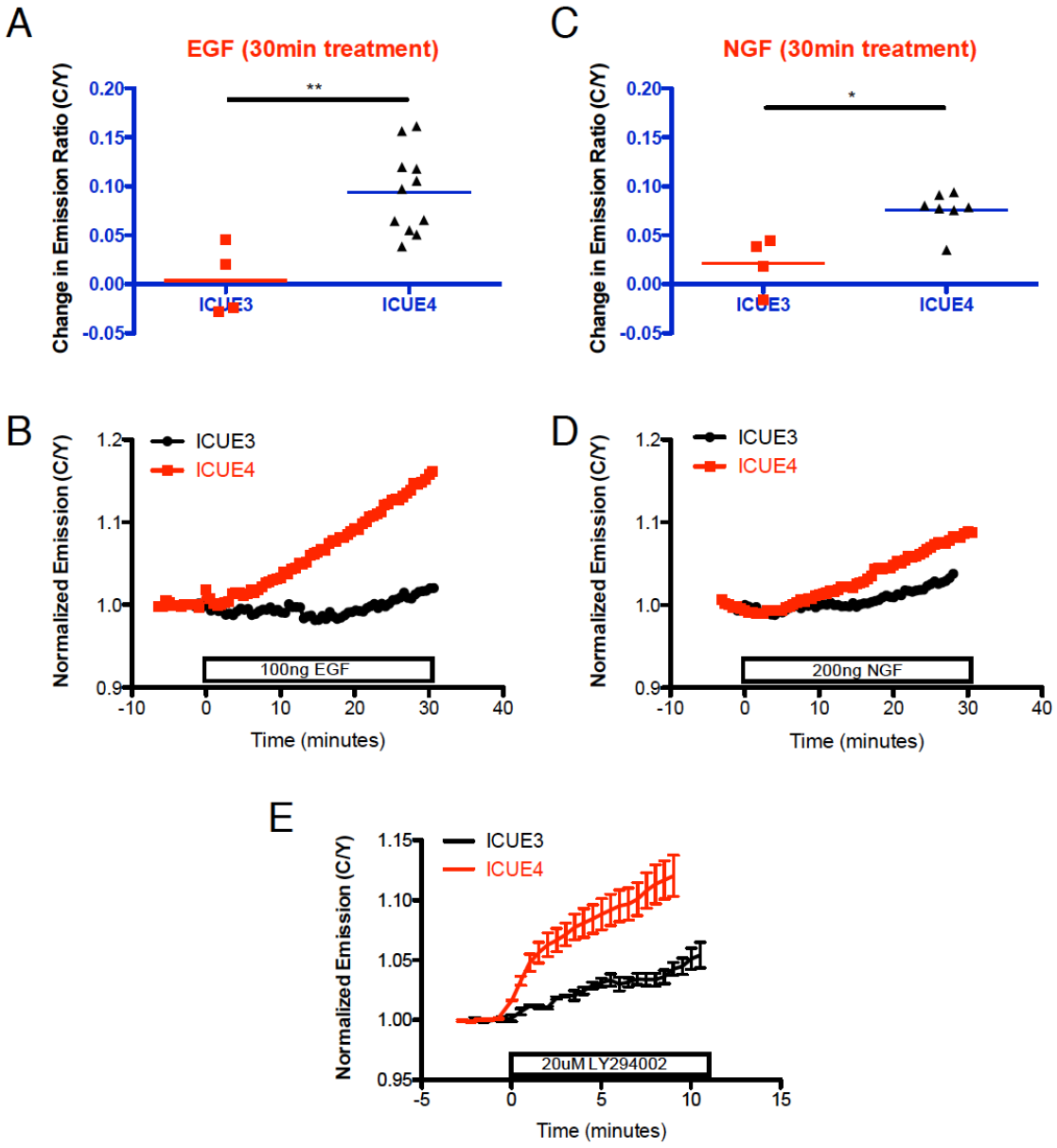

Figure 5.4 ICUE4 detects growth-factor induced cAMP in PC12 cells
(A) Quantification of ICUE3 and ICUE4 responses to 100ng/mL EGF and (B) 200ng/mL NGF. (B-C) Representative time course plot of ICUE3 and ICUE4 with either EGF or NGF treatments (E) Time course plot of ICUE3 and ICUE4 response to 20μM LY294002 (black n=4, red=5).

Cells are known to compartmentalized cAMP singling to where it is needed most to induce specific cellular responses. As a result, the concentration of cAMP is uniform throughout the cell. The differences in cAMP levels within various microdomains can be visualized using FRET-based reporters such as ICUE3. However, it has been shown to be insensitive to low cAMP concentrations. Therefore through structural studies, Dao *et a.l*, identified a key residue in Epac, that if mutated to mimic the tight binding of PKA tocAMP, could enhance the binding of Epac to cAMP. By incorporating this Q270E mutation in ICUE3, which utilizes Epac as its molecular switch, we demonstrated both *in vitro* and *in vivo* that ICUE4 has increased affinity for cAMP and significantly larger dynamic range. Furthermore, we employed ICUE4 in a setting where changes in cAMP levels are detectable by AKAR, but not ICUE3 due to the extremely low levels of cAMP and the ability of AKAR to amplify the cAMP signals. ICUE4 successfully detected growth-factor and LY294002 induced increase in cAMP levels in PC12 cells. As a result, ICUE4 will be useful in uncovering dynamic changes in cAMP levels that had once escaped our detection.

MATERIALS AND METHODS

In vitro fluorescence assays

After 48 hour transfection, HEK293T cells were spun and lysed in a buffer pH 7.4 containing 50mM Tris-HCl, 100mM NaCl, 1mM EDTA, 1mM PMSF, protease inhibitor cocktail (Roche), and 0.2% Triton X-100 in a Dounce homogenizer. Lysed cells were spun and 50 μL of Ni-NTA beads (Qiagen) was added to the supernatant. The beads were spun, washed once in buffer containing 10 mM imidazole, and eluted in buffer containing

100 mM imidazole. Purified protein was detected by Coomasie stain (Pierce Biotechnology) and western analysis using anti-GFP antibody (eBioscience). Fluorescence spectra of ICUE3 and ICUE4 were measured with excitation at 435 nm before and after addition of cAMP. Spectrum reading was taking between 450 to 600nm. Integration time was set to 0.5sec. Slit size for excitation wavelength was set to 1 while emission slit size was set to 5. FLuoromax-3 fluorimeter from Horiba scientific was used to take the spectrum reading. Each sample was read three times, and each reading was background subtracted and normalized to the CFP peak at 475 nm.

Cell Culture and Imaging

HEK293T cells were grown in DMEM cell culture media (Gibco) supplemented with 10% FBS and 1% penicillin/streptomycin at 37^{o}C with 5% CO_2. HEK293T cells were transfected with Lipofectamine 2000 (Invitrogen). For imaging, PC12 cells were washed with Hanks' balanced salt solution buffer and imaged in. For imaging, cells were washed once and then imaged in Hanks' balanced salt solution in the dark at 37°C, on a Zeiss Axiovert 200 M microscope with a cooled charge-coupled-device camera (MicroMAX BFT512; Roper Scientific, Trenton, NJ) controlled by METAFLUOR software (Molecular Devices, Sunnyvale, CA). Dual emission ratio imaging was performed using a 420DF20 excitation filter and a 450DRLP dichroic mirror and appropriate emission filters, 475DF40 for cyan fluorescent protein (CFP) and 535DF25 for yellow fluorescent protein (YFP). Exposure time was 50–500 ms. Images were taken every 20–30 s. Imaging data were analyzed with MetaFluor 6.2 software (Molecular Devices, Sunnyvale, CA). Cells were treated with drug as indicated, and images were analyzed

using ImageJ software (NIH). Fluorescence images were background corrected by deducting the background (regions with no cells) from the emission intensities of CFP or YFP. Traces were normalized by taking the emission ratio before addition of drugs as 1.

Chapter 6

Concluding Remarks

The ability of cells to recognize, adapt and respond to wide array of external conditions is critical for regulating various cellular processes in order to survive. Cells respond to these changes by modulating the inner workings of intracellular signaling pathways that ultimately alter cellular processes. In order for cells to achieve specific cellular responses, cells exploit the precise spatial localization and temporal dynamics of different signaling molecules. Investigation of these intricate signaling networks allows us to understand how these processes manifest and occasionally malfunction, all in the hopes of preventing and/or treating conditions that arise from dysregulation of signaling pathways. To gain a precise understanding of the mechanisms involved in these tight regulation of signal transduction, one needs to study these networks in their native environment. Utilizing FRET-based biosensors in conjunction with biochemical and molecular biology techniques, allows us to investigate intracellular signaling events in their native context. Specifically, with the help of FRET-based reporters, we were able to investigate the molecular determinants of cAMP/PKA signaling specificity in distinct cell-based systems.

With the aid of plasma membrane targeted KARs in conjunction with microfabrication devices, and AFM, we discovered the differential PKA activity levels in CHO-α4WT cells undergoing different degrees of physical confinement. In response to physical confinement, cells suppress PKA activity to activate components of cell migration that allow for efficient movement through confined spaces. PKA is negatively regulated by elevated intracellular calcium in confined cells via phosphodiesterase 1 (PDE1)-dependent mechanism and tunes myosin II/Rac1 activities to promote cell motility. The myosin II/Rac 1 pathway in turn suppresses PKA. This circuit activity is

amplified by double negative feedback, leading to maximized cell responses to confinement. We further demonstrate the existence of two confinement-sensing mechanisms that are mediated by the Ca^{2+}/PDE1/PKA and myosin II/Rac1 signaling modules, respectively. This study provides a novel paradigm by which confinement-induced signaling enables cells to adapt to different physical microenvironments.

In a second study, we used FRET-based biosensors for PKA and Akt activities targeted to distinct subcellular locations to elucidate the molecular mechanisms underlying GF signaling specificity in PC12 cells. In doing so, we first characterized the precise spatiotemporal patterns of EGF- and NGF-induced Akt activities throughout subcellular regions of PC12 cells. We have also revealed the tight spatiotemporal regulation of PKA activity on GF-stimulated Akt activity at the plasma membrane as well as the negative feedback from Akt to PKA. As a novel level of regulation underlying the GF signaling specificity in this classical system, we again present an example of signal transduction cross-talk where the precise spatiotemporal regulation of one signaling pathway controls the spatiotemporal regulation of another. Interestingly, we also observed that simply elevating cAMP levels through AC activation can induce neurite outgrowth. This is interesting because this effect bypasses the need for growth-factor receptor activation, which challenges the classically accepted hypothesis. Since Akt also has effect on PKA activity, the PKA-Akt crosstalk may play an important role in regulating PC12 differentiation. Collectively these findings have elucidated differential subcellular Akt activity specific to PC12 cells and new insights into additional mechanisms that are required for GF signaling specificity in PC12 cells.

Finally, while FRET-based biosensors have proven powerful tools to study the spatiotemporal regulation of signal transduction in the native cellular context, further improvement of these sensors in terms of sensitivity and versatility of detection is needed to facilitate the use of these tools in applications such as *in vivo* imaging, high throughput compound screening, and possibly co-imaging with optogentic tools. Thus, for the specific case of kinase activity detection, we have designed a series of BRET-based biosensors, which is generalizable both in terms of kinase specificity and readout, and can thus be used to sensitively track dynamic kinase activities in a variety of systems and formats. With the design of these sensors we have enhanced the molecular toolkit to detect various kinase activities, broadening the application of these tools for the use of tracking signal transduction in the native cellular context.

Throughout this work we have shown that proper signal transduction is necessary for the conversion of a specific environmental stimulant into a distinct cell fate, and it is thus critical that the cell tightly regulates signal transduction in both space and time. If this proper regulation is not maintained, the result can be detrimental to the cell, tissue, and/or organism, and this is the case in many diseased states. Therefore, understanding the molecular regulatory mechanisms underlying signal transduction in a given system, and identifying the molecular discrepancies in these signaling mechanisms between the normal and diseased states will facilitate the identification and characterization of molecular targets for therapeutic intervention. As cAMP is a ubiquitous second messenger and implicated in the regulation of a variety of physiological processes, the findings presented in this work are likely influence and will have implication in the further characterization of cAMP-mediated signaling specificity in a variety of systems.

REFERENCES

1. Finn, R.N. Vertebrate yolk complexes and the functional implications of phosvitins and other subdomains in vitellogenins. *Biology of reproduction* **76**, 926-935 (2007).
2. Burnett, G. & Kennedy, E.P. The enzymatic phosphorylation of proteins. *The Journal of biological chemistry* **211**, 969-980 (1954).
3. Madsen, N.B., Avramovic-Zikic, O., Lue, P.F. & Honikel, K.O. Studies on allosteric phenomena in glycogen phosphorylase b. *Molecular and cellular biochemistry* **11**, 35-50 (1976).
4. Helmreich, E., Michaelides, M.C. & Cori, C.F. Effects of substrates and a substrate analog on the binding of 5'-adenylic acid to muscle phosphorylase a. *Biochemistry* **6**, 3695-3710 (1967).
5. Simoni, R.D., Hill, R.L. & Vaughan, M. Carbohydrate Metabolism: Glycogen Phosphorylase and the Work of Carl F. and Gerty T.Cori. 1928-1943. *The Journal of biological chemistry* **277**, 18e (2002).
6. Sutherland, E.W. & Rall, T.W. Fractionation and characterization of a cyclic adenine ribonucleotide formed by tissue particles. *The Journal of biological chemistry* **232**, 1077-1091 (1958).
7. Walsh, D.A., Perkins, J.P. & Krebs, E.G. An adenosine 3',5'-monophosphate-dependant protein kinase from rabbit skeletal muscle. *The Journal of biological chemistry* **243**, 3763-3765 (1968).
8. Cohen, P. The regulation of protein function by multisite phosphorylation--a 25 year update. *Trends in biochemical sciences* **25**, 596-601 (2000).
9. Yoshizaki, H. & Okuda, S. Large-scale analysis of the evolutionary histories of phosphorylation motifs in the human genome. *GigaScience* **4**, 21 (2015).
10. Cohen, P. The role of protein phosphorylation in human health and disease. The Sir Hans Krebs Medal Lecture. *European journal of biochemistry / FEBS* **268**, 5001-5010 (2001).
11. Guan, K.L. & Dixon, J.E. Protein tyrosine phosphatase activity of an essential virulence determinant in Yersinia. *Science* **249**, 553-556 (1990).
12. MacKintosh, C., Beattie, K.A., Klumpp, S., Cohen, P. & Codd, G.A. Cyanobacterial microcystin-LR is a potent and specific inhibitor of protein phosphatases 1 and 2A from both mammals and higher plants. *FEBS letters* **264**, 187-192 (1990).
13. Cohen, P. The development and therapeutic potential of protein kinase inhibitors. *Current opinion in chemical biology* **3**, 459-465 (1999).
14. Miller, C.L. & Yan, C. Targeting cyclic nucleotide phosphodiesterase in the heart: therapeutic implications. *Journal of cardiovascular translational research* **3**, 507-515 (2010).
15. De Felice, F.G. *et al.* Cyclic AMP enhancers and Abeta oligomerization blockers as potential therapeutic agents in Alzheimer's disease. *Current Alzheimer research* **4**, 263-271 (2007).
16. Wettschureck, N. & Offermanns, S. Mammalian G proteins and their cell type specific functions. *Physiological reviews* **85**, 1159-1204 (2005).

17. Taylor, S.S., Buechler, J.A. & Yonemoto, W. cAMP-dependent protein kinase: framework for a diverse family of regulatory enzymes. *Annual review of biochemistry* **59**, 971-1005 (1990).
18. Herberg, F.W., Taylor, S.S. & Dostmann, W.R. Active site mutations define the pathway for the cooperative activation of cAMP-dependent protein kinase. *Biochemistry* **35**, 2934-2942 (1996).
19. Erlichman, J., Rosenfeld, R. & Rosen, O.M. Phosphorylation of a cyclic adenosine 3':5'-monophosphate-dependent protein kinase from bovine cardiac muscle. *The Journal of biological chemistry* **249**, 5000-5003 (1974).
20. Cadd, G.G., Uhler, M.D. & McKnight, G.S. Holoenzymes of cAMP-dependent protein kinase containing the neural form of type I regulatory subunit have an increased sensitivity to cyclic nucleotides. *The Journal of biological chemistry* **265**, 19502-19506 (1990).
21. de Rooij, J. *et al.* Epac is a Rap1 guanine-nucleotide-exchange factor directly activated by cyclic AMP. *Nature* **396**, 474-477 (1998).
22. Gloerich, M. & Bos, J.L. Epac: defining a new mechanism for cAMP action. *Annual review of pharmacology and toxicology* **50**, 355-375 (2010).
23. Holz, G.G., Kang, G., Harbeck, M., Roe, M.W. & Chepurny, O.G. Cell physiology of cAMP sensor Epac. *The Journal of physiology* **577**, 5-15 (2006).
24. Selvaratnam, R., Mazhab-Jafari, M.T., Das, R. & Melacini, G. The auto-inhibitory role of the EPAC hinge helix as mapped by NMR. *PloS one* **7**, e48707 (2012).
25. Rehmann, H., Das, J., Knipscheer, P., Wittinghofer, A. & Bos, J.L. Structure of the cyclic-AMP-responsive exchange factor Epac2 in its auto-inhibited state. *Nature* **439**, 625-628 (2006).
26. Rehmann, H. *et al.* Structure and regulation of the cAMP-binding domains of Epac2. *Nature structural biology* **10**, 26-32 (2003).
27. Ozaki, N. *et al.* cAMP-GEFII is a direct target of cAMP in regulated exocytosis. *Nature cell biology* **2**, 805-811 (2000).
28. Rangarajan, S. *et al.* Cyclic AMP induces integrin-mediated cell adhesion through Epac and Rap1 upon stimulation of the beta 2-adrenergic receptor. *The Journal of cell biology* **160**, 487-493 (2003).
29. Kiermayer, S. *et al.* Epac activation converts cAMP from a proliferative into a differentiation signal in PC12 cells. *Molecular biology of the cell* **16**, 5639-5648 (2005).
30. Chen, H. *et al.* 5-Cyano-6-oxo-1,6-dihydro-pyrimidines as potent antagonists targeting exchange proteins directly activated by cAMP. *Bioorganic & medicinal chemistry letters* **22**, 4038-4043 (2012).
31. Vliem, M.J. *et al.* 8-pCPT-2'-O-Me-cAMP-AM: an improved Epac-selective cAMP analogue. *Chembiochem : a European journal of chemical biology* **9**, 2052-2054 (2008).
32. Tsalkova, T., Mei, F.C. & Cheng, X. A fluorescence-based high-throughput assay for the discovery of exchange protein directly activated by cyclic AMP (EPAC) antagonists. *PloS one* **7**, e30441 (2012).
33. Zhang, C.L. *et al.* The cAMP sensor Epac2 is a direct target of antidiabetic sulfonylurea drugs. *Science* **325**, 607-610 (2009).

34. Metrich, M. *et al.* Role of the cAMP-binding protein Epac in cardiovascular physiology and pathophysiology. *Pflugers Archiv : European journal of physiology* **459**, 535-546 (2010).
35. McPhee, I. *et al.* Cyclic nucleotide signalling: a molecular approach to drug discovery for Alzheimer's disease. *Biochemical Society transactions* **33**, 1330-1332 (2005).
36. Hayes, J.S., Brunton, L.L. & Mayer, S.E. Selective activation of particulate cAMP-dependent protein kinase by isoproterenol and prostaglandin E1. *The Journal of biological chemistry* **255**, 5113-5119 (1980).
37. Fleischer, N., Rosen, O.M. & Reichlin, M. Radioimmunoassay of bovine heart protein kinase. *Proceedings of the National Academy of Sciences of the United States of America* **73**, 54-58 (1976).
38. Felder, C.C. Muscarinic acetylcholine receptors: signal transduction through multiple effectors. *FASEB journal : official publication of the Federation of American Societies for Experimental Biology* **9**, 619-625 (1995).
39. Steegborn, C. Structure, mechanism, and regulation of soluble adenylyl cyclases - similarities and differences to transmembrane adenylyl cyclases. *Biochimica et biophysica acta* **1842**, 2535-2547 (2014).
40. Zippin, J.H. *et al.* Compartmentalization of bicarbonate-sensitive adenylyl cyclase in distinct signaling microdomains. *FASEB journal : official publication of the Federation of American Societies for Experimental Biology* **17**, 82-84 (2003).
41. Schmid, A., Meili, D. & Salathe, M. Soluble adenylyl cyclase in health and disease. *Biochimica et biophysica acta* **1842**, 2584-2592 (2014).
42. Rahman, N., Buck, J. & Levin, L.R. pH sensing via bicarbonate-regulated "soluble" adenylyl cyclase (sAC). *Frontiers in physiology* **4**, 343 (2013).
43. Sunahara, R.K. & Taussig, R. Isoforms of mammalian adenylyl cyclase: multiplicities of signaling. *Molecular interventions* **2**, 168-184 (2002).
44. Hohl, C.M. & Li, Q.A. Compartmentation of cAMP in adult canine ventricular myocytes. Relation to single-cell free Ca2+ transients. *Circulation research* **69**, 1369-1379 (1991).
45. Lefkimmiatis, K. & Zaccolo, M. cAMP signaling in subcellular compartments. *Pharmacology & therapeutics* **143**, 295-304 (2014).
46. Herbst, K.J., Allen, M.D. & Zhang, J. Spatiotemporally regulated protein kinase A activity is a critical regulator of growth factor-stimulated extracellular signal-regulated kinase signaling in PC12 cells. *Molecular and cellular biology* **31**, 4063-4075 (2011).
47. Yan, C. *et al.* Molecular cloning and characterization of a calmodulin-dependent phosphodiesterase enriched in olfactory sensory neurons. *Proceedings of the National Academy of Sciences of the United States of America* **92**, 9677-9681 (1995).
48. Shakur, Y. *et al.* Regulation and function of the cyclic nucleotide phosphodiesterase (PDE3) gene family. *Progress in nucleic acid research and molecular biology* **66**, 241-277 (2001).

49. Rababa'h, A. *et al.* Compartmentalization role of A-kinase anchoring proteins (AKAPs) in mediating protein kinase A (PKA) signaling and cardiomyocyte hypertrophy. *International journal of molecular sciences* **16**, 218-229 (2015).
50. Carr, D.W. *et al.* Interaction of the regulatory subunit (RII) of cAMP-dependent protein kinase with RII-anchoring proteins occurs through an amphipathic helix binding motif. *The Journal of biological chemistry* **266**, 14188-14192 (1991).
51. Jarnaess, E. *et al.* Dual specificity A-kinase anchoring proteins (AKAPs) contain an additional binding region that enhances targeting of protein kinase A type I. *The Journal of biological chemistry* **283**, 33708-33718 (2008).
52. Means, C.K. *et al.* An entirely specific type I A-kinase anchoring protein that can sequester two molecules of protein kinase A at mitochondria. *Proceedings of the National Academy of Sciences of the United States of America* **108**, E1227-1235 (2011).
53. Kovanich, D. *et al.* Sphingosine kinase interacting protein is an A-kinase anchoring protein specific for type I cAMP-dependent protein kinase. *Chembiochem : a European journal of chemical biology* **11**, 963-971 (2010).
54. Lim, C.J. *et al.* Alpha4 integrins are type I cAMP-dependent protein kinase-anchoring proteins. *Nature cell biology* **9**, 415-421 (2007).
55. Gold, M.G., Gonen, T. & Scott, J.D. Local cAMP signaling in disease at a glance. *Journal of cell science* **126**, 4537-4543 (2013).
56. Halls, M.L. & Cooper, D.M. Regulation by Ca2+-signaling pathways of adenylyl cyclases. *Cold Spring Harbor perspectives in biology* **3**, a004143 (2011).
57. Seino, S. & Shibasaki, T. PKA-dependent and PKA-independent pathways for cAMP-regulated exocytosis. *Physiological reviews* **85**, 1303-1342 (2005).
58. Howe, A.K. Cross-talk between calcium and protein kinase A in the regulation of cell migration. *Current opinion in cell biology* **23**, 554-561 (2011).
59. Marshall, C.J. Specificity of receptor tyrosine kinase signaling: transient versus sustained extracellular signal-regulated kinase activation. *Cell* **80**, 179-185 (1995).
60. Smith, F.D., Langeberg, L.K. & Scott, J.D. Plugging PKA into ERK scaffolds. *Cell cycle* **10**, 731-732 (2011).
61. Smith, F.D. *et al.* AKAP-Lbc enhances cyclic AMP control of the ERK1/2 cascade. *Nature cell biology* **12**, 1242-1249 (2010).
62. Hunzicker-Dunn, M.E. *et al.* PKA and GAB2 play central roles in the FSH signaling pathway to PI3K and AKT in ovarian granulosa cells. *Proceedings of the National Academy of Sciences of the United States of America* **109**, E2979-2988 (2012).
63. Donati, G. & Watt, F.M. Stem Cell Heterogeneity and Plasticity in Epithelia. *Cell stem cell* **16**, 465-476 (2015).
64. Zardavas, D., Irrthum, A., Swanton, C. & Piccart, M. Clinical management of breast cancer heterogeneity. *Nature reviews. Clinical oncology* (2015).
65. Ni, Q. *et al.* Signaling diversity of PKA achieved via a Ca2+-cAMP-PKA oscillatory circuit. *Nature chemical biology* **7**, 34-40 (2011).
66. Fosbrink, M., Aye-Han, N.N., Cheong, R., Levchenko, A. & Zhang, J. Visualization of JNK activity dynamics with a genetically encoded fluorescent

biosensor. *Proceedings of the National Academy of Sciences of the United States of America* **107**, 5459-5464 (2010).
67. Cohen, L.B. *et al.* Changes in axon fluorescence during activity: molecular probes of membrane potential. *The Journal of membrane biology* **19**, 1-36 (1974).
68. Grynkiewicz, G., Poenie, M. & Tsien, R.Y. A new generation of Ca2+ indicators with greatly improved fluorescence properties. *The Journal of biological chemistry* **260**, 3440-3450 (1985).
69. Ross, W.N., Salzberg, B.M., Cohen, L.B. & Davila, H.V. A large change in dye absorption during the action potential. *Biophysical journal* **14**, 983-986 (1974).
70. Sample, V., Newman, R.H. & Zhang, J. The structure and function of fluorescent proteins. *Chemical Society reviews* **38**, 2852-2864 (2009).
71. VanEngelenburg, S.B. & Palmer, A.E. Fluorescent biosensors of protein function. *Current opinion in chemical biology* **12**, 60-65 (2008).
72. Depry, C., Allen, M.D. & Zhang, J. Visualization of PKA activity in plasma membrane microdomains. *Molecular bioSystems* **7**, 52-58 (2011).
73. Kunkel, M.T., Ni, Q., Tsien, R.Y., Zhang, J. & Newton, A.C. Spatio-temporal dynamics of protein kinase B/Akt signaling revealed by a genetically encoded fluorescent reporter. *The Journal of biological chemistry* **280**, 5581-5587 (2005).
74. Sample, V. *et al.* Regulation of nuclear PKA revealed by spatiotemporal manipulation of cyclic AMP. *Nature chemical biology* **8**, 375-382 (2012).
75. Herbst, K.J., Allen, M.D. & Zhang, J. Luminescent kinase activity biosensors based on a versatile bimolecular switch. *Journal of the American Chemical Society* **133**, 5676-5679 (2011).
76. Ni, Q., Titov, D.V. & Zhang, J. Analyzing protein kinase dynamics in living cells with FRET reporters. *Methods* **40**, 279-286 (2006).
77. Zhou, X. *et al.* Dynamic Visualization of mTORC1 Activity in Living Cells. *Cell reports* (2015).
78. DiPilato, L.M., Cheng, X. & Zhang, J. Fluorescent indicators of cAMP and Epac activation reveal differential dynamics of cAMP signaling within discrete subcellular compartments. *Proceedings of the National Academy of Sciences of the United States of America* **101**, 16513-16518 (2004).
79. Honda, A. *et al.* Spatiotemporal dynamics of guanosine 3',5'-cyclic monophosphate revealed by a genetically encoded, fluorescent indicator. *Proceedings of the National Academy of Sciences of the United States of America* **98**, 2437-2442 (2001).
80. Miyawaki, A., Griesbeck, O., Heim, R. & Tsien, R.Y. Dynamic and quantitative Ca2+ measurements using improved cameleons. *Proceedings of the National Academy of Sciences of the United States of America* **96**, 2135-2140 (1999).
81. Ananthanarayanan, B., Ni, Q. & Zhang, J. Signal propagation from membrane messengers to nuclear effectors revealed by reporters of phosphoinositide dynamics and Akt activity. *Proceedings of the National Academy of Sciences of the United States of America* **102**, 15081-15086 (2005).

82. Mehta, S. & Zhang, J. Using a kinase-inducible bimolecular switch to control enzyme activity in living cells. *Current protocols in chemical biology* **5**, 227-237 (2013).
83. Inglese, J. *et al.* High-throughput screening assays for the identification of chemical probes. *Nature chemical biology* **3**, 466-479 (2007).
84. Thorne, N., Inglese, J. & Auld, D.S. Illuminating insights into firefly luciferase and other bioluminescent reporters used in chemical biology. *Chemistry & biology* **17**, 646-657 (2010).
85. Hoshino, H. Current advanced bioluminescence technology in drug discovery. *Expert opinion on drug discovery* **4**, 373-389 (2009).
86. Jiang, L.I. *et al.* Use of a cAMP BRET sensor to characterize a novel regulation of cAMP by the sphingosine 1-phosphate/G13 pathway. *The Journal of biological chemistry* **282**, 10576-10584 (2007).
87. Kaczor, A.A. *et al.* Application of BRET for studying G protein-coupled receptors. *Mini reviews in medicinal chemistry* **14**, 411-425 (2014).
88. Xiong, T.C. *et al.* Imaging long distance propagating calcium signals in intact plant leaves with the BRET-based GFP-aequorin reporter. *Frontiers in plant science* **5**, 43 (2014).
89. Wolf, K. *et al.* Compensation mechanism in tumor cell migration: mesenchymal-amoeboid transition after blocking of pericellular proteolysis. *The Journal of cell biology* **160**, 267-277 (2003).
90. Liu, Y.J. *et al.* Confinement and low adhesion induce fast amoeboid migration of slow mesenchymal cells. *Cell* **160**, 659-672 (2015).
91. Sanz-Moreno, V. *et al.* Rac activation and inactivation control plasticity of tumor cell movement. *Cell* **135**, 510-523 (2008).
92. Xue, C. *et al.* Epidermal growth factor receptor overexpression results in increased tumor cell motility in vivo coordinately with enhanced intravasation and metastasis. *Cancer Res* **66**, 192-197 (2006).
93. Petrie, R.J., Koo, H. & Yamada, K.M. Generation of compartmentalized pressure by a nuclear piston governs cell motility in a 3D matrix. *Science* **345**, 1062-1065 (2014).
94. Hung, W.C. *et al.* Distinct signaling mechanisms regulate migration in unconfined versus confined spaces. *The Journal of cell biology* **202**, 807-824 (2013).
95. Stroka, K.M. *et al.* Water permeation drives tumor cell migration in confined microenvironments. *Cell* **157**, 611-623 (2014).
96. Jacobelli, J. *et al.* Confinement-optimized three-dimensional T cell amoeboid motility is modulated via myosin IIA-regulated adhesions. *Nature immunology* **11**, 953-961 (2010).
97. Balzer, E.M. *et al.* Physical confinement alters tumor cell adhesion and migration phenotypes. *FASEB journal : official publication of the Federation of American Societies for Experimental Biology* **26**, 4045-4056 (2012).
98. Doyle, A.D., Wang, F.W., Matsumoto, K. & Yamada, K.M. One-dimensional topography underlies three-dimensional fibrillar cell migration. *The Journal of cell biology* **184**, 481-490 (2009).

99. Petrie, R.J., Gavara, N., Chadwick, R.S. & Yamada, K.M. Nonpolarized signaling reveals two distinct modes of 3D cell migration. *The Journal of cell biology* **197**, 439-455 (2012).
100. Tozluoglu, M. *et al.* Matrix geometry determines optimal cancer cell migration strategy and modulates response to interventions. *Nat Cell Biol* **15**, 751-762 (2013).
101. Goldfinger, L.E., Han, J., Kiosses, W.B., Howe, A.K. & Ginsberg, M.H. Spatial restriction of alpha4 integrin phosphorylation regulates lamellipodial stability and alpha4beta1-dependent cell migration. *The Journal of cell biology* **162**, 731-741 (2003).
102. Howe, A.K. Cross-talk between calcium and protein kinase A in the regulation of cell migration. *Current opinion in cell biology* **23**, 554-561 (2011).
103. Newell-Litwa, K.A. & Horwitz, A.R. Cell migration: PKA and RhoA set the pace. *Curr Biol* **21**, R596-598 (2011).
104. Han, J. *et al.* Phosphorylation of the integrin alpha 4 cytoplasmic domain regulates paxillin binding. *The Journal of biological chemistry* **276**, 40903-40909 (2001).
105. Lim, C.J. *et al.* Integrin-mediated protein kinase A activation at the leading edge of migrating cells. *Molecular biology of the cell* **19**, 4930-4941 (2008).
106. Chen, L., Vicente-Manzanares, M., Potvin-Trottier, L., Wiseman, P.W. & Horwitz, A.R. The integrin-ligand interaction regulates adhesion and migration through a molecular clutch. *PloS one* **7**, e40202 (2012).
107. Schreiner, C.L. *et al.* Isolation and characterization of Chinese hamster ovary cell variants deficient in the expression of fibronectin receptor. *The Journal of cell biology* **109**, 3157-3167 (1989).
108. Nagai, T., Yamada, S., Tominaga, T., Ichikawa, M. & Miyawaki, A. Expanded dynamic range of fluorescent indicators for Ca(2+) by circularly permuted yellow fluorescent proteins. *Proc Natl Acad Sci U S A* **101**, 10554-10559 (2004).
109. Suchyna, T.M. *et al.* Identification of a peptide toxin from Grammostola spatulata spider venom that blocks cation-selective stretch-activated channels. *J Gen Physiol* **115**, 583-598 (2000).
110. Bender, A.T. & Beavo, J.A. Cyclic nucleotide phosphodiesterases: molecular regulation to clinical use. *Pharmacological reviews* **58**, 488-520 (2006).
111. Mika, D., Richter, W. & Conti, M. A CaMKII/PDE4D negative feedback regulates cAMP signaling. *Proceedings of the National Academy of Sciences of the United States of America* **112**, 2023-2028 (2015).
112. Westphal, R.S., Soderling, S.H., Alto, N.M., Langeberg, L.K. & Scott, J.D. Scar/WAVE-1, a Wiskott-Aldrich syndrome protein, assembles an actin-associated multi-kinase scaffold. *The EMBO journal* **19**, 4589-4600 (2000).
113. Yamashita, H., Ueda, K. & Kioka, N. WAVE2 forms a complex with PKA and is involved in PKA enhancement of membrane protrusions. *The Journal of biological chemistry* **286**, 3907-3914 (2011).
114. Fernandez-Gonzalez, R., Simoes Sde, M., Roper, J.C., Eaton, S. & Zallen, J.A. Myosin II dynamics are regulated by tension in intercalating cells. *Developmental cell* **17**, 736-743 (2009).

115. Ren, Y. *et al.* Mechanosensing through cooperative interactions between myosin II and the actin crosslinker cortexillin I. *Curr Biol* **19**, 1421-1428 (2009).
116. Thomas, G., Burnham, N.A., Camesano, T.A. & Wen, Q. Measuring the Mechanical Properties of Living Cells Using Atomic Force Microscopy. *Jove-J Vis Exp* (2013).
117. Charras, G. & Sahai, E. Physical influences of the extracellular environment on cell migration. *Nature reviews. Molecular cell biology* **15**, 813-824 (2014).
118. Bergert, M. *et al.* Force transmission during adhesion-independent migration. *Nat Cell Biol* **17**, 524-529 (2015).
119. Sawada, Y. *et al.* Force sensing by mechanical extension of the Src family kinase substrate p130Cas. *Cell* **127**, 1015-1026 (2006).
120. Nishiya, N., Kiosses, W.B., Han, J. & Ginsberg, M.H. An alpha4 integrin-paxillin-Arf-GAP complex restricts Rac activation to the leading edge of migrating cells. *Nature cell biology* **7**, 343-352 (2005).
121. Tkachenko, E. *et al.* Protein kinase A governs a RhoA-RhoGDI protrusion-retraction pacemaker in migrating cells. *Nat Cell Biol* **13**, 660-667 (2011).
122. Diviani, D., Abuin, L., Cotecchia, S. & Pansier, L. Anchoring of both PKA and 14-3-3 inhibits the Rho-GEF activity of the AKAP-Lbc signaling complex. *The EMBO journal* **23**, 2811-2820 (2004).
123. Wolenski, J.S. Regulation of calmodulin-binding myosins. *Trends Cell Biol* **5**, 310-316 (1995).
124. Sbrana, F. *et al.* Role for stress fiber contraction in surface tension development and stretch-activated channel regulation in C2C12 myoblasts. *American journal of physiology. Cell physiology* **295**, C160-172 (2008).
125. Pinco, K.A., He, W. & Yang, J.T. alpha4beta1 integrin regulates lamellipodia protrusion via a focal complex/focal adhesion-independent mechanism. *Molecular biology of the cell* **13**, 3203-3217 (2002).
126. Dikeman, D.A. *et al.* alpha4 beta1-Integrin regulates directionally persistent cell migration in response to shear flow stimulation. *American journal of physiology. Cell physiology* **295**, C151-159 (2008).
127. Hanley, W.D., Wirtz, D. & Konstantopoulos, K. Distinct kinetic and mechanical properties govern selectin-leukocyte interactions. *Journal of cell science* **117**, 2503-2511 (2004).
128. Raman, P.S., Alves, C.S., Wirtz, D. & Konstantopoulos, K. Single-molecule binding of CD44 to fibrin versus P-selectin predicts their distinct shear-dependent interactions in cancer. *Journal of cell science* **124**, 1903-1910 (2011).
129. Lemmon, M.A. & Schlessinger, J. Cell signaling by receptor tyrosine kinases. *Cell* **141**, 1117-1134 (2010).
130. Obara, Y., Labudda, K., Dillon, T.J. & Stork, P.J. PKA phosphorylation of Src mediates Rap1 activation in NGF and cAMP signaling in PC12 cells. *Journal of cell science* **117**, 6085-6094 (2004).
131. Ebinu, J.O. *et al.* RasGRP, a Ras guanyl nucleotide- releasing protein with calcium- and diacylglycerol-binding motifs. *Science* **280**, 1082-1086 (1998).

132. Santos, S.D., Verveer, P.J. & Bastiaens, P.I. Growth factor-induced MAPK network topology shapes Erk response determining PC-12 cell fate. *Nature cell biology* **9**, 324-330 (2007).
133. Gao, X. & Zhang, J. Spatiotemporal analysis of differential Akt regulation in plasma membrane microdomains. *Molecular biology of the cell* **19**, 4366-4373 (2008).
134. Toker, A. & Marmiroli, S. Signaling specificity in the Akt pathway in biology and disease. *Advances in biological regulation* **55**, 28-38 (2014).
135. Martelli, A.M. *et al.* The emerging multiple roles of nuclear Akt. *Biochimica et biophysica acta* **1823**, 2168-2178 (2012).
136. Xuan Nguyen, T.L. *et al.* Akt phosphorylation is essential for nuclear translocation and retention in NGF-stimulated PC12 cells. *Biochemical and biophysical research communications* **349**, 789-798 (2006).
137. Yao, H. *et al.* Cyclic adenosine monophosphate can convert epidermal growth factor into a differentiating factor in neuronal cells. *The Journal of biological chemistry* **270**, 20748-20753 (1995).
138. Xiao, L. *et al.* Protein phosphatase-1 regulates Akt1 signal transduction pathway to control gene expression, cell survival and differentiation. *Cell death and differentiation* **17**, 1448-1462 (2010).
139. Cosentino, C. *et al.* p85 regulatory subunit of PI3K mediates cAMP-PKA and estrogens biological effects on growth and survival. *Oncogene* **26**, 2095-2103 (2007).
140. Di Zazzo, E. *et al.* The p85 regulatory subunit of PI3K mediates cAMP-PKA and insulin biological effects on MCF-7 cell growth and motility. *TheScientificWorldJournal* **2014**, 565839 (2014).
141. Lou, L., Urbani, J., Ribeiro-Neto, F. & Altschuler, D.L. cAMP inhibition of Akt is mediated by activated and phosphorylated Rap1b. *The Journal of biological chemistry* **277**, 32799-32806 (2002).
142. Han, S.J. *et al.* Protein kinase B/Akt phosphorylation of PDE3A and its role in mammalian oocyte maturation. *The EMBO journal* **25**, 5716-5725 (2006).
143. Herbst, K.J., Allen, M.D. & Zhang, J. The cAMP-dependent protein kinase inhibitor H-89 attenuates the bioluminescence signal produced by Renilla Luciferase. *PloS one* **4**, e5642 (2009).
144. Pfleger, K.D. & Eidne, K.A. Illuminating insights into protein-protein interactions using bioluminescence resonance energy transfer (BRET). *Nature methods* **3**, 165-174 (2006).
145. Boute, N., Jockers, R. & Issad, T. The use of resonance energy transfer in high-throughput screening: BRET versus FRET. *Trends in pharmacological sciences* **23**, 351-354 (2002).
146. Jiang, L.I. *et al.* Use of a cAMP BRET sensor to characterize a novel regulation of cAMP by the sphingosine 1-phosphate/G13 pathway. *The Journal of biological chemistry* **282**, 10576-10584 (2007).
147. Prinz, A., Diskar, M., Erlbruch, A. & Herberg, F.W. Novel, isotype-specific sensors for protein kinase A subunit interaction based on bioluminescence resonance energy transfer (BRET). *Cellular signalling* **18**, 1616-1625 (2006).

148. Salahpour, A. *et al.* BRET biosensors to study GPCR biology, pharmacology, and signal transduction. *Frontiers in endocrinology* **3**, 105 (2012).
149. Xiong, T.C. *et al.* Imaging long distance propagating calcium signals in intact plant leaves with the BRET-based GFP-aequorin reporter. *Frontiers in plant science* **5**, 43 (2014).
150. Xu, C. *et al.* REV, A BRET-Based Sensor of ERK Activity. *Frontiers in endocrinology* **4**, 95 (2013).
151. Sample, V., Ni, Q., Mehta, S., Inoue, T. & Zhang, J. Controlling enzymatic action in living cells with a kinase-inducible bimolecular switch. *ACS chemical biology* **8**, 116-121 (2013).
152. Loening, A.M., Fenn, T.D., Wu, A.M. & Gambhir, S.S. Consensus guided mutagenesis of Renilla luciferase yields enhanced stability and light output. *Protein engineering, design & selection : PEDS* **19**, 391-400 (2006).
153. Weston, C.R. & Davis, R.J. The JNK signal transduction pathway. *Current opinion in cell biology* **19**, 142-149 (2007).
154. Miyamoto, T. *et al.* Compartmentalized AMPK Signaling Illuminated by Genetically Encoded Molecular Sensors and Actuators. *Cell reports* **11**, 657-670 (2015).
155. Sample, V., Ramamurthy, S., Gorshkov, K., Ronnett, G.V. & Zhang, J. Polarized activities of AMPK and BRSK in primary hippocampal neurons. *Molecular biology of the cell* **26**, 1935-1946 (2015).
156. Curtin, J.F. & Cotter, T.G. Anisomycin activates JNK and sensitises DU 145 prostate carcinoma cells to Fas mediated apoptosis. *British journal of cancer* **87**, 1188-1194 (2002).
157. Tsou, P., Zheng, B., Hsu, C.H., Sasaki, A.T. & Cantley, L.C. A fluorescent reporter of AMPK activity and cellular energy stress. *Cell metabolism* **13**, 476-486 (2011).
158. Allen, M.D. *et al.* Reading dynamic kinase activity in living cells for high-throughput screening. *ACS chemical biology* **1**, 371-376 (2006).
159. Allen, M.D. & Zhang, J. Subcellular dynamics of protein kinase A activity visualized by FRET-based reporters. *Biochemical and biophysical research communications* **348**, 716-721 (2006).
160. Gautier, A. *et al.* How to control proteins with light in living systems. *Nature chemical biology* **10**, 533-541 (2014).
161. Yi, J.J., Wang, H., Vilela, M., Danuser, G. & Hahn, K.M. Manipulation of endogenous kinase activity in living cells using photoswitchable inhibitory peptides. *ACS synthetic biology* **3**, 788-795 (2014).
162. Costa, W.S., Liewald, J. & Gottschalk, A. Photoactivated adenylyl cyclases as optogenetic modulators of neuronal activity. *Methods in molecular biology* **1148**, 161-175 (2014).
163. Stierl, M. *et al.* Light modulation of cellular cAMP by a small bacterial photoactivated adenylyl cyclase, bPAC, of the soil bacterium Beggiatoa. *The Journal of biological chemistry* **286**, 1181-1188 (2011).
164. Schroder-Lang, S. *et al.* Fast manipulation of cellular cAMP level by light in vivo. *Nature methods* **4**, 39-42 (2007).

165. Jansen, V. *et al.* Controlling fertilization and cAMP signaling in sperm by optogenetics. *eLife* **4** (2015).
166. Boute, N., Jockers, R. & Issad, T. The use of resonance energy transfer in high-throughput screening: BRET versus FRET. *Trends in pharmacological sciences* **23**, 351-354 (2002).
167. Hall, M.P. *et al.* Engineered luciferase reporter from a deep sea shrimp utilizing a novel imidazopyrazinone substrate. *ACS chemical biology* **7**, 1848-1857 (2012).
168. DiPilato, L.M. & Zhang, J. The role of membrane microdomains in shaping beta2-adrenergic receptor-mediated cAMP dynamics. *Molecular bioSystems* **5**, 832-837 (2009).
169. Gorshkov, K. & Zhang, J. Visualization of cyclic nucleotide dynamics in neurons. *Frontiers in cellular neuroscience* **8**, 395 (2014).
170. Liu, S. *et al.* Phosphodiesterases coordinate cAMP propagation induced by two stimulatory G protein-coupled receptors in hearts. *Proceedings of the National Academy of Sciences of the United States of America* **109**, 6578-6583 (2012).
171. Marley, A., Choy, R.W. & von Zastrow, M. GPR88 reveals a discrete function of primary cilia as selective insulators of GPCR cross-talk. *PloS one* **8**, e70857 (2013).
172. Nikolaev, V.O., Bunemann, M., Hein, L., Hannawacker, A. & Lohse, M.J. Novel single chain cAMP sensors for receptor-induced signal propagation. *The Journal of biological chemistry* **279**, 37215-37218 (2004).
173. Dao, K.K. *et al.* Epac1 and cAMP-dependent protein kinase holoenzyme have similar cAMP affinity, but their cAMP domains have distinct structural features and cyclic nucleotide recognition. *The Journal of biological chemistry* **281**, 21500-21511 (2006).
174. Kim, C., Cheng, C.Y., Saldanha, S.A. & Taylor, S.S. PKA-I holoenzyme structure reveals a mechanism for cAMP-dependent activation. *Cell* **130**, 1032-1043 (2007).

Curriculum Vitae

Jessica R. Yang

Jessicaryang28@gmail.com

103 East Mount Royal Ave. #901
Baltimore, MD 21202
+1 (949) 241-6181

EDUCATION

Johns Hopkins Medical School (August 2010-August 2015)
Baltimore, MD

- Ph.D. Candidate in Pharmacology and Molecular Sciences
- GRE 2009: V530; Q730
- Advisor: Jin Zhang Ph.D.

University of California, Irvine, School of Biological Sciences (August 2006- June 2010)
Irvine, CA
B.S. in Pharmaceutical Sciences

- GPA: 3.48, Science GPA: 3.5
- Advisor: Sheryl Tsai, Ph.D.
- Magna Cum Laude
- Dean's Honor List

RESEARCH EXPERIENCE

Graduate Student Research

Johns Hopkins University School of Medicine, Baltimore, MD, USA (Winter 2010-Spring 2015)

Pharmacology and Molecular Sciences, Ph.D. Candidate
Advisor: Dr. Jin Zhang
Thesis: Role of spatiotemporally regulated Protein Kinase A (PKA) in different cellular processes

- Project involved the development and usage of genetically encodable biosensors to detect cAMP/PKA signaling dynamics in living cells using fluorescent and bioluminescent proteins
- Used pharmacological intervention to monitor a series of dynamic signaling events in distinct biological processes, including insulin secretion, neuronal differentiation, and cell migration.
    - Determining the mechanism underlying growth-factor stimulated proliferation and differentiation of PC12 cells
        - Developing network map of PKA-AKT crosstalk in PC12

    - Determining and comparing mechanisms underlying cell migration in confined and unconfined spaces
        - Studying how PKA differentially regulates cell migration in confined and unconfined spaces
- Screening compound library for potential inhibitors of kinases
    - Developed FRET/BRET-based assay for single-cell imaging and high-throughput screen
- Acquired proficiencies in live cell fluorescence imaging, bioluminescence detection in single cell and 96 well formats, high-throughput compound screening, immuno-based assays, protein purification, tissue culture, mammalian cell fractionation, and molecular modeling
- Developed the creative ability to analyze many biological problems and data-sets and to devise solutions to solve various scientific challenges in a highly self-motivated manner
- Refined my verbal and written scientific communication skills to communicate in both a technical and simple manner
- Mentored and trained 2 students joining the lab

Graduate rotation student research

Johns Hopkins University School of Medicine, Baltimore, MD, USA (Fall 2010)

Pharmacology and Molecular Sciences, Ph.D. Candidate
Advisor: Philip Cole

University of California, Irvine (Fall 2007-Spring 2010)
Molecular Biology and Biochemistry Department, Research Assistant
Advisor: Sheryl Tsai, Ph.D.

- Conducted structural characterization of bacterial acyl-CoA carboxylase (ACCase) as a potential therapeutic target for Tuberculosis
    - Performed protein purifications/screenings/and crystallization
    - Conducted protein kinetic assays
- Mentored and trained 2 students joining the lab

PUBLICATIONS

- Robinson, K. H., **Yang, J. R**., & Zhang, J. (2014). FRET and BRET-Based Biosensors in Live Cell Compound Screens. In *Fluorescent Protein-Based Biosensors* (pp. 217-225). Humana Press.

- Huang, J., **Yang, J. R**., Zhang, J., & Yang, J. (2013). Total synthesis and structure–activity relationship study of the potent cAMP signaling

agonist (−)-alotaketal A. *Organic & biomolecular chemistry*, *11*(19), 3212-3222.

- Huang, J., **Yang, J. R**., Zhang, J., & Yang, J. (2012). Total synthesis of the potent cAMP signaling agonist (−)-alotaketal A. *Journal of the American Chemical Society*, *134*(21), 8806-8809.

ORAL PRESENTATIONS

- Undergraduate Research Opportunities Program (UROP) Symposium
  - **Spring 2007** Discovering and Developing: Crystallization of Hec1 and the Promise for Future Drug Design
  - **Spring 2008** Discovering and Developing: Detecting the Activity of AccB1420V by Kinetic Analysis
  - **Fall 2008** Discovering and Developing: Crystallizing AccD4

- Chemistry Summer Undergraduate Research Fellowship (Chem-SURF) Symposium
  - **Summer 2009** Discovering and Developing New Tuberculosis Therapeutics: Crystalizing AccD3/AccD4

HONORS

- Allergan Summer Research Fellowship (Summer 2009)
- Chemistry Summer Undergraduate Research Fellowship (Chem-SURF) (Summer 2009)
- Undergraduate Research Opportunities Program (UROP) Fellowship (2007-2008)

REFERENCES

Jin Zhang, Professor of Pharmacology
Johns Hopkins University School of Medicine
410-501-0713
jzhang32@jhmi.edu

Dr. Phil Cole, Professor and Char oof Pharmacology
Johns Hopkins University School of Medicine
410-614-8849
pcole@jhmi.edu